

Aus dem Max-Planck-Institut für Kolloid- und Grenzflächenforschung

Towards a Library of Functional Block Copolymers –  
Synthesis and Colloidal Properties

Dissertation

Zur Erlangung des akademischen Grades

“doctor rerum naturalium“

(Dr. rer. nat.)

in der Wissenschaftsdisziplin

Kolloid- und Polymerchemie

eingereicht an der

Mathematisch-Naturwissenschaftlichen Fakultät

der Universität Potsdam

von

**Justyna Justynska**

geboren in Gliwice, Polen

Potsdam, im April 2005

Die vorliegende Arbeit entstand in der Zeit von Januar 2003 bis April 2005  
am Max-Planck-Institut für Kolloid- und Grenzflächenforschung in Potsdam-Golm  
unter Betreuung von Prof. Dr. Markus Antonietti.

Gutachter: Prof. Dr. M. Antonietti  
Dr. habil. H. Motschmann  
Prof. Dr. S. Förster

Tag der mündlichen Prüfung: 01. September 2005

*“A scientist in his laboratory is not a mere technician:  
he is also a child confronting natural phenomena  
that impress him as though they were fairy tales.”*

Maria Skłodowska-Curie (1867–1934)



# CONTENTS

<b>1</b>	<b>Introduction .....</b>	<b>3</b>
<b>2</b>	<b>Fundamentals.....</b>	<b>4</b>
2.1	Block copolymers .....	4
2.2	Anionic polymerisation .....	5
2.3	Polymer analogue reactions .....	8
2.4	Phase behaviour .....	10
2.4.1	In bulk.....	10
2.4.2	In solution.....	12
2.4.3	In the presence of additional interactions.....	15
<b>3</b>	<b>Characterisation methods.....</b>	<b>19</b>
3.1	Size exclusion chromatography.....	19
3.2	Light scattering methods .....	21
3.2.1	Static light scattering .....	22
3.2.2	Dynamic light scattering.....	25
3.3	Analytical ultracentrifugation.....	26
3.4	Atomic force microscopy .....	29
<b>4</b>	<b>Results and discussion.....</b>	<b>31</b>
4.1	Radical addition of $\omega$ -functional mercaptanes .....	31
4.1.1	Modification of 1,2- and 1,4-polybutadiene.....	32
4.1.2	Modification of PB-PEO block copolymers.....	36
4.1.2.1	Introduction of ester functionalities.....	39
4.1.2.2	Introduction of ionic groups .....	42
4.1.2.3	Introduction of cysteine.....	45
4.1.2.4	Introduction of diol functionalities.....	48
4.1.2.5	Introduction of fluorinated side chains.....	50
4.1.3	Modification of PB-PS block copolymers.....	52

4.2	Self-organisation of modified block copolymers.....	55
4.2.1	Ionic block copolymers.....	56
4.2.1.1	PEO-polyanion block copolymers.....	57
4.2.1.2	PEO-polycation block copolymers.....	60
4.2.2	Diol-modified block copolymer.....	64
4.2.3	Fluoro-modified block copolymer.....	67
4.2.4	Influence of introduced groups on the self-organisation behaviour.....	71
4.3	Block copolymer complexes.....	72
4.3.1	Polyion complexes of ionic block copolymers with equal lengths of the oppositely charged blocks.....	73
4.3.2	Polyion complexes of ionic block copolymers with unequal lengths of the oppositely charged blocks.....	77
4.3.3	Hydrogen-bonded complexes in toluene.....	79
<b>5</b>	<b>Summary and outlook.....</b>	<b>82</b>
<b>6</b>	<b>Experimental part.....</b>	<b>85</b>
6.1	Solvents and Reagents.....	85
6.2	Synthetic procedures.....	85
6.2.1	Preparation of precursors by anionic polymerisation.....	85
6.2.1.1	Synthesis of 1,2-PB precursors.....	85
6.2.1.2	Synthesis of PB-PEO precursors.....	86
6.2.1.3	Synthesis of PB-PS precursor.....	87
6.2.2	Radical addition of $\omega$ -functional mercaptanes.....	88
6.2.2.1	Modification of PB homopolymers.....	88
6.2.2.2	Modification of PB-PEO block copolymers.....	90
6.2.2.3	Modification of PB-PS block copolymers.....	97
6.3	Experimental techniques.....	98
<b>7</b>	<b>Appendix.....</b>	<b>100</b>
<b>8</b>	<b>Abbreviations.....</b>	<b>105</b>
<b>9</b>	<b>Acknowledgements.....</b>	<b>107</b>
<b>10</b>	<b>Literature.....</b>	<b>109</b>

## 1 INTRODUCTION

Understanding the principles of self-organisation exhibited by block copolymers requires the combination of synthetic and physicochemical knowledge. The ability to synthesise block copolymers with desired architecture facilitates the ability to manipulate their aggregation behaviour, thus providing the key to nanotechnology.<sup>1,2</sup> Apart from relative block volumes, the size and morphology of the produced nanostructures is controlled by the effective incompatibility between the different blocks.<sup>3</sup> Since polymerisation techniques allowing for the synthesis of well-defined block copolymers are restricted to a limited number of monomers, the ability to tune the incompatibility is very limited. Nevertheless, *Polymer Analogue Reactions* can offer another possibility for the production of functional block copolymers by chemical modifications of well-defined polymer precursors. Therefore, by applying appropriate modification methods both volume fractions and incompatibility, can be adjusted. Moreover, copolymers with introduced functional units allow utilization of the concept of molecular recognition in the world of synthetic polymers.<sup>4</sup>

The present work describes a modular synthetic approach towards functional block copolymers. Radical addition of  $\omega$ -functional mercaptanes was employed for the introduction of diverse functional groups to polybutadiene-containing block copolymers. Various modifications of 1,2-polybutadiene-poly(ethylene oxide) block copolymer precursors are described in detail. Furthermore, extension of the concept to 1,2-polybutadiene-polystyrene block copolymers is demonstrated. Further investigations involved the self-organisation of the modified block copolymers. Formed aggregates in aqueous solutions of block copolymers with introduced carboxylic acid, amine and hydroxyl groups as well as fluorinated chains were characterised. Study of the aggregation behaviour allowed general conclusions to be drawn regarding the influence of the introduced groups on the self-organisation of the modified copolymers. Finally, possibilities for the formation of complexes, based on electrostatic or hydrogen-bonding interactions in mixtures of block copolymers bearing mutually interacting functional groups, were investigated.

## 2 FUNDAMENTALS

### 2.1 Block copolymers

Block copolymers consist of covalently connected sequences built of different monomeric species. In the most simple case, two homopolymeric blocks may be linked together forming a linear AB diblock copolymer. By adding a third block, it is possible to obtain a triblock copolymer, which, depending on the nature of the third sequence, can be of the ABA, BAB or ABC type. Extension of this concept leads to the formation of multiblock copolymers. Besides the linear type of arrangement exist other copolymer architectures, such as stars or brushes (Figure 2.1).



Figure 2.1. Various architectures of block copolymers: a) diblock copolymer, b) triblock copolymer, c) star, d) brush.

Different blocks, each block exhibiting many of the physical characteristics of the homopolymer, connected together yield a material with combined properties. Depending on their chemical composition and molecular structure, block copolymers reveal interesting physicochemical properties allowing them to find use in a multitude of applications.<sup>5</sup> They can be used as stabilizers, emulsifiers, dispersing agents, elastomeric materials and surfactants as well as in drug delivery, cosmetics and many other industrial applications.

There are many techniques for the synthesis of block copolymers; living, controlled anionic and radical polymerisation being the most commonly used. The older technique of anionic polymerisation is a well established method allowing preparation of block copolymers with desired block lengths and very low polydispersities.<sup>6</sup> Some of the copolymers prepared by anionic polymerisation have become commercially available products, e.g. Kraton (thermoplastic elastomers composed of polystyrene and polybutadiene) or Pluronics (triblock copolymers of poly(ethylene oxide) and poly(propylene oxide) used as surfactants).<sup>1</sup>



In recent years, a significant progress has occurred in the field of radical polymerisation.<sup>7</sup> Living/controlled techniques such as ATRP (*Atom Transfer Radical Polymerisation*) and RAFT (*Reversible Addition-Fragmentation Chain Transfer Polymerisation*) are based, in principle, on the dynamic equilibrium between a very small fraction of propagating free radicals and a majority of dormant species. This decreases the rate of termination and allows better control over the molecular weight distribution. The main advantage of controlled radical methods is their tolerance to a large variety of functional groups and low sensitivity to impurities. They allow for the preparation of copolymers from diverse monomers e.g. styrene, (meth)acrylates or dienes.

In some cases, block copolymers can be also synthesised by coupling reactions between different homopolymers containing functional groups<sup>8-10</sup> or sequential living cationic polymerisation. The latter is mostly used for polymerisation of isobutylene<sup>11,12</sup> or vinyl ethers.<sup>13,14</sup>

## 2.2 Anionic polymerisation

Anionic polymerisation proceeds in the presence of anionic active centres and includes the following kinetic steps: initiation, propagation, and termination. This type of polymerisation can be applied to a wide range of monomers, among them:

- vinyl monomers (styrene and dienes);
- polar vinyl monomers (acrylates and acrylonitriles);
- heterocyclic monomers (oxiranes, sulfides, siloxanes and lactones).

In the case of the first two groups, the negative active centre is localized on the carbon atom (carbanion) whereas in the polymerisation of heterocycles the negative charge is localized on the heteroatom (O, S). Formation of the anionic active centres is induced by the addition of initiators, usually alkyl or aryllithium reagents, alkali-metal suspensions, organic radical ions or Grignard reagents. In appropriate solvents, initiators undergo spontaneous dissociation into initiating anions, which subsequently react with monomer molecules and initiate the polymerisation. Propagation proceeds often in the simultaneous presence of a few forms of reaction intermediates (ion pairs), equal in the relation to their chemical constitution but

different according to the strength of ion-ion interactions.<sup>6,15</sup> The coexistence of various forms of active centres can be represented as follows (Figure 2.2):<sup>16</sup>

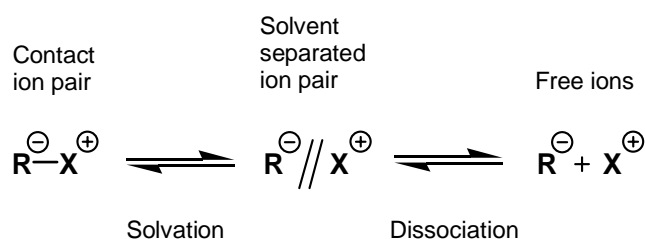


Figure 2.2. Winstein diagram illustrating the coexistence of various forms of active centres in anionic polymerisation.<sup>16</sup>

Each of these types of intermediates can participate as reactive propagating species in anionic polymerisation. Hence, polymerisation rates and stereospecificities depend strongly on the equilibrium between different ion pairs, which can be regulated by the polarity of the solvent, nature of the counter ion, temperature and presence of additives (solvating agents e.g. LiCl, crown ethers).<sup>6,15,17</sup>

Under appropriate conditions, anionic polymerisation can be performed in the “*living way*” and in the ideal case, exhibit neither chain transfer nor termination reactions. *Living anionic polymerisation* demands an inert atmosphere or high-vacuum technique without access of humidity, oxygen and other electrophilic impurities.<sup>6</sup> Another condition, which has to be fulfilled in order to perform the polymerisation in a controlled way, is rapid initiation, so that almost all chains can start their growth at the same time and grow at the same rate until the complete consumption of monomer. Under these conditions the degree of polymerisation  $DP$  of the synthesised polymer can be easily calculated from the initial molar ratios of monomer  $[M]_0$  and initiator  $[I]_0$ :

$$DP = \frac{[M]_0}{[I]_0} \quad (2.1)$$

For an ideal living process, nearly monodisperse polymers, characterized by a Poissonian distribution of molecular weights, can be synthesized. The polydispersity index  $PDI$  is determined as:

$$PDI = \frac{M_w}{M_n} = 1 + \frac{DP}{(DP+1)^2} \approx 1 + \frac{1}{DP}, \quad \text{for } DP \gg 1 \quad (2.2)$$

Since first described in 1956 by Szwarc,<sup>18,19</sup> living anionic polymerisation has become a significant method for the synthesis of homopolymers as well as tailored block copolymers. In the absence of a termination step, active centres remain active even after the exhaustion of monomer. This allows the so called step-wise synthesis of copolymers, just by simple addition of the second kind of monomer into the living system, which will then add to the existing chains and increase their degree of polymerisation.<sup>20,21</sup> However, the newly formed active centre has to be a weaker nucleophile (exhibit a relatively lower reactivity) than the already present carbanion. This is why the sequence of polymerised monomers plays an important role. The nucleophilicity of carbanions can be estimated on the basis of the  $pK_a$  values of their conjugated acids.<sup>22</sup> In a similar way, functionalised block copolymers bearing specific end groups may be obtained by terminating the “living” polymer with a suitable reagent.<sup>23-26</sup> For example, living polybutadiene chains terminated with ethylene oxide gain hydroxyl functionality<sup>27</sup> and can subsequently be used as macroinitiators for the synthesis of various polybutadiene-poly(ethylene oxide) copolymers.

The main limitations of anionic polymerisation are difficulties in polymerising polar monomers, bearing e.g. carboxyl, amino or hydroxyl groups, which may participate in termination or chain transfer reactions. In some cases, suitable protecting groups can be applied, but the obtained derivatives must be stable under the polymerisation conditions, i.e. they should not undergo side reactions with the initiator or the living chain end.<sup>28</sup>

## 2.3 Polymer analogue reactions

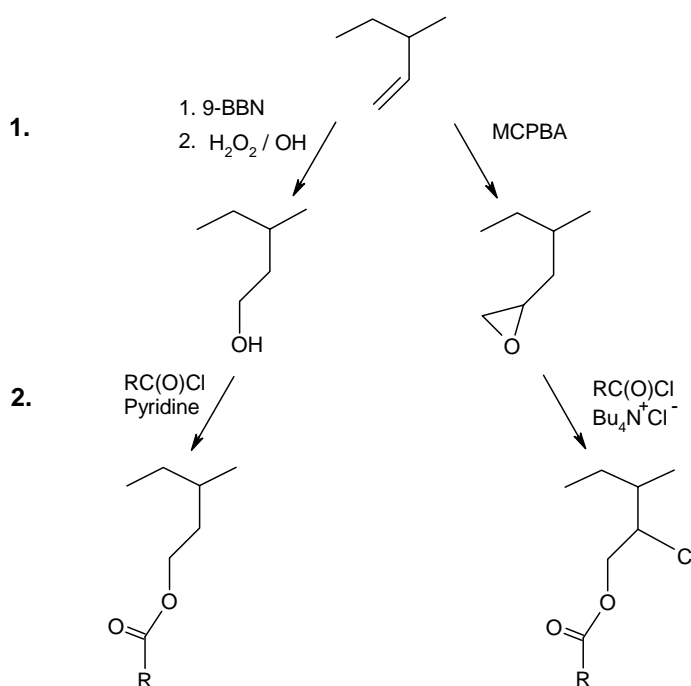
Synthesis of new block copolymer systems in which individual blocks bear diverse functional groups is a subject of continuous interest. However, the range of monomers, which can be used (by generally applied synthetic methods) for the preparation of well-defined block copolymers is limited. The chemical modification of precursor block copolymers, also known as *Polymer Analogue Reactions*, gives access to new types of functional copolymers, revealing novel distinctive properties. In the case of block copolymers, readily available precursors with predetermined molecular weight, narrow molecular weight distribution, desired block lengths and architecture are used for further chemical modifications.<sup>1</sup> Applied polymer analogue reactions should then lead to a change in the chemical composition of the modified block without an occurrence of undesired side reactions. The initial degree of polymerisation, polymer architecture and polydispersity ought to remain unchanged. Thus, applied methods must be mild enough to avoid cross-linking or degradation of the precursors but at the same time permit the quantitative transformation into the copolymer bearing the desired functional groups.

For example, poly(vinyl alcohol) belongs to the group of polymers, which cannot be synthesised directly. This is because the monomer (vinyl alcohol) as the unstable enolic form of acetic aldehyde is unable to undergo polymerisation. Copolymers containing poly(vinyl alcohol) block can be obtained e.g. from benzyl protected poly(vinyl ether).<sup>29,30</sup> Similarly, it is possible to prepare poly(methacrylic acid) by applying catalytic hydrogenolysis of poly(benzyl methacrylate). Other methods for the synthesis of poly(methacrylic acid) are hydrolysis of trimethylsilyl methacrylate at room temperature using aqueous methanol<sup>31</sup> and polymerisation of (meth)acrylic esters, e.g.: tert-butyl ester, and their subsequent hydrolysis.<sup>21,32,33</sup> Block copolymers with a (meth)acrylic acid sequence are often used as ionomers, that are copolymers with an electrolyte content of less than 15 mol%.<sup>34</sup> Other examples of chemical modification reactions resulting in block ionomers are quaternization of poly(vinylpyridine) with methyl iodide,<sup>35</sup> and sulfonation of polystyrene using either H<sub>2</sub>SO<sub>4</sub>/P<sub>2</sub>O<sub>5</sub> (for complete sulfonation)<sup>36</sup> or acyl sulfates (for partial sulfonation).<sup>37</sup>

An important class of polymer analogue reactions is the hydrogenation of unsaturated polymers. Butadiene- or isoprene-containing polymers can be hydrogenated using p-toluenesulfonyl hydrazine,<sup>38,39</sup> heterogeneous Pd/CaCO<sub>3</sub> catalyst as reported by Rosedale

and Bates<sup>40</sup>, or a homogenous rhodium catalytical system based on Wilkinson's catalyst as described by Mohammadi and Rempel.<sup>41</sup> Commercially available thermoplastic elastomers (Kraton) have also been prepared by the hydrogenation method.<sup>1</sup>

In some cases, polymer analogue reactions consist of two steps: in the first step, the formation of a reactive intermediate occurs, followed by the second step involving the reaction with an appropriate functional component. Reactive intermediates can be produced by means of epoxidation<sup>42</sup> as well as hydroxylation via hydroboration with 9-borabicyclo[3,3,1]nonane (9-BBN) and subsequent oxidation with H<sub>2</sub>O<sub>2</sub>/NaOH.<sup>43</sup> The following reaction of the reactive intermediate with e.g. functional acid chlorides, leads to the preparation of diverse functionalised copolymers.<sup>44-46</sup> Among these are copolymers with perfluorinated side chains.<sup>47-49</sup> The described synthetic route is presented in Scheme 2.1.. Schlaad *et al.* utilized this approach for the preparation of diblock copolymers bearing  $\beta$ -dicarbonyl (acetoacetoxy) residues revealing chelating properties and interesting aggregation behaviour.<sup>50</sup>



Scheme 2.1. Two-step modification approach : 1. Hydroboration with 9-Bora-bicyclo[3,3,1]nonan (9-BBN) or epoxidation with m-Chlorbenzoic acid (MCPBA); 2. Esterification with acid chloride.<sup>49</sup>

## 2.4 Phase behaviour

### 2.4.1 In bulk

One of the well-known features of polymers is their immiscibility, which occurs as a result of entropic reasons. Practically this means that the mixing of two different polymers, with dissimilar physicochemical characteristics, results in macroscopic phase separation. Block copolymers of an AB type, in which two chemically different blocks are linked together via covalent bonding, also exhibit phase separation, but on the smaller, microscopic scale.<sup>51</sup> This microscopic separation is possible through the simultaneous existence of two opposite forces in the system: long-range repulsive and short-range attractive forces.<sup>52</sup> Incompatibility of the two blocks causes long-range repulsive interactions whereas the covalent bond, which links the blocks together, is responsible for the short-range attractive force (Figure 2.3.a).

Microphase-separated copolymers can form various periodically ordered structures of the lengthscale between 1-100 nm.<sup>53</sup> The type of morphology produced depends on the first approximation of the copolymer composition, represented as the volume ratio ( $\phi = V_A/V_B$ ) of the individual blocks, determining the curvature radius  $R$  of the interface as shown in Figure 2.3.b.<sup>52</sup>

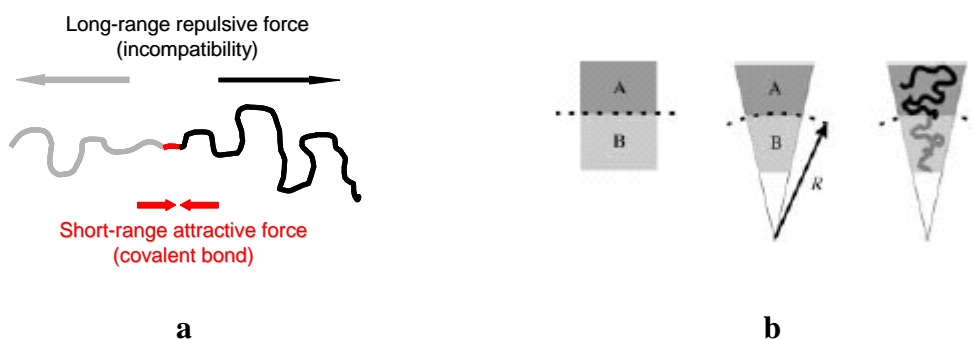


Figure 2.3. a) Schematic representation of two simultaneously present interactions leading to the self-organisation of block copolymers. b) Local geometry and the curvature of domains and interfaces;  $A$ ,  $B$  – domains;  $R$  – curvature radius of the interface (for a planar interface  $R = \infty$ ).<sup>52</sup>

The most commonly observed bulk morphologies of microphase-separated block copolymers are ordered continuous phases such as bcc-packed spheres (*BCC*), hexagonally ordered cylinders (*HEX*), lamellae (*LAM*), and bicontinuous *gyroid* structures (Figure 2.4).

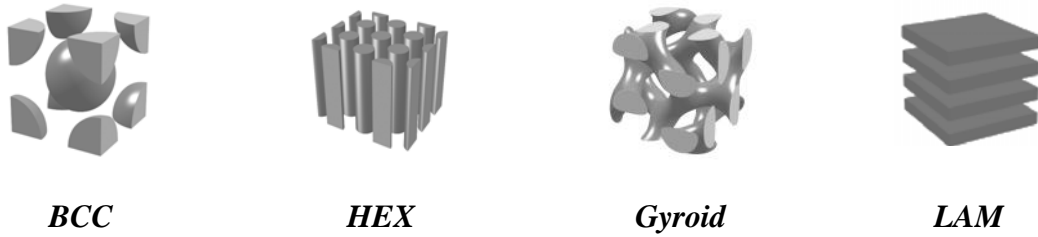


Figure 2.4. Commonly observed bulk morphologies of microphase-separated block copolymers.<sup>1</sup>

Phase behaviour of an AB diblock copolymer in bulk can be described by following parameters:<sup>51</sup>

- The total degree of polymerisation,  $N$ , resulting from the sum of the degrees of polymerisation of the individual blocks;  $N = N_A + N_B$ ;
- The Flory-Huggins interaction parameter,  $\chi$ , representing the strength of repulsive interactions between both blocks;
- The copolymer composition,  $f$ , describing the geometry factor;  $f_A = N_A/N$ .

According to Leibler, the microphase separation of block copolymers can be illustrated in a phase diagram, parameterised in terms of  $\chi N$  versus the block length ratio,  $f$ .<sup>54</sup> Matsen and Bates derived an exemplary phase diagram (Figure 2.5) from theoretical calculations outlining the types of morphologies available for the phase-separated AB block copolymer.<sup>55</sup>

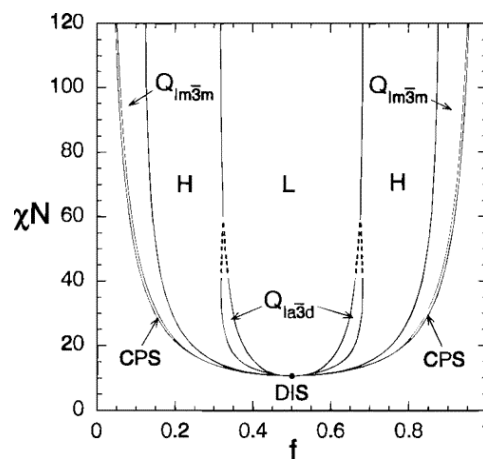


Figure 2.5. Theoretical phase diagram for block copolymers: L – Lamellae, H – hexagonal cylinders,  $Q_{la3d}$  – bicontinuous  $la3d$  cubic,  $Q_{lm3m}$  – BCC packed spheres, CPS – close packed spheres, DIS – disordered phase.<sup>55</sup>

The tendency for microphase separation is dependent on the term  $\chi N$ , which includes both enthalpic and entropic contributions. It is known that the Flory-Huggins parameter,  $\chi$ , is

inversely proportional to the temperature, i.e. the lower the temperature the higher the  $\chi$  value. At higher temperatures the chains are homogeneously mixed, on decreasing the temperature till the point where  $\chi N$  exceeds a critical value  $(\chi N)_{ODT}$  (where *ODT* means order-disorder transition), microphase separation takes place leading to the formation of microdomains of A and B blocks.<sup>56,57</sup> There are three regimes, categorized by the magnitude of the  $\chi N$  value:<sup>53</sup>

- $\chi N \sim 10$  – *Weak Segregation Limit (WSL)*, where the polymer blocks are highly miscible;
- $\chi N \sim 10-100$  – *Strong Segregation Limit (SSL)*, where the regime of stable morphologies occurs;
- $\chi N \gg 100$  – *Super Strong Segregation Limit (SSSL)*, postulated by Khokhlov<sup>58</sup> for systems in which the phase interface consists only of covalent bonds connecting the A and B blocks (the domains contain essentially pure components).

#### 2.4.2 In solution

Block copolymers undergo specific separation not only in bulk but also in solution. By bringing an AB block copolymer into the solvent, which acts as a good solvent for block B but not for block A, one can induce the spontaneous self-organisation process, called micellisation.<sup>59</sup> Produced aggregates, which in the easiest case, are spherical micelles, consist of a core, containing the insoluble block A surrounded by a corona of the soluble block B. As is the case for low molecular surfactants, in dilute solutions of block copolymers, spherical or cylindrical micelles<sup>60,61</sup> as well as more complex vesicular aggregates<sup>62,63</sup> can be formed (Figure 2.6). However, the dynamics of the aggregate formation and equilibration is for block copolymers in solution much slower, comparing to low molecular weight surfactants, due to much lower diffusion coefficients.



Figure 2.6. Possible morphologies of block copolymer aggregates occurring in dilute solutions.



The observed morphology depends strongly on the shape of the individual molecules constituting the aggregate and can be predicted from the so-called critical packing parameter,  $P$ , described in Israelachvili's model for surfactant micelles, as follows:<sup>64</sup>





$$P = \frac{v}{a \cdot l} \quad (2.3)$$

where  $v$  is the molar volume of the surfactant molecule,  $a$  is the area per hydrophilic head group and  $l$  is the contour length of the hydrophobic alkyl chain. The relation between the packing parameter and the morphology of the aggregate is presented in Table 2.1. An important parameter, which is related to the size of the micelle is the aggregation number,  $Z$ . This is the number of copolymer chains incorporated into one micelle. Förster *et al.* demonstrated that for strongly segregating systems, a general correlation between  $Z$  and the degree of polymerisation of insoluble  $N_A$  and soluble  $N_B$  block is described as:<sup>65</sup>

$$Z = Z_0 N_A^2 N_B^{-0.8} \quad (2.4)$$

$Z_0$  is related to the Flory-Huggins parameter,  $\chi$ , (which considers in solution both polymer/polymer and polymer/solvent interactions) as well as the packing parameter,  $P$ , and is known for many block copolymer and surfactant systems. Hence, the aggregation number can be tuned by the variation in the lengths of the blocks.<sup>1</sup>

Table 2.1. Morphology of aggregates in dependence on the packing parameter,  $P$ .

Packing parameter $P$	Molecule Geometry	Morphology
$< 1/3$		Spherical micelles
$1/3 - 1/2$		Cylindrical micelles
$1/2 - 1$		Vesicles, flexible bilayers
1		Lamellae, planar bilayers

By considering the relative block lengths of the individual segments  $N_A$  and  $N_B$ , two kinds of micellar structures can be distinguished: in the case where  $N_A \ll N_B$  a “*hairy micelle*” is formed (the core is much smaller than the corona) and, conversely, when  $N_A \gg N_B$ , a “*crew cut*”

*micelle*” is formed (the core is much larger than the corona). The third group of micelles represents the so-called “*amphiphilic micelles*”, characterised by a large interaction parameter,  $\chi$ .<sup>61</sup> Basic scaling relations between the micelle size (radius,  $R$ ), the aggregation number and the degree of polymerisation are summarized in the Table 2.2.

Table 2.2. Basic scaling relations between micelle size  $R$ , aggregation number  $Z$  and degree of polymerisation,  $N$ .

Micelle	Radius $R$	Aggregation number $Z$
hairy	$R \sim N_A^{3/5}$	$Z \sim N_A^{4/5}$
crew cut	$R \sim N_A^{2/3}$	$Z \sim N_A$
amphiphilic	$R \sim N_A$	$Z \sim N_A^2$

The formation of vesicular aggregates is more complex and proceeds in two steps.<sup>66</sup> First the formation of a bilayer occurs, then the bilayer closes to form a vesicle. A schematic illustration of this process is presented in Figure 2.7. Control of the architecture of block copolymer vesicles in solution has been extensively studied by the group of Eisenberg.<sup>67,68</sup>

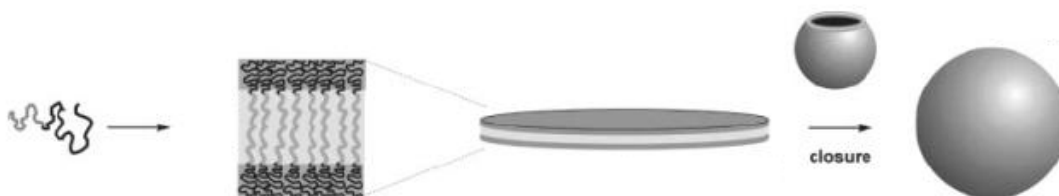


Figure 2.7. The mechanism of a vesicle formation.<sup>66</sup>

Besides the above-mentioned parameters, control over the size and morphology of block copolymer aggregates can be achieved by the manipulation of solution conditions. Thus, it is possible to prepare different aggregate architectures from the same copolymer by varying, among the others, the nature and composition of the applied solvent, the polymer concentration, the content of water in the solvent mixture and the presence of additives.<sup>69,70</sup>

### 2.4.3 In the presence of additional interactions

Block copolymers of the AB type reveal interesting phase behaviour; however, all possible morphologies resulting from the phase separation of such copolymers have already been predicted. A more complex behaviour can be observed for copolymers having an increased number of incompatible blocks or exhibiting non-linear molecular architectures.<sup>3</sup> ABC triblock copolymers organize in diverse, previously unknown three-dimensional structures<sup>71</sup> as described by Stadler *et al.* the *knitting pattern* morphology represented in Figure 2.8.<sup>72</sup> Another interesting example is shown by Li *et al.*, who used a microarm triblock copolymer, consisting of a water soluble poly(ethylene oxide) block and two hydrophobic but immiscible segments (hydrocarbon and perfluorinated polyether), for the formation of multicompartiment micelles (Figure 2.8).<sup>73</sup>

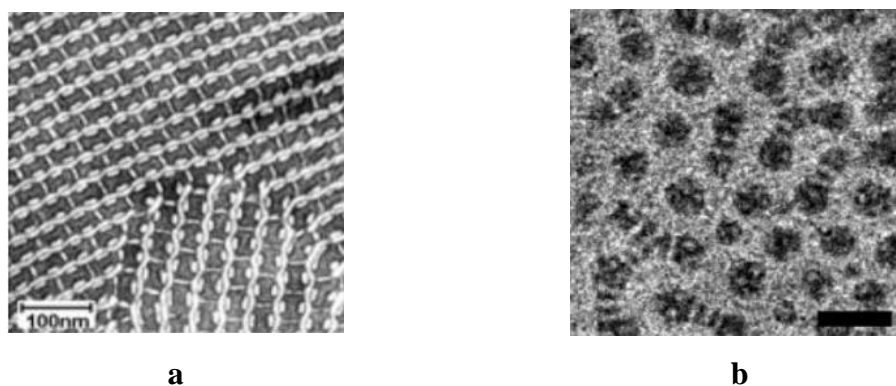


Figure 2.8. Self-assembly of ABC triblock copolymers: a) TEM micrograph of the *knitting pattern*;<sup>72</sup> b) Cryo-TEM image of multicompartiment micelles, the scale bar indicates 50 nm.<sup>73</sup>

In order to achieve greater structural complexity and functionality one can combine self-organisation with molecular recognition. According to the concept of J.M. Lehn, the diversity and complexity of superstructures is related to the number of simultaneously present noncovalent interactions;<sup>74</sup> molecules which exhibit complementary interactions are able to recognize each other and form a supramolecule.<sup>75</sup> Hence by the introduction of additional energy contributions, originating from noncovalent interactions, the preparation of complex macromolecular assemblies may be possible. This approach has attracted increasing attention in the past few years; energy contributions originating from dipole-dipole, hydrogen bonding, van der Waals and electrostatic interactions are being applied to the self-organisation of polymers.<sup>4,76,77</sup> Many experimental studies deal with the preparation of complex mesostructures by making use of rod-coil block copolymers.<sup>78</sup> Dipole-dipole interactions between the rod-like segments have a decisive influence on the observed morphology.

Unusual phases such as the *zigzag lamellar* phase prepared from polystyrene-poly(hexyl isocyanate) have been reported.<sup>79,80</sup> Another example is the *undulated lamellar* morphology described by Schlaad et. al., who examined the solid-state structures of polystyrene-poly(Z-L-lysine) block copolymers with respect to the polymer's architecture and the secondary structure of the polypeptide.<sup>81</sup> A rich polymorphism of complex mesostructures such as helices and filaments can be obtained by introduction of additional specific interactions in a rod-coil system, as reported for charged polystyrene-poly(isocyanodipeptide)s (Figure 2.9).<sup>82,83</sup>

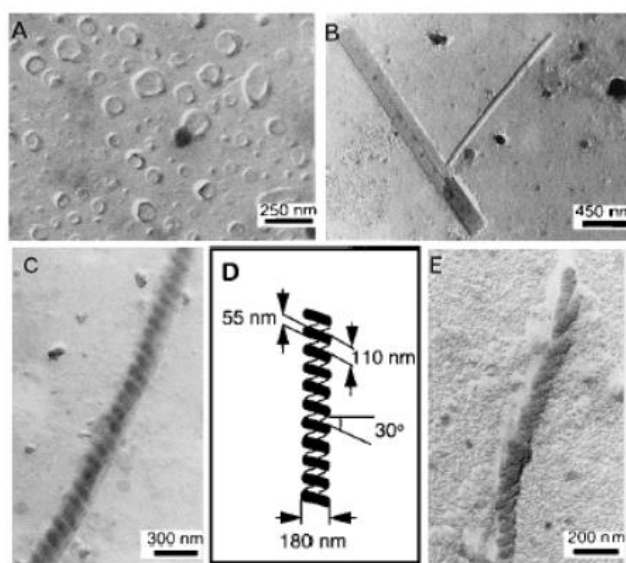


Figure 2.9. TEM micrographs of the morphologies observed for charged polystyrene-poly(isocyanodipeptide): (A) vesicles, (B) bilayer filaments, (C) left-handed superhelix, (D) schematic representation of the helix and (E) right-handed helical aggregate.<sup>82</sup>

Interesting self-assembly behaviour has been also revealed by systems containing polyelectrolytes. Mutual electrostatic interactions occurring in the mixture of oppositely charged chains were found to act as a driving force for the formation of polyion complex *PIC* micelles or interpolyelectrolyte complexes *IPEC* of oppositely charged block ionomers. This strategy has been adopted by several groups for the production of various micellar<sup>84</sup> or vesicular<sup>85</sup> aggregates as well as solid state structures.<sup>86</sup> Kataoka *et al.* have prepared monodisperse *PIC* micelles from a mixture of oppositely charged poly(ethylene glycol)-polylysine and poly(ethylene glycol)-poly(aspartic acid) in an aqueous medium<sup>87</sup> and have studied the chain length recognition in the process of *PIC* micelles formation<sup>88</sup> as well as the effect of the charged segment length on the micelle system's physicochemical properties.<sup>89</sup> Potential application of polyelectrolyte micelles as carriers in the field of drug delivery has

also been investigated.<sup>90,91</sup> Interesting examples of unusual *IPEC* morphologies have been presented by Gohy *et al.* who prepared *bucklelike* aggregates by mixing poly(2-vinylpyridinium)-poly(ethylene oxide) with poly(4-styrenesulfonate) (Figure 2.10.a).<sup>92</sup> The same research group also prepared micelles with segregated coronal chains consisting of poly(ethylene oxide) and polystyrene (Figure 2.10.b).<sup>93</sup>

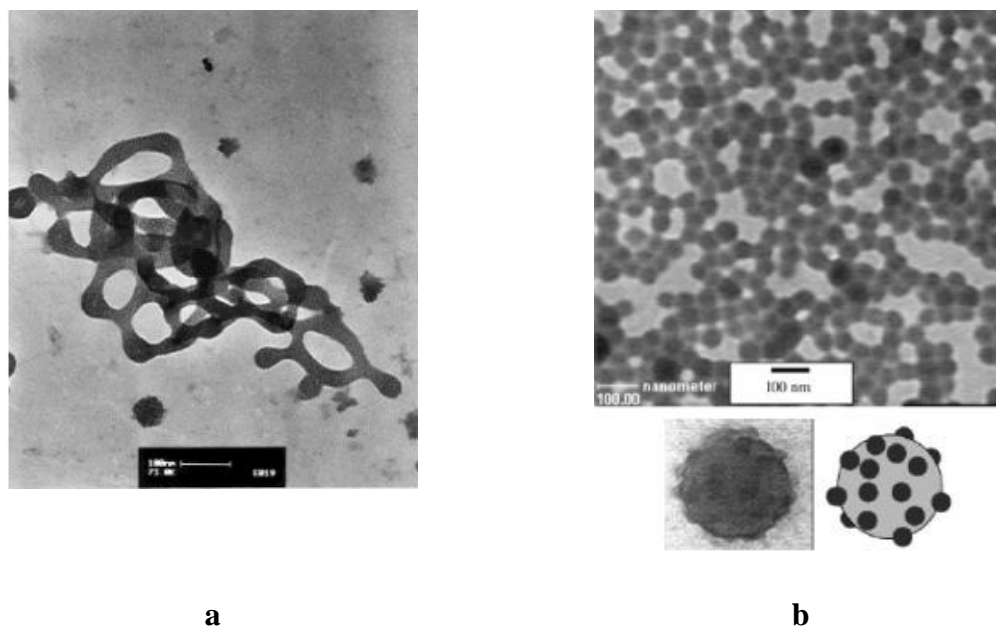


Figure 2.10. TEM micrographs of unusual IPCE morphologies: a) *bucklelike* aggregates,<sup>92</sup> b) micelle with segregated coronal chains; scale bars indicate 100 nm.<sup>93</sup>

The concept of molecular recognition based on multiple hydrogen bonding interaction has been extensively applied to the self-organisation of polymers by the group of Rotello.<sup>94</sup> This group has also studied the influence of various types of recognition units on the phase behaviour and physical properties of diblock copolymers.<sup>95</sup> Interesting triblock copolymers containing self-complementary sequences interacting *via* three-point hydrogen bonding were synthesised by Bazzi *et al.*; where they show that variation of the triblock copolymer sequence results in a dramatic change of the self-organisation properties.<sup>96</sup>

The above examples illustrate that by applying the concept of molecular recognition to the self-organisation of polymers, one can create unusual, highly ordered supramolecular assemblies. Specific interactions between molecules, when appropriately used, may present the universal tool allowing for the preparation of complex polymeric morphologies, which ideally reveal superior properties. These self-organized assemblies, also termed “*host-guest*” systems are widely present in biological systems. Well-defined and appropriately

functionalised materials are necessary for the utilization of the concept of molecular recognition in the world of synthetic polymers. Unfortunately, the synthesis of suitable polymers is often the limiting step in the whole concept. Thus, the development of convenient methods allowing for the preparation of macromolecules bearing mutually interacting functional groups is of great importance. For this purpose, the modular synthetic approach towards functional block copolymers has been evolved. Radical addition of  $\omega$ -functional mercaptanes was employed for the introduction of various functional groups into polybutadiene containing block copolymers. Furthermore, the phase behaviour of the modified block copolymers has been investigated.

## 3 CHARACTERISATION METHODS

### 3.1 Size exclusion chromatography

Size exclusion chromatography (SEC), also known as gel permeation chromatography (GPC), represents a chromatographic method widely used in the analysis of polymer molecular weights and molecular weight distributions. Columns utilized in SEC are packed with porous material (silica or cross-linked polymer gel), and solvent (mobile phase, eluent) is forced through the column at a flow of  $\sim 1$  ml/min. A sample (dissolved in the same solvent) is introduced into the column and passes through the column with the eluent stream. In order to realize pure SEC mode it is necessary to exclude any interaction between the solute and the packing material. It is also important, that the selected eluent is well suited to the analysed sample. Separation of polymer molecules in the column is based on their hydrodynamic volume. Small molecules are able to penetrate into the pores of the packing material, thus their average migration rate is slow. When a molecule experiences steric hindrance in permeation inside a pore, it continues moving with the eluent flow. Hence, larger molecules reach the end of the column faster than the molecules having smaller size. The concentration of eluted molecules is monitored by a suitable detector and, as a function of time or elution volume ( $V_e$ ), gives a so-called elution curve. Commonly, refractive index (RI) and/or ultraviolet-visible (UV-Vis) detectors are utilized. Molecules, the size of which is larger than the pore size of packing material elute at a so-called exclusion limit and cannot be separated. The elution volume corresponding the exclusion limit is called void volume ( $V_o$ ). In order to separate molecules, their elution volumes have to lay between  $V_o$  and  $V_o + V_i$ , where  $V_i$  represents the total volume of pores (inner volume). The elution volume,  $V_e$ , can be expressed as

$$V_e = V_o + k_{GPC}V_i \quad (3.1)$$

where  $k_{GPC}$  is the distribution coefficient. The latter describes the ratio of the mean concentration of molecules inside and outside the pores ( $0 \leq k_{GPC} \leq 1$ ).

SEC is a relative method, therefore molecular weights of analysed polymers can be determined only after calibrating the system in terms of  $V_e$ . Calibration is performed using polymer standards with known molecular weights and narrow molecular weight distributions.

Plot of the molecular weight of the standards *versus* their elution volume gives the calibration curve ( $\log M = f(V_e)$ ). As already mentioned the concentration of eluted molecules,  $c_i$ , in any chromatographic fraction,  $i$ , is measured. Using the calibration curve it is possible to determine the molecular weight corresponding to each chromatographic fraction. Thus, for the analysed sample, the number-average ( $M_n$ ) and weight-average ( $M_w$ ) molecular weights (equations (3.2) and (3.3), respectively) as well as polydispersity index ( $PDI = M_w/M_n$ ) can be calculated.

$$M_n = \frac{\sum_i c_i}{\sum_i c_i / M_i} \quad (3.2)$$

$$M_w = \frac{\sum_i c_i M_i}{\sum_i c_i} \quad (3.3)$$

The calibration curve can be used for determining the molecular weight of a certain polymer only when used standards were of the same chemical nature and applied eluent was of the same type. In the case of polymers, for which a suitable calibration curve is not available, it is possible to apply a so-called “universal calibration”.<sup>97</sup> According to Fox and Flory, the hydrodynamic volume of molecule,  $V_h$ , is proportional to the intrinsic viscosity,  $[\eta]$ , and the molecular weight

$$V_h \propto [\eta]M \quad (3.4)$$

with

$$[\eta] = \lim_{c \rightarrow 0} \frac{\eta_{sp}}{c} \quad (3.5)$$

where  $\eta_{sp}$  is the specific viscosity of the polymer. For two different polymers exhibiting the same  $V_h$  in solution it is

$$[\eta_1]M_1 = [\eta_2]M_2 \quad (3.6)$$

The intrinsic viscosity is related to the polymer molecular weight by Mark-Houwink equation



$$[\eta] = KM^\alpha \quad (3.7)$$

where  $K$  and  $\alpha$  are the specific constants known for many polymer-solvent combinations. Thus it is possible to calculate the calibration curve for the second polymer

$$\log M_2 = \frac{1}{1+\alpha_2} \log \frac{K_1}{K_2} + \frac{1+\alpha_1}{1+\alpha_2} \log M_1 \quad (3.8)$$

Values of  $M_n$ ,  $M_w$  and  $PDI$  obtained from SEC measurements of copolymers are only apparent, since the detected concentrations are not true for copolymers and a suitable calibration is usually not available. Absolute values of  $M_n$  for diblock copolymer systems described in this thesis were calculated in the classical way combining SEC with  $^1\text{H}$  NMR. The first block of a copolymer was characterised using SEC and values of  $M_n$ ,  $M_w$  and  $PDI$  were determined using suitable calibration curve (1,2-PB and universally calibrated curve from PS standards). Knowing the molecular weight of the first block and calculating the copolymer composition, from the peak integrals assigned to the different comonomers in the  $^1\text{H}$  NMR spectrum, it was possible to calculate the  $DP$  of the second block.

### 3.2 Light scattering methods

When a beam of monochromatic light passes a system, in which no absorption of the light occurs, the transmission is still not complete. Molecules present in the system interact with the incident electromagnetic wave and their electrons start to behave like an oscillating dipole. These oscillating dipoles act as electromagnetic radiation sources, and therefore the molecules emit light, called scattered light. This light is scattered in all directions and has mostly the same wavelength as the incident beam. In the year 1869, John Tyndall systematically investigated the phenomenon of light scattering and discovered that the intensity of the scattered light depends on the wavelength of the incident light as well as on the angle of detection.<sup>98</sup> Two years later, Lord Rayleigh developed the first theoretical description of light scattering basing on the theory of electromagnetic waves.<sup>99</sup>

### 3.2.1 Static light scattering

Static light scattering (SLS) is used to provide the information on the size, shape and mass of the analysed particles as well as on the interactions between the particles in solution. In this method the intensity of elastically scattered light is measured as a function of scattering angle,  $\theta$ , (Figure 3.1).

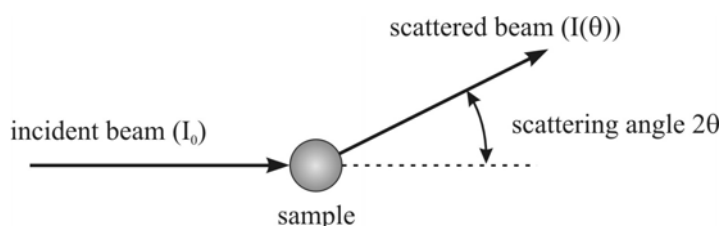


Figure 3.1. Schematic illustration of the scattering process.

The relationship between the intensity of the scattered light at the angle  $\theta$ ,  $I(\theta)$ , and the initial intensity of the vertically polarised light,  $I_0$ , is presented in equation (3.9)

$$\frac{I(\theta)}{I_0} = \frac{16 \cdot \pi^2 \cdot \alpha^2}{\lambda_0^4 \cdot r^2} \quad (3.9)$$

where  $\alpha$  is the polarisability of the molecules,  $\lambda_0$  is the wavelength of the used light in vacuum and  $r$  is the distance between sample and detector. It can be seen that the scattered intensity depends strongly on the wavelength of the light and on the polarisability of the scattering centres (molecules). For a liquid two-component system, Peter Debye<sup>100,101</sup> has shown the following dependence

$$\langle \Delta \alpha^2 \rangle \propto n_0^2 R T c \left( \frac{\partial n}{\partial c} \right)^2 \left( \frac{\partial \Pi}{\partial c} \right)_T \quad (3.10)$$

where  $n_0$  is the refractive index of the solvent,  $R$  is the gas constant,  $T$  is the absolute temperature,  $c$  is the concentration,  $n$  is the refractive index of the sample and  $\Pi$  is the osmotic pressure. Debye found out that the additional scattering of light by a solution results from local fluctuations in the concentration of the solute. He considered the local fluctuations, present due to random thermal motion, to be opposed by the osmotic pressure of the solution. Thus, the equation (3.11) presents the so-called Rayleigh ratio  $R(\theta)$  of the scattering due to solute as

$$R(\theta) = \frac{I(\theta)r^2}{I_0} = \frac{4\pi^2}{\lambda_0^4 N_A} \cdot n_0^2 RTc \left( \frac{\partial n}{\partial c} \right)^2 \left( \frac{\partial \Pi}{\partial c} \right)_T \quad (3.11)$$

where  $N_A$  is the Avogadro's number. In real, such as colloidal or polymer, solutions it is necessary to subtract the scattering of the solvent from the whole scattering intensity. The equation (3.11) can be expressed in the reciprocal form<sup>101</sup>

$$\frac{Kc}{R(\theta)} = \frac{1}{RT} \cdot \left( \frac{\partial \Pi}{\partial c} \right)_T \quad (3.12)$$

were

$$K = \frac{4\pi^2}{\lambda_0^4 N_A} \cdot n_0^2 \left( \frac{\partial n}{\partial c} \right)^2 \quad (3.13)$$

The osmotic module  $(\partial \Pi / \partial c)_T$  can be expanded into a power series as follows

$$\left( \frac{\partial \Pi}{\partial c} \right)_T = RT \left( \frac{1}{M_w} + 2A_2c + 3A_3c^2 + \dots \right) \quad (3.14)$$

where  $M_w$  is the weight-average molecular weight of the solute and  $A_2, A_3, \dots$  are virial coefficients describing interactions between the particles in solution.

By introducing equation (3.14) into equation (3.12) and neglecting the higher order terms of  $c$  one obtains

$$\frac{Kc}{R(\theta)} = \frac{1}{M_w} + 2A_2c \quad (3.15)$$

The above equation is true for small particles, which diameter is smaller than  $\lambda/20$ . In the case of bigger particles the scattering is shape dependent. Therefore it is necessary to introduce the angle dependent form factor,  $P(q)$ ;<sup>102</sup>  $q$  represents the scattering vector defined as

$$q = \frac{4\pi n_0}{\lambda_0} \cdot \sin(\theta) \quad (3.16)$$

$P(q)$  can be approximated by

$$P(q) = 1 - \frac{1}{3} \langle R_g^2 \rangle q^2 + \dots \quad (3.17)$$

where  $R_g$  is the radius of gyration. The above is true for the particles, for which  $qR_g < 1$  (the form factor is identical regardless of the particle shape). Introducing  $P(q)$  into equation (3.15) yields

$$\frac{Kc}{R(\theta)} = \frac{1}{M_w} + \frac{1}{3} \frac{\langle R_g^2 \rangle}{M_w} q^2 + 2A_2c \quad (3.18)$$

For data evaluation a so-called Zimm plot<sup>103</sup> is used, where  $Kc/R(\theta)$  is plotted versus  $q^2 + kc$  (where  $k$  is an arbitrary constant). For a series of concentrations and angles, the extrapolation  $q \rightarrow 0$  and  $c \rightarrow 0$  provides the value of  $M_w$ , whereas  $R_g$  and  $A_2$  are obtained from the slopes of the  $q^2$  and  $c$  dependence, respectively.

In the case of particles, for which  $qR_g > 1$ , the shape of the particles causes that the scattered light is significantly dependent on the detection angle. Thus, the shape of the particles can be distinguished from the shape of the curve in a Zimm or Kratky plot<sup>104</sup> (Figure 3.2). The latter, is parameterised in terms of  $q^2 R(\theta)$  versus  $q$ .

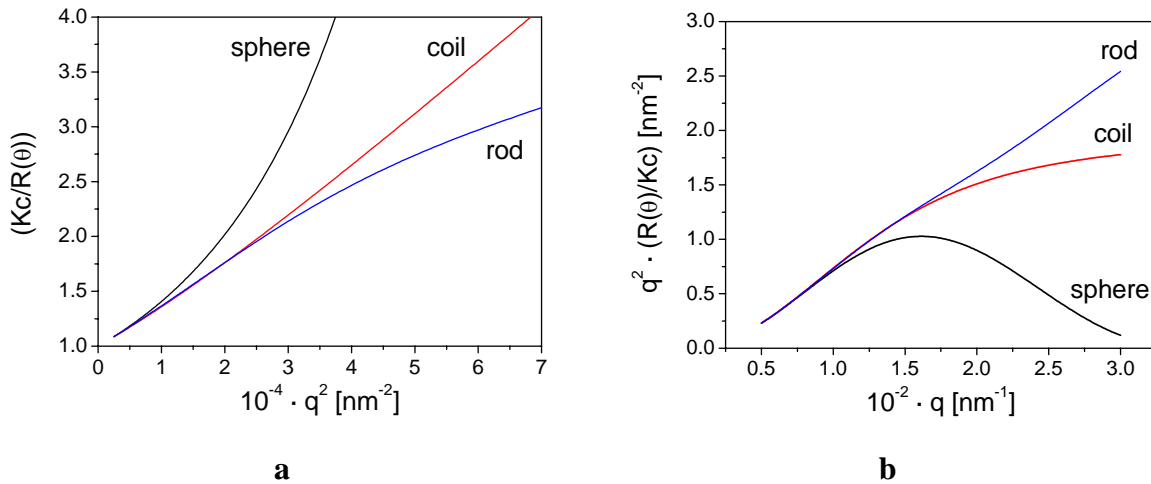


Figure 3.2. a) Zimm plot and b) Kratky plot of a sphere, a coil and a rod having  $R_g = 100$  nm.

### 3.2.2 Dynamic light scattering

Dynamic light scattering (DLS) is used to determine the size and polydispersity of particles present in an analysed system. This method involves measuring the temporal fluctuations of the intensity of scattered light. The numbers of photons entering a detector are recorded and analysed by a digital correlator. The separation in time between photon countings is the correlation time,  $\tau$ . The intensity-time correlation function,  $g_2(t)$  can be expressed as<sup>105</sup>

$$g_2(t) = \frac{\langle I(t)I(t+\tau) \rangle}{\langle I(t) \rangle^2} \quad (3.19)$$

Using the Siegert relation,<sup>106</sup> the above function can be transformed into the electric field correlation function,  $g_1(t)$

$$g_1(t) = \sqrt{\frac{g_2(t) - b}{b}} \quad (3.20)$$

$$g_1(t) = \frac{\langle E(t)E(t+\tau) \rangle}{\langle E(t) \rangle^2} \quad (3.21)$$

where  $b$  is the experimentally determined baseline,  $E$  is the electric field strength.

In the case of highly diluted systems containing monodisperse and relatively small particles ( $qR_g < 1$ ),  $g_1(t)$  can be expressed as a single exponential function

$$g_1(t) = B \cdot \exp(-q^2 Dt) \quad (3.22)$$

where  $B$  is the signal to noise ratio and  $D$  is the translational diffusion coefficient.

For polydisperse systems containing large particles ( $qR_g > 1$ ),  $g_1(t)$  has a multi-exponential decay. Thus, this function has to be considered as a superposition of several exponential functions with different diffusion coefficients

$$g_1(t) = \langle e^{-\Gamma t} \rangle = \int_0^{\infty} e^{-\Gamma t} G(-\Gamma) d\Gamma \quad (3.23)$$

where

$$\Gamma = D_{app}(q)q^2 \quad (3.24)$$

In the limit of small  $q$  one obtains

$$\lim_{q \rightarrow 0} D_{app}(q) = D_z \quad (3.25)$$

where  $D_z$  is the z-averaged diffusion coefficient.

For the evaluation of the data presented in this thesis, the analysis of the distribution function  $G(\Gamma)$  by inverse Laplace-Transformation was carried out using the program *Contin*.<sup>107</sup>

Assuming that the analysed particles are hard spheres, it is possible to calculate their hydrodynamic radius,  $R_h$ , applying the Stokes-Einstein equation

$$R_h = \frac{k_B T}{6\pi\eta_0 D} \quad (3.26)$$

where  $k_B$  is the Boltzmann constant,  $T$  is the absolute temperature and  $\eta_0$  is the viscosity of the solvent.

### 3.3 Analytical ultracentrifugation

Analytical ultracentrifugation (AUC) represents a valuable technique for determination of the molecular weight as well as the hydrodynamic and thermodynamic properties of macromolecules and colloids. It was developed in the 1920's by Thé Svedberg,<sup>108</sup> who introduced two extensively used methods: sedimentation velocity and sedimentation equilibrium. From the sedimentation velocity experiments, which were applied for this thesis, sedimentation coefficient distributions can be obtained. Sedimentation coefficients can be used for the calculation of molecular weight and hydrodynamic properties of the sample. The method of sedimentation equilibrium is used for the absolute determination of the weight-average molecular weight and the polydispersity of the sample. In both AUC methods, the data obtained represent a record of the concentration distribution in the sample cell at a given time. This can be achieved using for example absorption or interference measurements

because both the absorbance and refractive index of the sample are proportional to the sample concentration.<sup>109</sup>

A solute particle suspended in the solvent, which is subjected to a centrifugal field experiences three different forces, as presented in Figure 3.3. The downward force is the centrifugal force,  $F_c$ , which is proportional to the mass of the particle,  $m$ , and to the square of the angular velocity,  $\omega$ . The two upwards forces are the buoyancy force,  $F_b$ , and the frictional force,  $F_f$ . The buoyancy force is proportional to the weight of the fluid displaced by the particle,  $\rho_0 V$ , whereas the frictional force is proportional to the velocity of the particle,  $u$ .

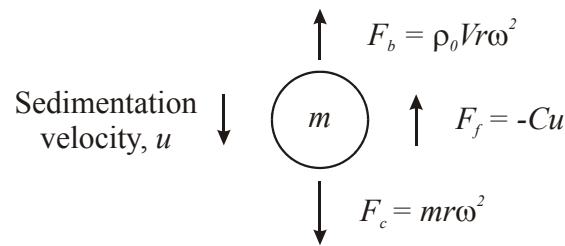


Figure 3.3. Forces acting on the particle subjected to a centrifugal force.

Hence, the effective force exerted on the particle can be written as

$$F_{eff} = m \frac{du}{dt} = F_c + F_b + F_f = mr\omega^2 - \rho_0 Vr\omega^2 - Cu \quad (3.27)$$

where  $r$  is the distance of the sample from the centre of rotation,  $\rho_0$  is the density of the solvent,  $V$  is the volume of the particle and  $C$  is the frictional coefficient of the particle.

Within a short period of time, the three forces come into balance

$$F_c + F_b + F_f = 0 \quad (3.28)$$

and then the particle moves with the sedimentation velocity,  $u_s$ . Rearranging equation (3.27) gives

$$m(1 - \bar{v}\rho_0)r\omega^2 = Cu_s \quad (3.29)$$

where  $\bar{v}$  is the partial specific volume of the particle. The frictional coefficient,  $C$ , is not known explicitly and must be eliminated by other quantity, which is dependent on it and can

be measured experimentally. Usually, this quantity is the diffusion coefficient,  $D$ . It was shown by Nernst<sup>110</sup> that this coefficient in an infinitely dilute solution can be expressed as

$$D = \frac{RT}{N_A C} \quad (3.30)$$

where  $R$  is the gas constant,  $T$  is the absolute temperature and  $N_A$  is the Avogadro's number. It is expected that the frictional coefficient for diffusion should be the same as that for sedimentation, thus equation 3.28 can be written as

$$m(1 - \bar{v}\rho_0)r\omega^2 = \left(\frac{N_A D}{RT}\right)^{-1} u_s \quad (3.31)$$

The sedimentation coefficient,  $s$ , is defined as

$$s = \frac{u_s}{\omega^2 r} \quad (3.32)$$

Introducing  $s$  into equation (3.31) the Svedberg equation can be finally obtained

$$M_w = N_A m = \frac{sRT}{D(1 - \bar{v}\rho_0)} \quad (3.33)$$

According to this equation molecular weight,  $M_w$ , of particles in solution can be determined by measurement of the sedimentation coefficient,  $s$ , the diffusion coefficient,  $D$ , and the partial specific volume of the particle in solution,  $\bar{v}$ . It was found, however, that the experimental values of  $s$  and  $D$  depend significantly on the concentration of the solution. Furthermore, the Nernst equation is valid only in the limit of infinite dilution, hence the values of  $s$  and  $D$  have to be extrapolated to zero concentration. The Svedberg equation is then more properly written as

$$M_w = N_A m = \frac{s_0 RT}{D_0(1 - \bar{v}\rho_0)} \quad (3.34)$$

where  $s_0$  and  $D_0$  represent values extrapolated to zero concentration.



From the shape of the sedimenting boundary, one can determine the distribution of the sedimentation coefficient,  $g(s)$ , which is the measure of the polydispersity of the particles. Applying the method of Signer and Gross,<sup>111</sup> the experimental data of the concentration gradient can be directly transformed into the distribution of the sedimentation coefficient

$$g(s) = \frac{1}{c_0} \frac{dc_0}{ds} = \frac{1}{c_0} \frac{dc}{dr} \left( \frac{r}{r_m} \right)^2 (r\omega^2 t) \quad (3.35)$$

where  $c_0$  is the initial concentration,  $r_m$  is the radial position of the meniscus. This method is a simplification of a rather complex problem and is exclusively applicable when the spreading of the boundary is only due to heterogeneity of the sample and diffusion as well as self-sharpening effects are negligible.

From the fringe shift, measured by an interference detector in the sedimentation velocity experiment, it is possible to calculate the concentration of the sedimenting solute in the sample

$$\Delta c = \frac{I\lambda}{(dn/dc)a} \quad (3.36)$$

where  $I$  is the fringe shift,  $\lambda$  is the wavelength of the used laser,  $dn/dc$  is the refractive index increment of the polymer in solution and  $a$  is the thickness of the measurement cell.

### 3.4 Atomic force microscopy

Atomic force microscopy (AFM), invented in 1986 by Binnig, Quate and Gerber,<sup>112</sup> is nowadays one of the most extensively used imaging techniques for characterisation of surfaces on the molecular and atomic scale. In this technique, a very tiny tip (5 – 50 nm), attached to the underside of a cantilever, is scanned over a surface. The movement of the sample is performed by means of a precise piezo-electric crystal, which is capable of sub-angstrom resolution in three dimensions. The sample is scanned by moving it in raster mode, and the force between the tip and the sample is measured. Since this force is very small it is not measured directly, instead, the up and down movement of the tip is detected. A laser beam is reflected from the mirrored surface on the backside of the cantilever onto a position-sensitive photodiode. A small deflection of the cantilever tilts the reflected beam and changes

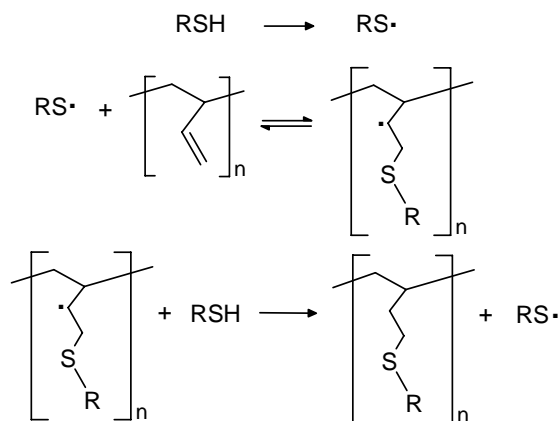
its position on the photodiode. In contrast to the optical microscopy, the lateral resolution of the AFM is determined by the size of the tip.

According to the interaction between the tip and the surface of the sample, the AFM can be operated in three principle modes: the contact, the non-contact and the tapping mode. In the contact mode, the tip scans the sample with a constant force in close contact with the surface. As a tip moves, the cantilever bends according to the changes in the topography. The piezo-electric crystal moves the sample vertically in order to maintain a constant force between the tip and sample. Therefore, the height profile of the sample can be directly obtained for the movement of the piezo-electric crystal. In the non-contact mode, the vibrating tip scans the sample from a distance of about 5 – 15 nm above the surface. Bending of the cantilever is caused by attractive forces (van der Waals) acting between the tip and the sample surface. In the tapping mode, the cantilever is oscillated near its resonant frequency (100 – 400 kHz) and with an amplitude between 10-150 nm. As the tip touches the surface, the cantilever oscillation is reduced due to energy loss. The reduction in oscillation amplitude is used to identify and measure surface features. The advantage of the tapping mode is that the contact between the tip and the sample is very short. Thus, problems associated with friction, adhesion or electrostatic forces are overcome. The tapping mode is being extensively applied since it allows for the imaging of surfaces, which can be easily damaged such as polymers<sup>113</sup> or biological tissues.<sup>114</sup>

## 4 RESULTS AND DISCUSSION

### 4.1 Radical addition of $\omega$ -functional mercaptanes

Well-defined block copolymers possessing covalently attached reactive functionalities have found much interest for the production of materials with tailored properties. However, polymerisation of monomers bearing functional groups is often difficult and poorly controlled. As mentioned in Section 2.3 an alternative pathway is to use well-defined block copolymers, obtained e.g. by sequential anionic polymerisation, as precursors for further chemical modifications. There are various possibilities for the introduction of functional groups onto the polymer backbone depending on the chemistry of the precursor block copolymer.<sup>1</sup> Nevertheless, the most desirable route is one of a general nature, allowing for the preparation of a series of different functional block copolymers from one precursor copolymer. In this work, it is demonstrated that the free-radical addition of  $\omega$ -functional mercaptanes onto unsaturated monomer units can represent such a synthetic strategy. This addition reaction tolerates the presence of many functional groups including  $-\text{OH}$ ,  $-\text{NH}_2$  and  $-\text{COOH}$  groups, and proceeds mostly in an anti-Markownikoff fashion as presented in Scheme 4.1



Scheme 4.1. The mechanism of the free radical addition of  $\omega$ -functional mercaptanes.

Radical addition of  $\omega$ -functional mercaptanes is well established in synthetic organic chemistry<sup>115</sup> but has not yet been extensively applied to polymeric systems. Mostly, the reports of such addition to polymers include the use of mercaptanes in the modification of

natural and synthetic rubbers.<sup>116-120</sup> The use of 2-mercaptoethanol for increasing the hydroxyl functionality in hydroxyl-terminated polybutadienes (HTPBs)<sup>121</sup> and the synthesis of phosphonated polybutadiene by addition of a phosphorus-containing mercaptanes were also described.<sup>122</sup> Though, of interest to note, is that in none of these cases does addition of the mercaptane occur to completion. Schapman *et al.*<sup>123</sup> have performed the modification of polybutadiene with (3-mercaptopropyl)triethoxysilane and have studied the influence of both mercaptane and initiator concentration on the progress of the reaction. In the modification of butadiene-containing copolymers, the free radical addition of mercaptanes has been employed to introduce carboxyl and ester functionalities into styrene/butadiene random copolymers (SBR).<sup>124,125</sup>

In this thesis, the radical addition of  $\omega$ -functional mercaptanes to well-defined 1,2-polybutadiene block containing precursors for the preparation of a series of functional block copolymers is presented. The whole is divided as follows: first, the exemplary modifications of 1,2- and 1,4-polybutadiene homopolymers are presented to demonstrate the differences in their reactivity with  $\omega$ -functional mercaptanes. Then, the modifications of 1,2-polybutadiene-poly(ethylene oxide) and 1,2-polybutadiene-polystyrene block copolymer precursors are described. The free radical addition of  $\omega$ -functional mercaptanes as a modular chemical approach towards well-defined functional block copolymers is discussed in detail.

#### 4.1.1 Modification of 1,2- and 1,4-polybutadiene

1,3-Butadiene belongs to the group of monomers having conjugated double bonds. The polymerisation of this monomer can occur in two different modes, referred to as 1,2- and 1,4-polymerisation.<sup>126</sup> Consequently, the obtained products can be of the 1,2-type (1,2-adduct), which has pendant unsaturation, or the 1,4-type (1,4-adduct) where unsaturation is present along the polymer chain (Figure 4.1). Additionally, the 1,4-adduct shows isomerism: cis and trans isomers can be distinguished. The type of product obtained in majority depends strongly on the experimental conditions applied in the polymerisation process. Lithium alkyl-based anionic polymerisation of 1,3-butadiene in THF produces mostly vinyl unsaturations (1,2-type), in contrast to the almost pure 1,4-polymers formed in non-polar solvents such as hexane.<sup>127</sup>

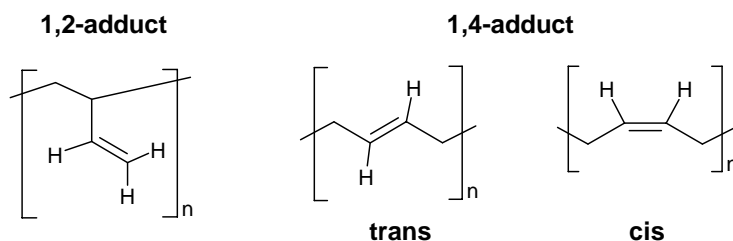
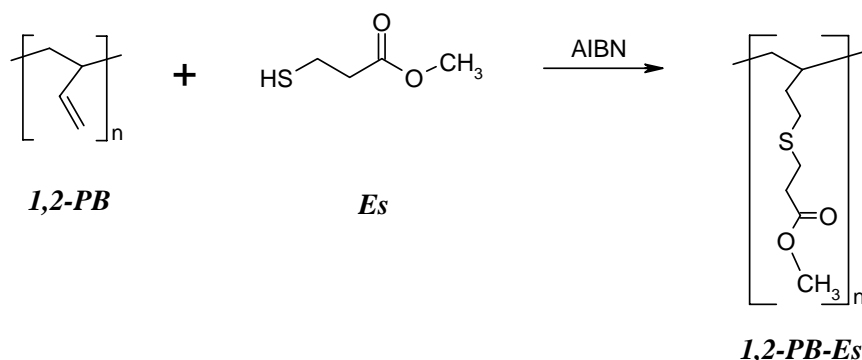


Figure 4.1. The microstructure of 1,2- and 1,4-type of polybutadiene.

The 1,2- and 1,4-types of polybutadiene exhibit different reactivities. In 1948, Serniuk *et al.* applied the addition of aliphatic mercaptanes to polybutadiene to obtain further information on the structure of butadiene polymers and copolymers.<sup>128</sup> According to these studies, the polybutadiene double bonds that predominantly undergo saturation are those present in the polymer chains as vinyl side groups (1,2-adduct). This is consistent with the work of Romani *et al.*, which shows that the addition of thioglycolic acid to double bonds in styrene/butadiene random copolymers (SBR) does not involve the internal double bonds (1,4-adduct).<sup>125</sup> However these observations concern only random polybutadiene-containing copolymers. In order to confirm the difference in the reactivities of 1,2- and 1,4-polybutadiene, modifications of the two types of polybutadiene homopolymers were performed. The modification reaction should satisfy the following two basic requirements: (i) addition of thiyl radicals should be quantitative and (ii) cross-linking of the polybutadiene chains must be avoided. Only when these cases are satisfied, the modification approach can be applied for the modification of polybutadiene-containing block copolymers.

Polybutadiene of the 1,2-type (*1,2-PB*) was synthesised by anionic polymerisation of 1,3-butadiene in THF using *sec*-BuLi as initiator (section 6.2.1.1). The content of 1,2-adduct in the polymer, calculated on the basis of <sup>1</sup>H NMR spectroscopy,<sup>129</sup> was found to be 93%. The polybutadiene of the 1,4-type (*1,4-PB*) was a commercial product from Aldrich, with a 99% content of 1,4-adduct. Both PBs were reacted under the same experimental conditions with the same ω-functional mercaptane, namely methyl-3-mercaptopropionate (*Es*). *Es* was chosen as the exemplary mercaptane because the ester function is easily detected by spectroscopic methods and both precursor and modified product can be analysed by size exclusion chromatography (SEC) under the same conditions. The modification reactions were performed under inert argon atmosphere; the precursor polymers were dissolved in THF and reacted at reflux temperature in the presence of AIBN (*N,N*-azobis(isobutyronitrile)) as the radical source. The experimental details are presented in section 6.2.2.1.

The modification of *1,2-PB* was carried out over 24 h (Scheme 4.2). During this time gelation of the reaction mixture, which would indicate cross-linking of the PB, was not observed. The modified polymer, isolated in 70% gravimetric yield, was characterized by SEC as well as  $^1\text{H}$  NMR and FT-IR spectroscopy.



Scheme 4.2 The introduction of ester functionalities to 1,2-polybutadiene (*1,2-PB*).

The  $^1\text{H}$  NMR spectrum of the modification product is presented in Figure 4.2. The signals originating from the unsaturated PB units,  $\delta = 4.80\text{--}5.60$  ppm, disappear completely upon modification, indicating that the mercaptane had been quantitatively added to the vinyl as well as the in chain double bonds (7% of 1,4-type units). Simultaneously, characteristic signals of the introduced ester group ( $-\text{COOCH}_3$ ) at  $\delta = 3.60$  ppm and of the newly formed thioether linkages ( $-\text{CH}_2\text{SCH}_2-$ ) at  $\delta = 2.60$  and 2.75 ppm can be observed. The signal at  $\delta = 2.60$  ppm is splitted into three lines and can therefore be assigned to the methylene protons (*d'*) of the anti-Markownikoff product. Whether or not any Markownikoff product was formed (c.f. work of Boileau *et al.*<sup>130</sup>) could not be confirmed. FT-IR analysis confirmed the disappearance of double bonds and the presence of the ester function in the polymer after modification. The modified polymer and the precursor were identical in terms of molecular weight distributions as indicated by the SEC chromatograms depicted in Figure 4.3. The fact that the modified polymer eluted faster in the SEC mode than the precursor could be attributed to a larger hydrodynamic volume of the functionalised block in comparison to the parent polymer. These results suggest that under the applied conditions the modification of *1,2-PB* occurred quantitatively and the isolated modified polymer was free of cross-linked products.

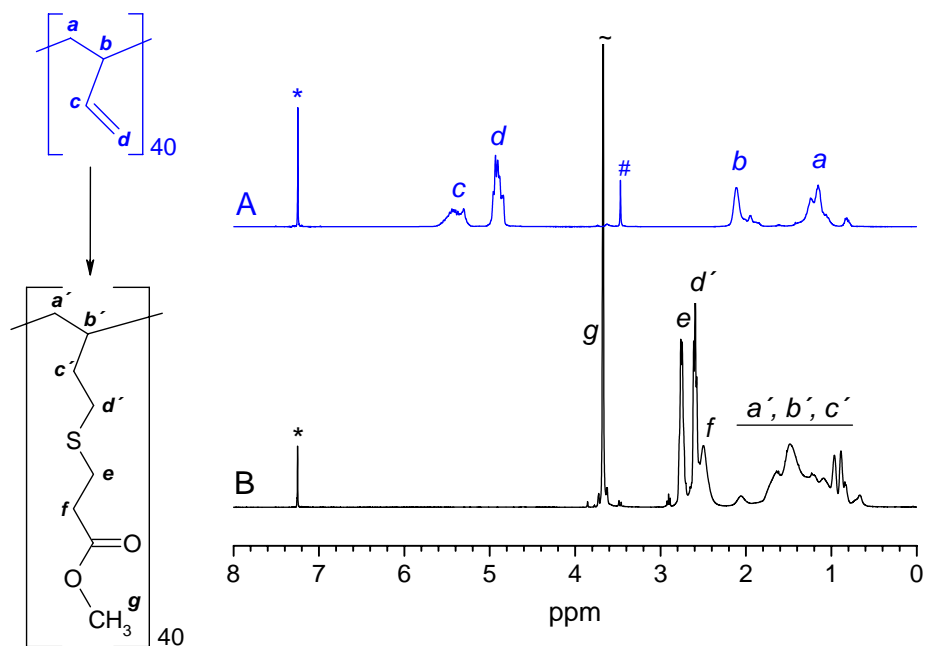


Figure 4.2.  $^1\text{H}$  NMR spectrum of the 1,2-polybutadiene, *1,2-PB* (A) and of the 1,2-polybutadiene modified with methyl-3-mercaptopropionate, *1,2-PB-Es* (B); \* solvent peak ( $\text{CDCl}_3$ ), # THF traces (from the synthesis).

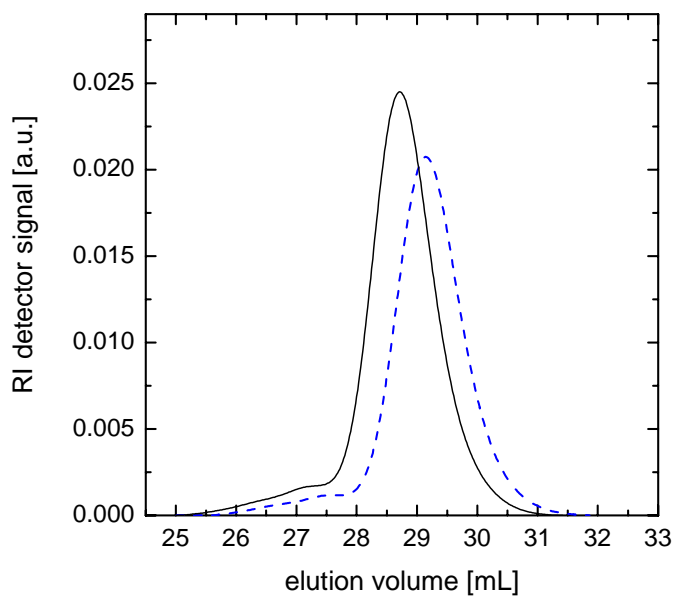


Figure 4.3. SEC chromatograms of the 1,2-polybutadiene modified with methyl-3-mercaptopropionate, *1,2-PB-Es* (solid line) compared to the precursor 1,2-polybutadiene, *1,2-PB*, (dashed line); eluent: THF.

The modification of the internal double bonds in *1,4-PB* proceeded differently that of *1,2-PB* discussed above. After 1h, strong gelation of the mixture occurred, indicating that cross-linking between the PB chains took place. The isolated product had a jelly-like consistency and was insoluble in common solvents; therefore detailed analysis on this product could not be performed.

The course of the free radical addition of  $\omega$ -functional mercaptanes to PB chains is strongly dependent on the microstructure of the precursor polymer. The modification of *1,2-PB* proceeded smoothly, yielding quantitatively modified polymer, whereas the modification of *1,4-PB* produced a cross-linked product under the same experimental conditions. Thus, further additions to PB-PEO copolymers were performed on precursors with a high content of 1,2-adduct.

#### 4.1.2 Modification of PB-PEO block copolymers

Polybutadiene-poly(ethylene oxide), PB-PEO, block copolymers utilized in this approach were prepared by sequential anionic polymerisation of 1,3-butadiene and ethylene oxide according to the procedure described in section 6.2.1.2. The chemical structure of the obtained copolymers was confirmed by  $^1\text{H}$  NMR analysis. Copolymer compositions were calculated by comparing peak integrals assigned to the different comonomers; the peak integral corresponding to the double bond protons in PB appearing at  $\delta = 4.75\text{-}5.60$  ppm was set in ratio to that assigned to the PEO backbone protons appearing at  $\delta = 3.60$  ppm. As indicated by SEC, the products displayed a narrow molecular weight distribution (polydispersity index,  $\text{PDI} \leq 1.08$ ) and did not contain any homopolymer impurities. The molecular characteristics of the precursor block copolymers are summarized in Table 4.1.

Table 4.1. Molecular characteristics of PB-PEO precursor block copolymers (n, m: number-average of butadiene and ethylene oxide units, respectively).

Precursor label	n <sup>a</sup>	m <sup>b</sup>	PDI <sup>a</sup>	PB 1,2 units <sup>b</sup> %
<i>P1</i>	25	75	1.05	97
<i>P2</i>	40	132	1.08	93
<i>P3</i>	40	273	1.06	93

As determined by: <sup>a</sup> SEC (calibrated with 1,2-PB standards), <sup>b</sup>  $^1\text{H}$  NMR.



Due to the negligible content of the 1,4-adduct, the structure of the PB-PEO block copolymer precursors will be presented as shown in Figure 4.4.

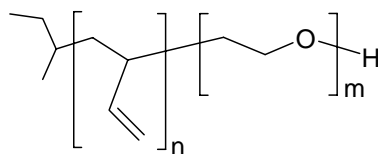


Figure 4.4. The general structure of the PB-PEO block copolymer precursors used for the modification with  $\omega$ -functional mercaptanes.

For the modification of PB-PEO block copolymers various, commercially available  $\omega$ -functional mercaptanes were utilized (Table 4.2).

Table 4.2.  $\omega$ -Functional mercaptanes applied for the modification of PB-PEO copolymers.

Mercaptane - chemical name	Structure	Label
Methyl-3-mercaptopropionate		<i>Es</i>
3-mercaptopropionic acid		<i>Ac</i>
2-aminoethanethiol hydrochloride		<i>Am·HCl</i>
2-(diethylamino)ethanethiol hydrochloride		<i>TAm·HCl</i>
3-mercapto-1,2-propanediol		<i>Di</i>
1H,1H,2H,2H-perfluorooctanethiol		<i>Fl</i>
N-acetyl-L-cysteine methyl ester		<i>PCys</i>

Typically, the radical addition of mercaptanes to PB-PEO was performed as described below (the experimental details are presented in section 6.2.2.2); modifications of the described procedure will be noted when required.

PB-PEO and AIBN were dissolved in THF to give a ~3 wt % solution. In most cases, reaction solutions were homogeneous, except when the mercaptanes carried ammonium groups. After addition of the mercaptane, the solution was degassed and heated to about 70 °C under an argon atmosphere. The molar ratio of reactants was  $[C=C]_0:[RSH]_0:[AIBN]_0 = 1:10:0.33$ . An excess of the mercaptane with respect to the PB degree of unsaturation was used since the overall aim was to modify the maximum number of double bonds. Maximum conversion of vinyl double bonds was reached within 24 hours ( $^1\text{H NMR}$ ), except when the mercaptane was *Fl*. Crude products were precipitated several times into an appropriate nonsolvent, filtered, re-dissolved in water and dialyzed (molecular weight cut-off: 1 kDa) against bi-distilled water. After freeze-drying, the modified copolymer samples were isolated as colourless (sometimes light yellow) powdered materials, in a 55 - 90% yield. The samples did not contain detectable amounts of mercaptane, as indicated by GC, FT-IR and the lack of mercaptane odour. Modified block copolymers were characterized by means of spectroscopy ( $^1\text{H NMR}$  and FT-IR) and size exclusion chromatography (SEC). An overview of the performed modification reactions is presented in Figure 4.5. This extensive illustration depicts the versatility of the chemical modification method applied.

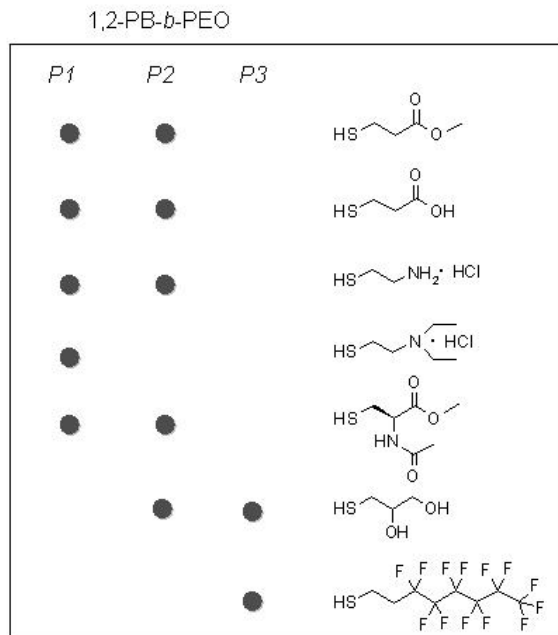
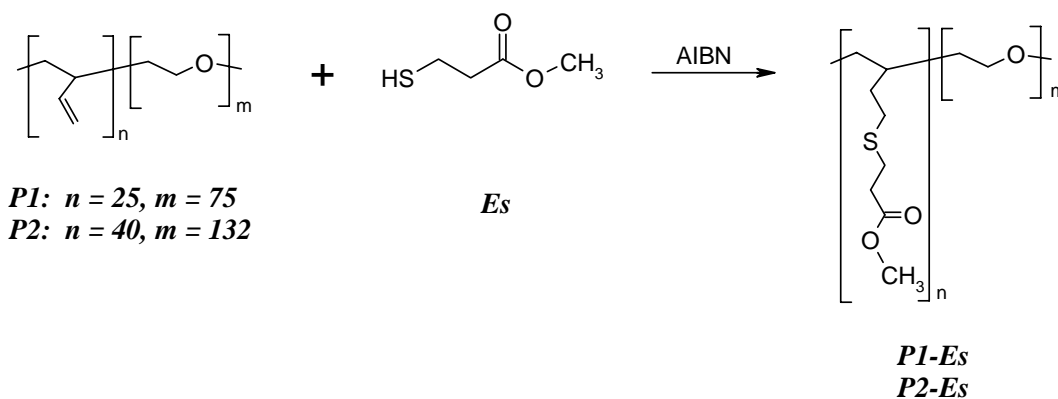


Figure 4.5. Overview on the performed modification reactions: various functional groups introduced to the three different precursor block copolymers.

#### 4.1.2.1 Introduction of ester functionalities

Similar to the exemplary modification of PBs, the introduction of ester functionalities (methyl-3-mercaptopropionate, *Es*) onto PB-PEO block copolymers was performed. The general equation of this reaction is given in Scheme 4.3.



Scheme 4.3. Introduction of ester functionalities to PB-PEO block copolymer precursors.

The modification reactions were performed with two PB-PEO samples, *P1* and *P2* according to the procedure described in section 6.2.2.2. Isolated yields, percentage of the remaining C=C bonds (the yield of modification), and PDI of the obtained products are summarised in Table 4.3.

Table 4.3. Isolated yields, percentage of the remaining C=C bonds, and PDIs of PB-PEO block copolymers modified with methyl-3-mercaptopropionate (*Es*).

Product label	Isolated yield <sup>a</sup> %	C=C content (PB) <sup>b</sup> %	PDI <sup>c</sup>
<i>P1-Es</i>	55	< 5	1.05
<i>P2-Es</i>	57	< 5	1.08

As determined by: <sup>a</sup> Gravimetry, <sup>b</sup> <sup>1</sup>H NMR, <sup>c</sup> SEC.

The chemical structure of the modified block copolymers was confirmed by <sup>1</sup>H NMR and FT-IR analyses. NMR was used to estimate the yield of modification by consideration of the intensity of the PB double bond signals relative to PEO. The exemplary NMR spectrum of the *P1-Es* sample (Figure 4.6) did not reveal any traces of unsaturated PB 1,2-units ( $\delta = 4.80\text{-}5.10$  ppm), indicating that the addition of *Es* to the PB block segment had been achieved in a quantitative yield, i.e. greater than 95%. Although the characteristic signal of the methyl ester group ( $\delta \sim 3.6$  ppm) could not be observed due to the overlapping signal of

PEO backbone protons (appearing also at  $\delta \sim 3.6$  ppm), the addition of the mercaptane could be confirmed by the presence of thioether linkage signals at  $\delta \sim 2.6$  and 2.8 ppm.

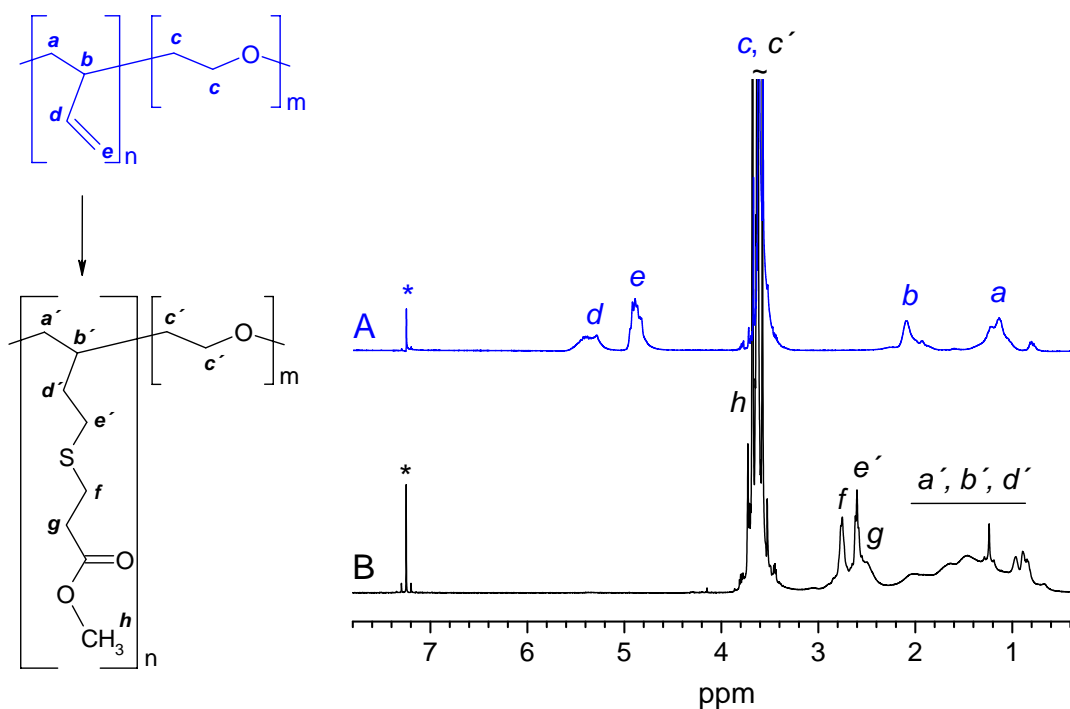


Figure 4.6.  $^1\text{H}$  NMR spectrum of the parent PB-PEO block copolymer, *PI* (A) and the PB-PEO sample modified with methyl-3-mercaptopropionate, *PI-Es* (B); \* solvent peak ( $\text{CDCl}_3$ ).

The FT-IR spectrum of *PI-Es* (Figure 4.7) shows the carbonyl stretching band  $\nu$  ( $\text{C}=\text{O}$ ), of the ester units at  $\tilde{\nu} = 1736 \text{ cm}^{-1}$  while the characteristic absorption band of vinyl double bonds  $\nu$  ( $\text{C}=\text{C}$ ), observed for the parent PB-PEO at  $1640 \text{ cm}^{-1}$  is absent.<sup>131</sup> Also the two distinct absorption bands of alkenes at around  $993$  and  $906 \text{ cm}^{-1}$ , originating from the out-of-plane  $\gamma$  ( $\text{C}-\text{H}$ ) bending vibrations as well as characteristic alkene stretching band  $\nu$  ( $\text{C}-\text{H}$ ) above  $3000 \text{ cm}^{-1}$  disappeared. The lack of stretching  $\nu$  ( $\text{S}-\text{H}$ ) resonance at around  $2600 \text{ cm}^{-1}$  indicates that ester groups are indeed covalently attached to the polymer backbone, and that the product is free of mercaptane impurities.

SEC analysis shows that *PI-Es* exhibits the same molecular weight distribution as the precursor *PI* (Figure 4.8). This proves that intermolecular radical cross-linking of the PB segments did not occur under the selected experimental conditions. Due to the somewhat larger hydrodynamic volume of ester-functional units, *PI-Es* eluted slightly faster than *PI*. It is noteworthy that the *PI-Es* sample showed a distinct UV absorption at  $\lambda = 260 \text{ nm}$  (inset in Figure 4.8), which probably originates from the ( $n \rightarrow \sigma^*$ ) transition of the thioether moieties.

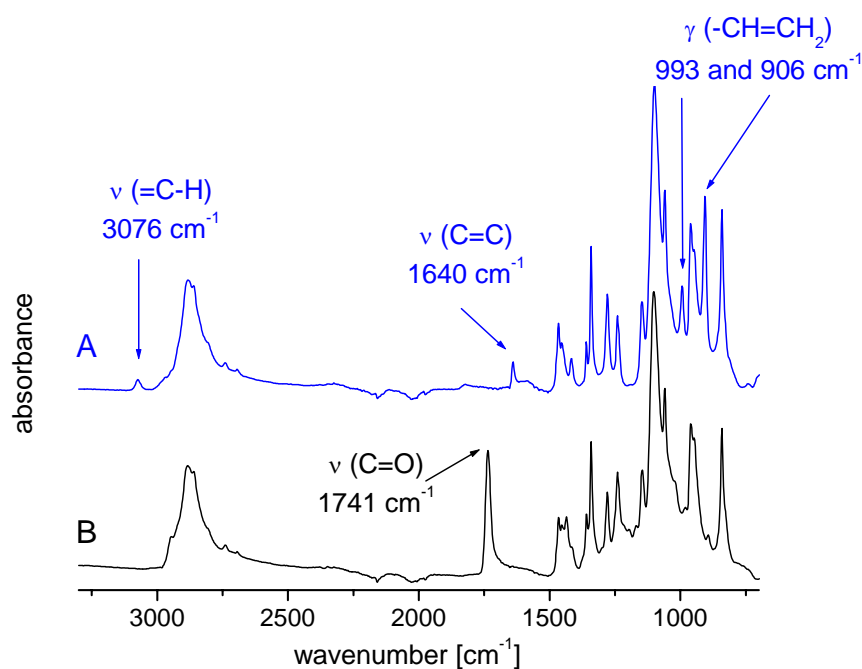


Figure 4.7. FT-IR spectra of the parent PB-PEO, *PI* (A) and the PB-PEO block copolymer sample modified with methyl-3-mercaptopropionate, *PI-Es* (B).

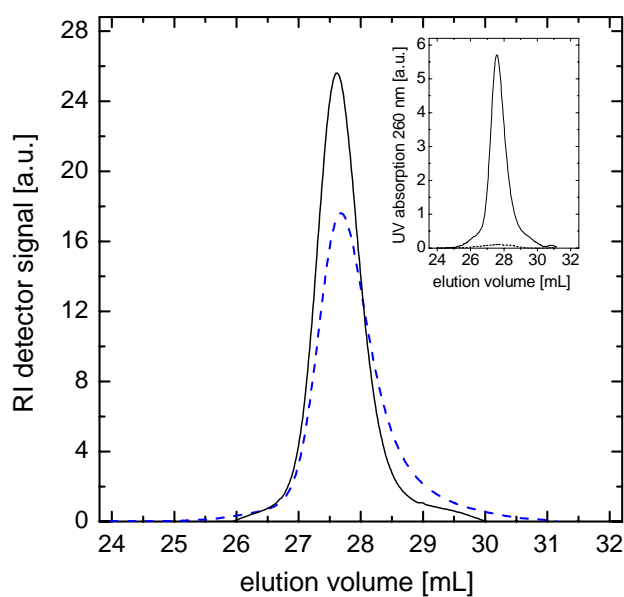


Figure 4.8. SEC chromatograms of the PB-PEO block copolymer bearing ester functionalities after the modification with methyl-3-mercaptopropionate, *PI-Es* (solid line) and the precursor PB-PEO, *PI*, (dashed line); eluent: THF.

#### 4.1.2.2 Introduction of ionic groups

In the frame of this approach three different  $\omega$ -functional mercaptanes were utilized: (i) 3-mercaptopropionic acid (*Ac*), containing carboxylic group, which allows for the presence of negative charges on the polymer chains when converted into the salt form; (ii) 2-aminoethanethiol hydrochloride (*Am·HCl*) and (iii) 2-(diethylamino)ethanethiol hydrochloride (*TAm·HCl*) allow for the introduction of positive charges on the polymer chain. Figure 4.9 depicts the chemical structures of the utilized mercaptanes.

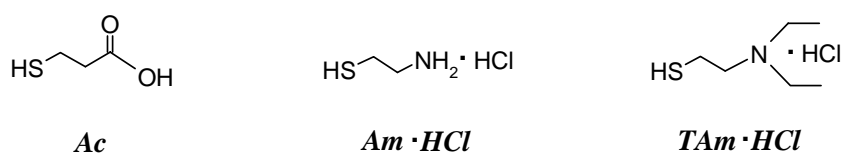


Figure 4.9. Chemical structures of the mercaptanes used in the synthesis of ionic block copolymers: 3-mercaptopropionic acid (*Ac*), 2-aminoethanethiol hydrochloride (*Am·HCl*), 2-(diethylamino)ethanethiol hydrochloride (*TAm·HCl*).

The modification reactions were performed for two precursor block copolymers, *P1* (PB<sub>25</sub>-PEO<sub>75</sub>) and *P2* (PB<sub>40</sub>-PEO<sub>132</sub>), the experimental details are described in section 6.2.2.2. The reaction mixtures during addition of *Am·HCl* and *TAm·HCl* were inhomogeneous, as these mercaptanes are insoluble in THF. Nevertheless, practically quantitative modification yields could be obtained. More important than solubility of the mercaptanes seems to be that the block copolymer chains dissolve either as unimers or as aggregates with PB solvating corona. Thus, THF was utilized as a solvent, since it is a good solvent for PB but not such a good for PEO. Obtained products were isolated in 60-78% gravimetric yields.

The chemical structure of the modified block copolymers was confirmed by <sup>1</sup>H NMR and FT-IR analyses. Similar to the addition reaction of *Es*, the modification yields were estimated on the basis of <sup>1</sup>H NMR, by consideration the relative intensities of the remaining PB double bond signals (for spectra see appendix I). FT-IR analyses performed on the copolymers functionalised with *Ac* (Figure 4.10) show the absorption band related to the carbonyl stretching of the aliphatic carboxylic acid,  $\nu$  (C=O), at 1717 cm<sup>-1</sup>, when the obtained products were in the protonated form. For samples converted into the sodium salt absorption bands originating from asymmetric ( $\nu_{as}$ ) and symmetric ( $\nu_s$ ) stretching vibrations in the carboxylate ion could be observed at 1572 and 1395 cm<sup>-1</sup> respectively.

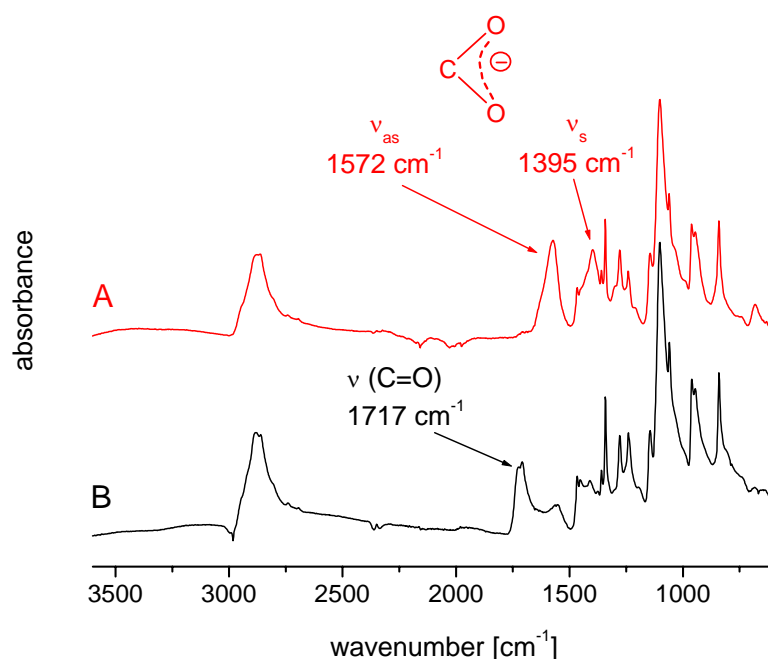


Figure 4.10. FT-IR spectra of the PB-PEO block copolymer modified with 3-mercaptopropionic acid, *P2-Ac*: sample were the introduced groups exist as carboxylate ions (A) and sample were the introduced groups are in the carboxylic acid form (B).

The samples modified with *Am·HCl* and *TAm·HCl* show broad absorption bands of ammonium salts  $\nu(-\text{NH}_3^+)$  at around  $2800\text{ cm}^{-1}$ . In the spectra of *P2-Am·HCl* (Figure 4.11), the distinct absorption bands arising from bending ( $\delta$ ) of the  $-\text{NH}_3^+$  group can be observed around  $1575\text{ cm}^{-1}$ . The N–H bending band of the tertiary amine salt could not be observed in the spectra of *PI-TAm·HCl*; it is known that this band is weak and of no practical value.<sup>131</sup> For all samples, the characteristic absorption bands of vinyl double bonds, observed for the precursor copolymers at around  $3075$ ,  $1640$  as well as  $993$  and  $906\text{ cm}^{-1}$  were absent. Again, the S–H stretching resonance at  $\sim 2600\text{ cm}^{-1}$  could not be observed. Thus, the products were free of mercaptane impurities and the introduced functionalities were, indeed, covalently attached to the polymer backbone.

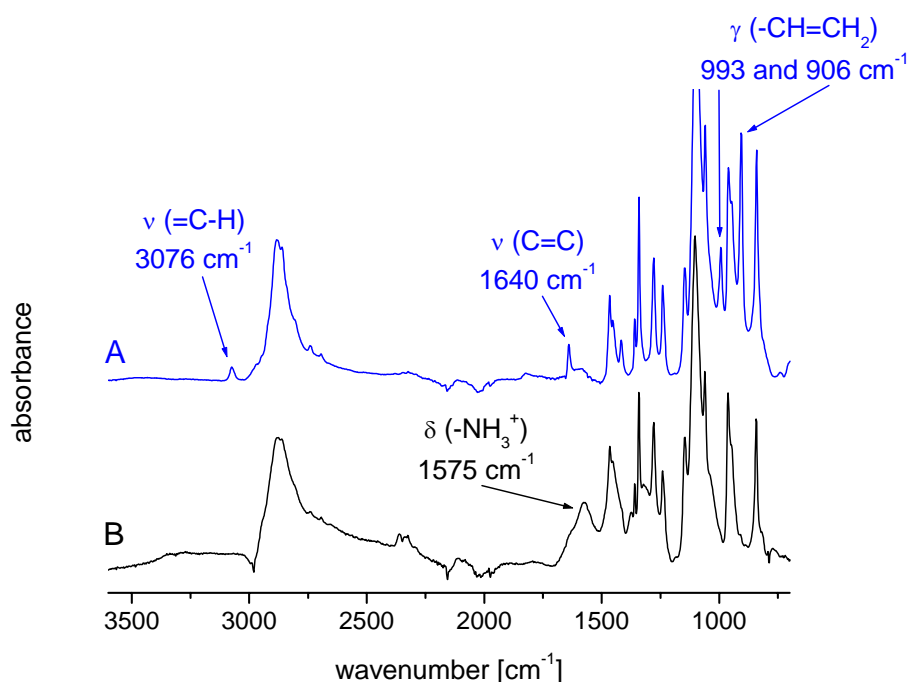


Figure 4.11. FT-IR spectra of the parent PB-PEO block copolymer, *P2* (A) and the PB-PEO sample modified with 2-mercaptoethylamine hydrochloride, *P2-Am·HCl* (B).

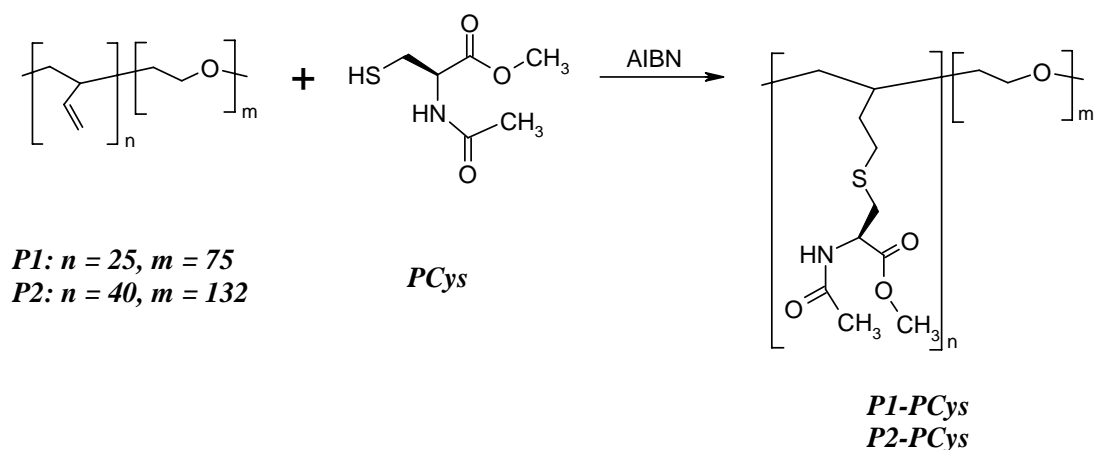
The characterization of the carboxyl- and amino-functionalised copolymers with aqueous SEC as well as SEC using organic eluents was not possible due to aggregation phenomena in common solvents. Nevertheless, we have shown in the model reaction with *Es* (section 4.1.2.1) that under the selected conditions cross-linking of PB chains can be avoided preserving the narrow molecular weight distribution of the parent PB-PEOs. Since the obtained products do not exhibit swelling behaviour, which is typical for cross-linked polymers, and are soluble in many common solvents, it can be concluded that the cross-linking side reaction did not take place.

In this investigation, it is shown that the addition of ω-functional mercaptanes represents an alternative method for the production of ionic block copolymers. The main advantage of this method is the possibility to introduce various charged groups to a well-defined and homopolymer-free precursor block copolymer. Additionally, oppositely charged groups can be attached to the same block copolymer, which leads to the production of ionic block copolymers with identical lengths of the oppositely charged segments.



### 4.1.2.3 Introduction of cysteine

The amino acid cysteine contains the reactive –SH group besides the typical amine and carboxylic acid functions. Therefore, it should be possible to attach cysteine to the double bonds of the polymer chain via radical addition. It has been previously mentioned that the radical addition of mercaptanes bearing amine hydrochlorides or carboxylic acid groups leads to the modified product, and that these functions do not disrupt the addition process (section 4.1.2.2). Hence, similar result could be expected when cysteine is utilized in the modification reaction. However, attempts to add the free cysteine to the precursor PB-PEO copolymer (*P1*) were unsuccessful: no conversion was observed after a reaction time of 24 h. The same was true when the amine group of cysteine was first converted into ammonium chloride. A third attempt for modification of the polymer chains involved the use of cysteine with protected amine and acid functions, namely N-acetyl-L-cysteine methyl ester, *PCys*. For this approach the two precursor block copolymers *P1* and *P2* were utilized; Scheme 4.4 depicts the general equation of the performed functionalization reactions.



Scheme 4.4. The general reaction equation of the radical addition of N-acetyl-L-cysteine methyl ester (*PCys*) to the PB-PEO precursor block copolymers.

<sup>1</sup>H NMR analysis showed that the modification yield in the reaction of *P1* with *PCys* was practically quantitative (see appendix I). In the modification of *P2*, the percentage of remaining double bonds was found to be about 10%. Figure 4.12 presents the exemplary <sup>1</sup>H NMR spectrum of *P2-PCys* sample, containing the characteristic signals of the newly introduced *PCys*. Protons of the protecting methyl ester and acetyl –CH<sub>3</sub> groups are observed at  $\delta = 3.75$  ppm and  $\delta = 2.0$  ppm, respectively. The relative intensities of these signals, when

set in ratio with the intensity of the signal originating from the PEO protons ( $\delta \sim 3.70$ - $3.40$  ppm), confirm the high yield of modification in the sample *P1-PCys*. This seems not to be the case for the *P2-PCys* sample, where these ratios correspond to the modification yield about 50%. However, this number changes with the applied measurement conditions including solvent and temperature, and possibly aggregation of the modified copolymer has an influence on the detected intensity values.

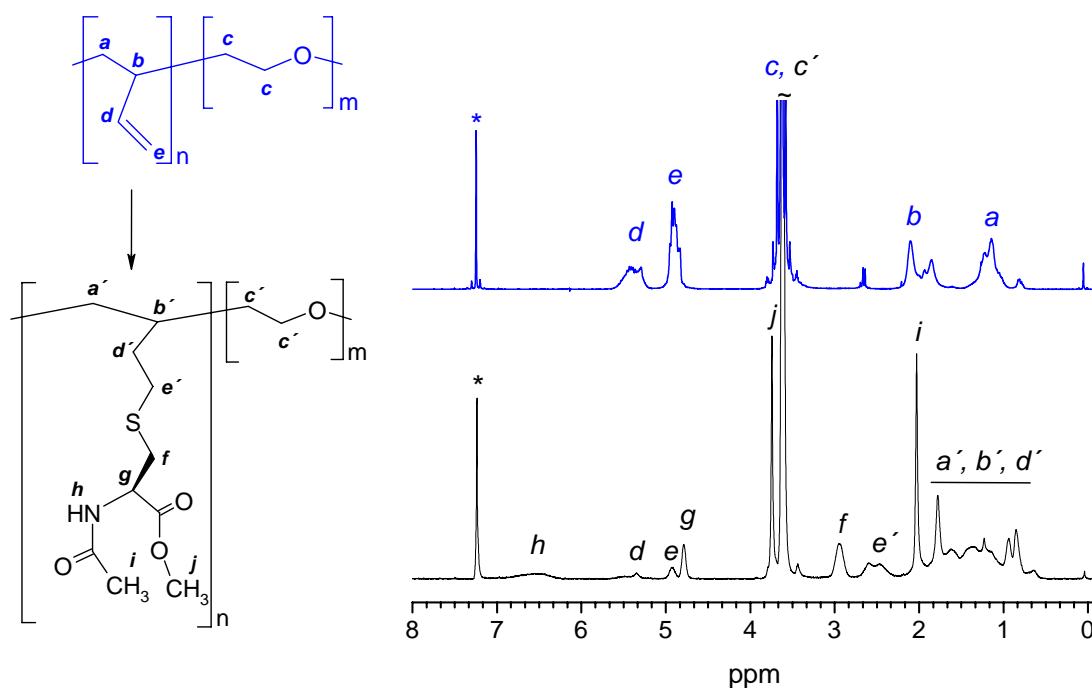


Figure 4.12.  $^1\text{H}$  NMR spectrum of the PB-PEO block copolymer modified with N-acetyl-L-cysteine methyl ester, *P2-PCys*; \* solvent peak ( $\text{CDCl}_3$ ).

FT-IR analysis (Figure 4.13) shows a distinct absorption band originating from the carbonyl stretching of the ester group,  $\nu(\text{C}=\text{O})$ , at  $\tilde{\nu} = 1736 \text{ cm}^{-1}$ . The characteristic Amide I band ( $\text{C}=\text{O}$  stretching) of the N-monosubstituted amide group is observed at  $1657 \text{ cm}^{-1}$  and the Amide II band (mainly N–H bending) is observed at  $1531 \text{ cm}^{-1}$ .<sup>132</sup> Furthermore, the N–H stretching absorption band is present at around  $3280 \text{ cm}^{-1}$ . The molecular weight distributions of the modified copolymers are similar to that of the precursor block copolymers, as indicated by SEC (Figure 4.14). The molecular characteristics of the copolymers modified with *PCys* are summarized in Table 4.4.

Table 4.4. Chemical characteristics of the PB-PEO copolymers modified with N-acetyl-L-cysteine methyl ester, *PCys*.

Sample	Isolated yield <sup>a</sup> %	C=C content (PB) <sup>b</sup> %	PDI <sup>c</sup>
<i>P1-PCys</i>	n.d. <sup>d</sup>	< 5	1.07
<i>P2-PCys</i>	83	~ 10	1.12

As determined by: <sup>a</sup> Gravimetry, <sup>b</sup> <sup>1</sup>H NMR, <sup>c</sup> SEC, <sup>d</sup> not determined.

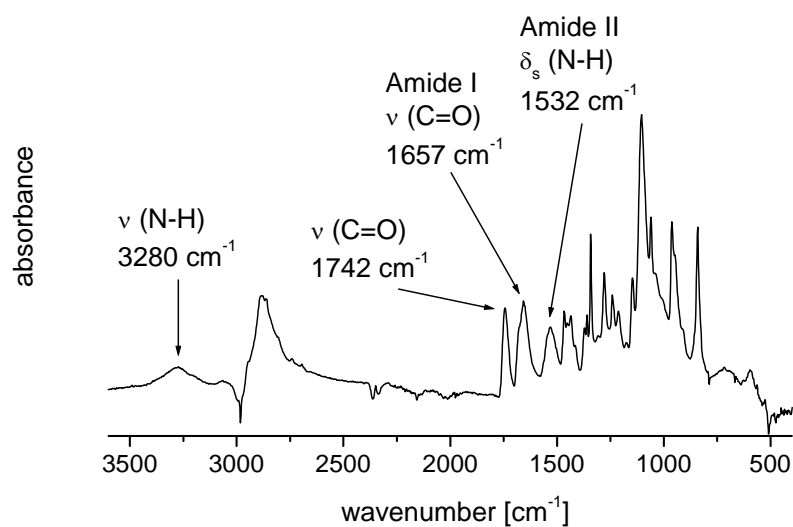


Figure 4.13. FT-IR spectrum of PB-PEO block copolymer modified with N-acetyl-L-cysteine methyl ester, *P2-PCys*.

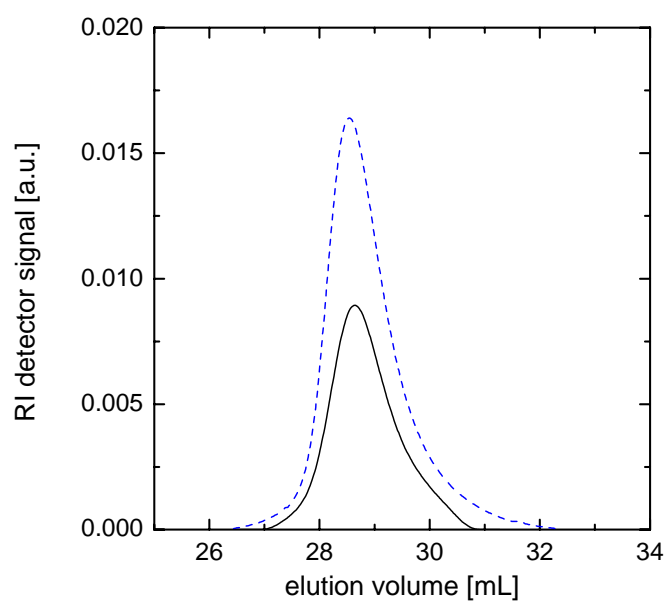
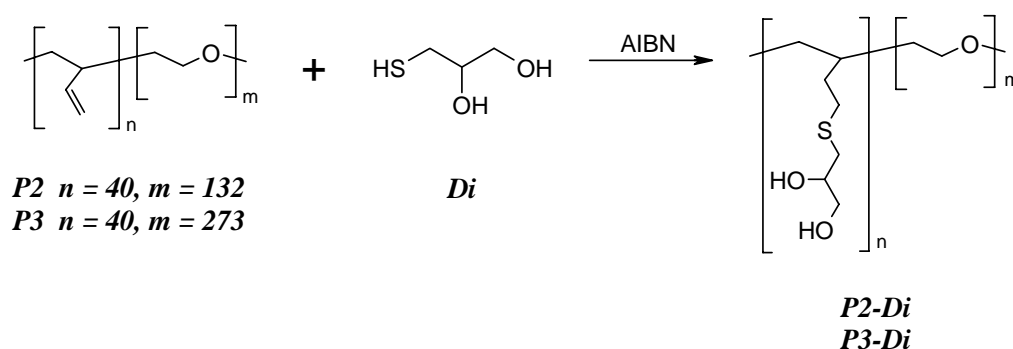


Figure 4.14. SEC chromatograms of the PB-PEO block copolymer modified with N-acetyl-L-cysteine methyl ester, *P1-PCys*, (solid line, signal magnified 10 times) and the parent PB-PEO copolymer, *P1* (dashed line); eluent: NMP.

The radical addition of *PCys* to the PB-PEO block copolymers may represent the first step towards synthetic polymers with oligopeptide sequences in the side chains. Further development of this approach may result in such polymers finding application in so-called “molecular chimeras” – polymers containing covalently bonded synthetic and natural (peptide) blocks.

#### 4.1.2.4 Introduction of diol functionalities

In this study, the addition reaction of 3-mercapto-1,2-propanediol (*Di*) to *P2* and *P3* precursor PB-PEOs for the preparation of highly hydroxyl-functionalised block copolymers (Scheme 4.5) was applied.



Scheme 4.5. Preparation of hydroxyl-functionalised block copolymers.

The modification reactions were performed under conditions as described in detail in section 6.2.2.2. The resulting products were characterised by SEC,  $^1\text{H}$  NMR and FT-IR; their chemical characteristics are summarised in Table 4.5.

Table 4.5. Chemical characteristics of hydroxyl-functionalised copolymers.

Sample	Isolated yield <sup>a</sup> %	C=C content (PB) <sup>b</sup> %	PDI <sup>c</sup>
<i>P2-Di</i>	88	< 5	1.09
<i>P3-Di</i>	83	< 5	n.d. <sup>d</sup>

As determined by: <sup>a</sup> Gravimetry, <sup>b</sup>  $^1\text{H}$  NMR, <sup>c</sup> SEC, <sup>d</sup> not determined.

The modification yields were greater than 95%, as calculated on the basis of  $^1\text{H}$  NMR analysis. The presence of hydroxyl functionalities was confirmed by FT-IR analysis, where the broad absorption band originating from the stretching of O–H functions could be observed at  $\tilde{\nu} = 3350\text{ cm}^{-1}$  (for NMR and FT-IR spectra see appendix I). Figure 4.15 depicts the SEC

chromatograms of *P2-Di* and the precursor block copolymer, *P2*. As can be seen, the modified copolymer elutes considerably faster than the parent PB-PEO, indicating that the hydrodynamic volume increases after the addition of the mercaptane to the polymeric chains. The narrow molecular weight distribution of the functionalised copolymer was preserved, as was the case for the copolymers with introduced ester groups (section 4.1.2.1). As a result, one can conclude that the transformation proceeds smoothly, in the absence of undesired cross-linking.

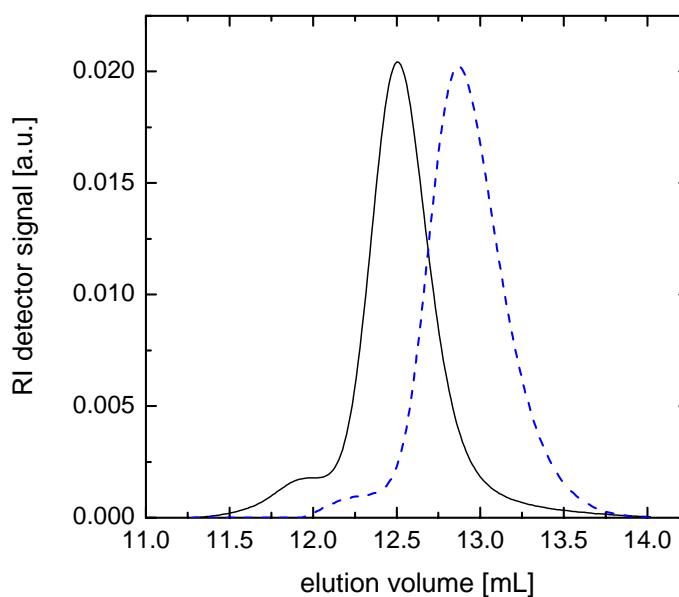
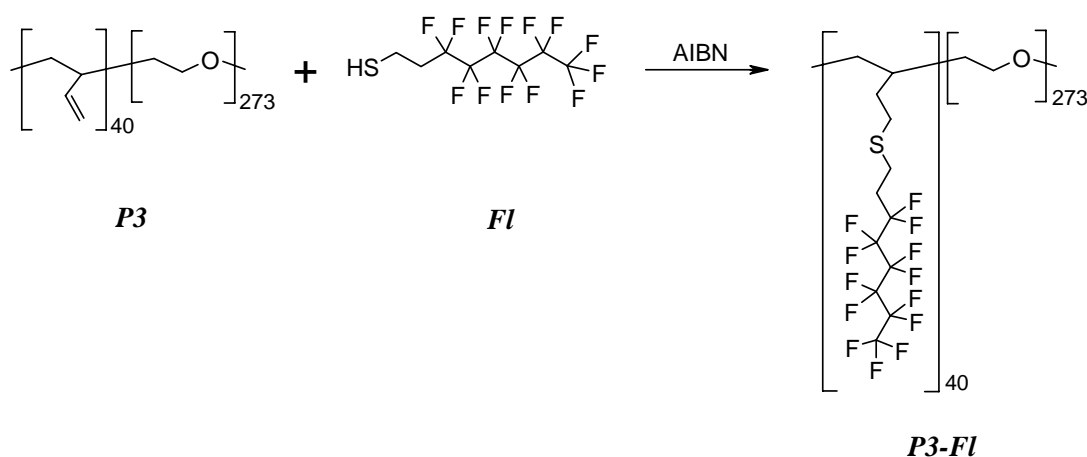


Figure 4.15. SEC chromatograms of the PB-PEO block copolymer modified with 3-mercapto-1,2-propanediol, *P2-Di* (solid line) and the parent PB-PEO copolymer, *P2* (dashed line, signal magnified 5 times); eluent: NMP.

To date, hydroxyl-containing mercaptanes have been utilised to increase the functionalization degree of hydroxyl-terminated polybutadienes (HTPB). These polymers are used as components in the industrial synthesis of polyurethanes due to their exceptional softness. Commercially available HTPBs are often obtained by anionic polymerisation of butadiene followed by termination with propylene oxide; however, the average hydroxyl functionality of these polymers is quite low. Hence, the interest arises to increase the hydroxyl functionality of HTPBs by a polymer modification reaction. Such an attempt has been reported by Boutevin *et al.* who described the synthesis and use of HTPB for polyurethane resins modified by radical addition of 2-mercaptoethanol.<sup>121</sup> The polymers with introduced diol functionalities can also be used as hydrogen donors in the polymer complexes based on hydrogen bonding (see section 4.3.3) or for reversible acetal-type linkage.

#### 4.1.2.5 Introduction of fluorinated side chains

For this modification reaction 1H,1H,2H,2H-perfluorooctanethiol, *Fl*, was used, which adds to the PB-PEO copolymer, resulting in a copolymer containing a segment grafted with partially fluorinated side chains (Scheme 4.6). Because of introduction of the relatively long and strongly hydrophobic fluorinated side chains, a change in the hydrophobic-hydrophilic balance of the modified PB-PEO copolymer could be expected. In order to counterbalance this effect, the modification reactions were performed with precursor *P3* containing a relatively long PEO segment.



Scheme 4.6. Grafting of a PB-PEO block copolymer precursor (*P3*) with 1H,1H,2H,2H-perfluorooctanethiol (*Fl*).

After a 24 h reaction, performed under conditions as described in section 6.2.2.2, the yield of modification reached 84% ( $^1\text{H}$  NMR analysis, percentage of unreacted double bonds). Addition of the second portion of AIBN radical initiator and extension of the reaction time to 48 h raised the degree of modification to 89%. The presence of C–F bonds in the modified copolymer was confirmed by FT-IR spectroscopy (Figure 4.16), the characteristic absorption band showing at about  $1200\text{ cm}^{-1}$ .

SEC analysis was performed in THF and revealed a significant shift in the elution time of the modified copolymer, *P3-Fl*, in comparison to the parent *P3*, indicating the increased hydrodynamic volume of the polymer after modification (Figure 4.17). Furthermore, both samples exhibited a similar narrow molecular weight distribution, PDI  $\sim 1.06$  which confirms that the modified copolymer did not contain any cross-linked product.

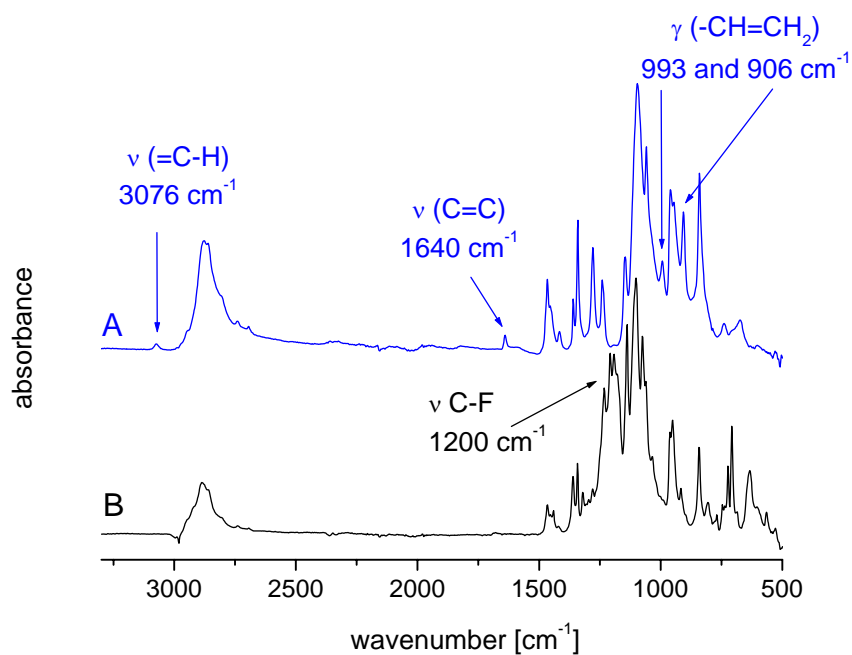


Figure 4.16. FT-IR spectrum of the parent PB-PEO block copolymer, *P3* (A) in comparison to the PB-PEO sample modified with 1H,1H,2H,2H-perfluorooctanethiol, *P3-Fl* (B).

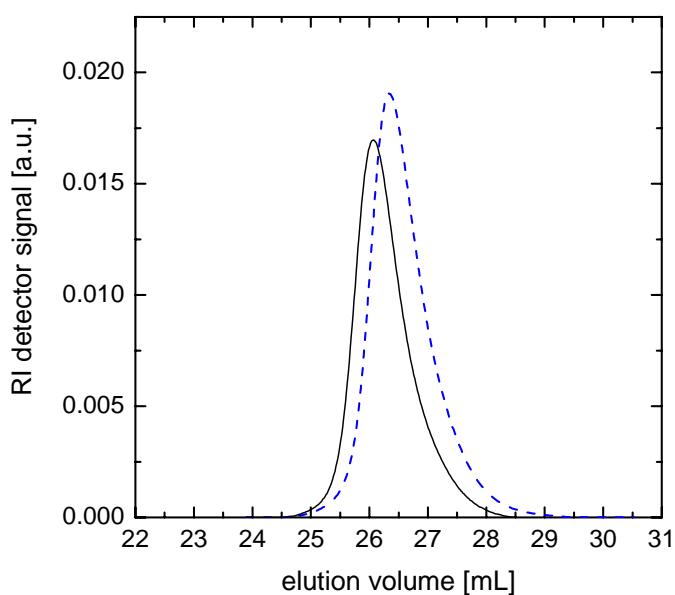


Figure 4.17. SEC chromatograms of the PB-PEO block copolymer modified with 1H,1H,2H,2H-perfluorooctanethiol, *P3-Fl* (solid line, signal magnified 3.5 times) and the precursor PB-PEO copolymer, *P3* (dashed line); eluent: THF.

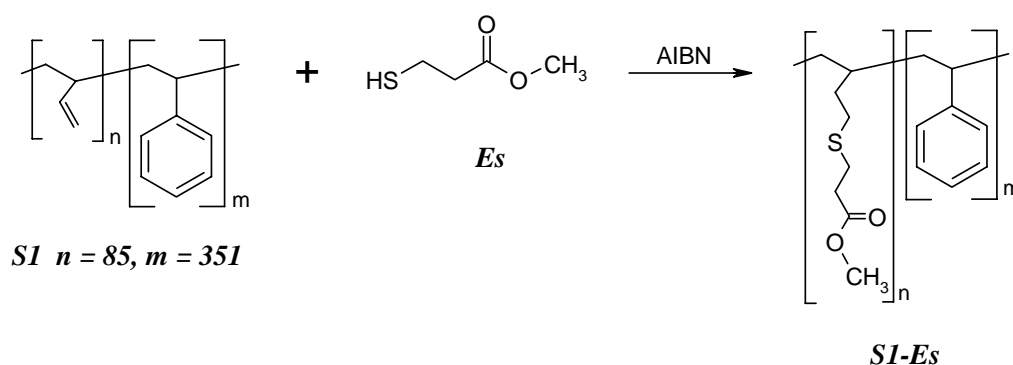
Tailoring the nature of the side chains allows for tuning of the block copolymer properties; typically, introduction of the partially fluorinated side chains results in a lowering

of the surface energy and qualifies such copolymers for applications that require reduced friction.<sup>133</sup> Besides low surface energy, fluorinated block copolymers exhibit good solubility in supercritical carbon dioxide (sc-CO<sub>2</sub>) predisposing them towards applications as surfactants in emulsion polymerisation of monomers insoluble in sc-CO<sub>2</sub>.<sup>134</sup> Copolymers containing fluorocarbon segments are often among the more difficult to synthesise, hence the development of appropriate polymer modification methods, which give facile access to such copolymers, is of great importance.

#### 4.1.3 Modification of PB-PS block copolymers

Since the radical addition of  $\omega$ -functional mercaptanes to PB-PEO block copolymers was found to proceed well for various tested mercaptanes, we attempted to extend the concept by applying this method for the modification of polybutadiene-polystyrene, PB-PS, block copolymers. The PB-PS precursor used throughout these studies was prepared by sequential anionic polymerisation of 1,3-butadiene and styrene by employing the procedure described in section 6.2.1.3. The number-average degrees of polymerisation of the PB and PS block were 85 and 351 respectively; the measured polydispersity index was 1.15. According to <sup>1</sup>H NMR analysis, the content of the butadiene 1,2-adduct in the copolymer was 97%.

The radical addition of mercaptanes to PB<sub>85</sub>-PS<sub>351</sub> (*SI*) was performed similarly as for PB-PEO copolymers, using THF as solvent and AIBN as radical initiator. The experimental details are described in section 6.2.2.3. Exemplary modification was performed using methyl-3-mercaptopropionate (*Es*), which was made to react with the *SI* block copolymer precursor as depicted in Scheme 4.7.



Scheme 4.7. The reaction scheme for the modification of *PB*<sub>85</sub>-*PS*<sub>351</sub> block copolymer precursor (*SI*) with methyl-3-mercaptopropionate (*Es*).



The obtained product was analysed using  $^1\text{H}$  NMR and FT-IR spectroscopy as well as SEC. The latter technique revealed a slight change in the elution time for the modified copolymer, *SI-Es*, comparing to the parent *SI* (Figure 4.18). The molecular weight distribution of *SI-Es* was similar to that measured for the precursor block copolymer ( $PDI = 1.18$ ), implying the absence of cross-linking reactions during the modification process.

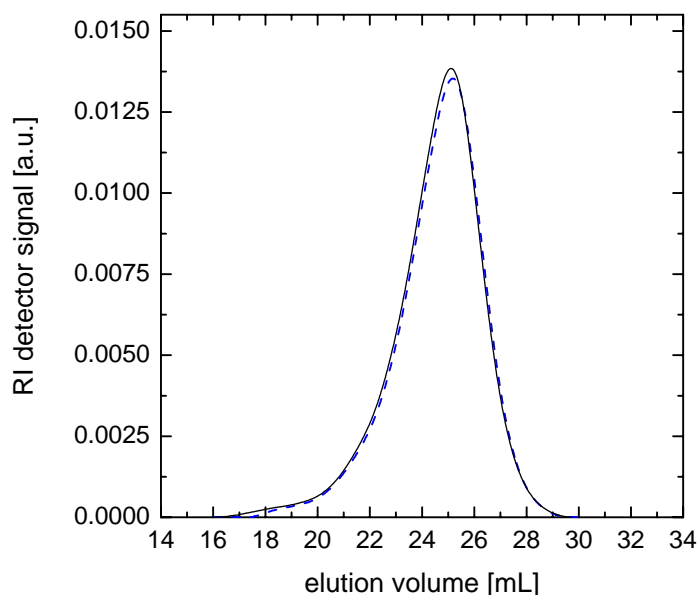


Figure 4.18. SEC chromatograms of the PB-PS block copolymer modified with methyl-3-mercaptopropionate, *SI-Es* (solid line) and the precursor PB-PS copolymer, *SI* (dashed line).

FT-IR analysis showed a distinct absorption band originating from carbonyl stretching of the ester group,  $\nu(\text{C}=\text{O})$ , at  $\tilde{\nu} = 1734\text{ cm}^{-1}$ . In the  $^1\text{H}$  NMR spectra (Figure 4.19), the signal of the newly introduced methyl ester groups can be observed at  $\delta = 3.60$  ppm and the peaks characteristic for the thioether linkage are present at  $\delta = 2.60$  and 2.50 ppm. Furthermore the complete disappearance of the PB double bond signals ( $\delta = 5.60\text{-}4.75$  ppm) indicates a quantitative modification. However, the ratio of the integral of the methyl ester peak with respect to the integral of the peak arising from the two protons in the PS benzyl ring (*ortho*-position,  $\delta = 6.85\text{-}6.25$  ppm) gives a modification yield of just 86% (for the sample measured in  $\text{CDCl}_3$  at r.t.). Interestingly, however, the value for the yield of modification depended on the measurement conditions including solvent (DMF: 71%), temperature (40 °C,  $\text{CDCl}_3$ : 59%) and pulse delay time (long  $\sim 15$  min: 65%), as was the case for the PB-PEO block

copolymer modified with *PCys* (sample *P2-PCys*, section 4.1.2.3). The dependence of the calculated yield of modification on the conditions probably arises from the differences in the solubility of both blocks. The poorly soluble block is due to its immobility not detected by NMR. Of importance to note is that the signal originating from the unreacted double bonds was absent in all the  $^1\text{H}$  spectra, run under varying measurement conditions. Thus, it seems reasonable to treat the amount of remaining double bonds as the determinant for the modification yield, especially since cross-linking, which may also cause the removal of double bonds, does not occur, as indicated by SEC.

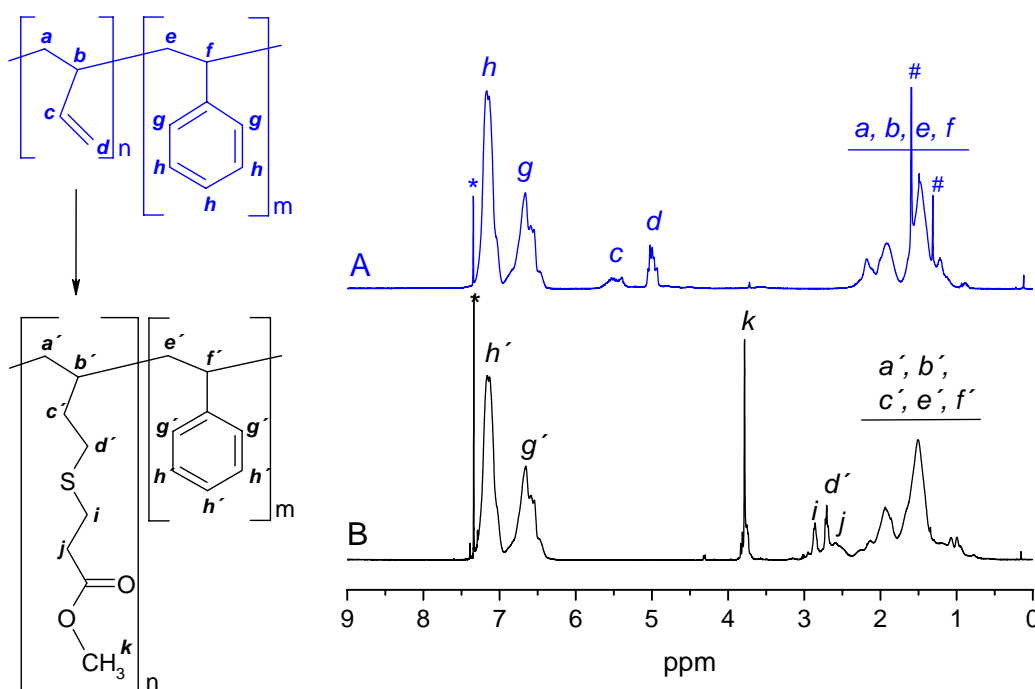


Figure 4.19.  $^1\text{H}$  NMR spectrum of the parent PB-PS block copolymer, *SI* (A) and the spectrum of the PB-PS block copolymer modified with methyl-3-mercaptopropionate, *SI-Es* (B); \*solvent peak ( $\text{CDCl}_3$ ), # solvent traces.

PB-PS block copolymers are often used as precursors for further chemical modifications. It has been reported that a wide variety of functional groups can be introduced to such copolymers by making use of two-step approaches. In the first step, reactive intermediates are prepared by means of epoxidation<sup>42</sup> or hydroxylation<sup>43</sup> of the double bonds of polybutadiene, which in the second step react with e.g. functional acid chlorides<sup>44-46</sup> *via* ring opening or esterification reactions yielding functionalised copolymers (section 2.3). However the one-step synthetic approach may represent an interesting alternative for the introduction of various functionalities to PB-PS block copolymers.

## 4.2 Self-organisation of modified block copolymers

One of the most fundamental properties of block copolymers is their ability to form various organized structures in dilute solutions (section 2.4.2). Self-organisation phenomena occur when the solvent introduced is selective for one of the blocks. The process is driven by minimisation of the contact between the insoluble block and the solvent, leading to spontaneous association of the copolymer chains. The size and shape of the formed aggregates are controlled by various factors, which, among many others, are: the Flory-Huggins interactions parameter, the degree of polymerisation of the individual copolymer blocks and the volume fractions of the blocks. The self-organisation of block copolymers in selective solvents has been intensively studied in the past 20-30 years.<sup>59,135</sup> Nevertheless, new synthetic methods are being continuously developed allowing easier access to interesting block copolymer materials,<sup>136-138</sup> hence sustaining interest in the field.

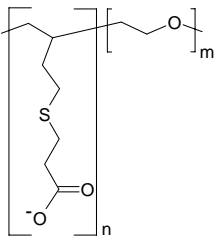
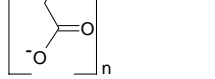
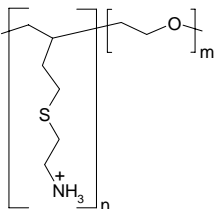
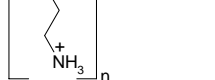
In the previous sections the modification of PB-PEO block copolymer precursors was described. The applied approach allowed for the attachment of various functions to the PB segment, including the carboxylic acid, amine or hydroxyl (diol) functions as well as fluorinated chains. The following studies concern the influence of the introduced groups on the self-organisation of the modified block copolymers. Firstly, the aggregation behaviour of ionic block copolymers in phosphate buffer solution is described. Then, investigations of the self-organisation of the diol-modified copolymer and the copolymer with introduced fluorinated chains in aqueous solutions are presented. Finally, general observations concerning the influence of the introduced groups on the self-organisation of modified block copolymers are discussed.

Characterisation of the aggregates was performed using dynamic and static light scattering (DLS/SLS), analytical ultracentrifugation (AUC), and atomic force microscopy (AFM); the principle of the above methods is described in section 3. From DLS measurements the hydrodynamic radius,  $R_h$ , was determined whereas SLS provided the radius of gyration,  $R_g$ , the second virial coefficient,  $A_2$ , and the apparent molecular weight of the aggregates,  $M_w^{\text{app}}$ . AUC provided the sedimentation coefficient distribution,  $g(s)$ , and the mean value of sedimentation coefficient,  $s$ . AFM micrographs allowed for the visualisation of the aggregates. Analysis was carried out using graphite substrate, on which the solutions were spin-coated.

### 4.2.1 Ionic block copolymers

Ionic block copolymers utilized in these studies have been synthesized *via* radical addition of suitable mercaptanes to the double bonds of PB in PB-PEO precursor block copolymers, as described in section 4.1.2.2. They consist of a segment bearing functional groups, which can be charged under appropriate conditions, and a water-soluble PEO block. For the self-assembly investigations, copolymers with carboxylic acid and primary amine functions have been selected. The structures and molecular characteristics of those copolymers are presented in Table 4.6.

Table 4.6. Molecular characteristics of PEO-polyion block copolymers (n, m: number-average of functionalised and ethylene oxide units, respectively).

PEO-polyion	Structure	Label	n	m
PEO-polyanion		<i>P1-Ac</i>	25	75
		<i>P2-Ac</i>	40	132
PEO-polycation		<i>P1-Am</i>	25	75
		<i>P2-Am</i>	40	132

The solvent utilized for these copolymers was a pH 7.2 phosphate buffer. The copolymers contain carboxylic acid or primary amine groups, therefore pH value around 7.2 should assure possibly high degree of ionisation of both types of functional groups, analogous to the system described by Harada and Kataoka.<sup>87</sup> At this pH, these block copolymers seem to be double hydrophilic since they contain a segment, which is highly charged, and a second segment, which is highly water-soluble (PEO block). Under the same conditions, for instance, in the solution of PEO-PAA (PAA – poly(acrylic acid)) no aggregates were observed. However, in the copolymers analysed here, charged groups are connected to a hydrocarbon backbone *via* a relatively long hydrophobic thioether spacer, the presence of which in every of the modified units leads to the self-organisation of these copolymers.

#### 4.2.1.1 PEO-polyanion block copolymers

The solutions of *PI-Ac* and *P2-Ac* in phosphate buffer (27 mM NaH<sub>2</sub>PO<sub>4</sub> in water, pH = 7.2), after 24 h of stirring, were opaque indicating that the copolymers formed aggregates. Dilute solutions (0.25 – 1.0 g/L) were examined by dynamic and static LS to obtain information on the size and shape of the formed aggregates. DLS showed the presence of large objects with hydrodynamic radii  $R_h \sim 256$  nm and 208 nm, respectively; the corresponding so-called dynamic Zimm plots are presented in Figure 4.20. SLS provided further information on the examined samples, such as the radius of gyration,  $R_g$ , the second virial coefficient,  $A_2$ , and the molecular weight of the aggregates,  $M_w^{\text{app}}$ , which are summarised in Table 4.7. These values were determined from Guinier-plots by extrapolation to  $q \rightarrow 0$  and  $c \rightarrow 0$  of data obtained from concentration- and angle-dependent measurements. Zimm plots could not be applied since the extrapolated values of  $M_w^{\text{app}}$  were too close to zero. Therefore small variations could lead to significant changes of the calculated  $M_w^{\text{app}}$  and  $R_g$  values. The extrapolation of the Guinier plot can be performed with higher accuracy since the data are displayed on a logarithmic scale.

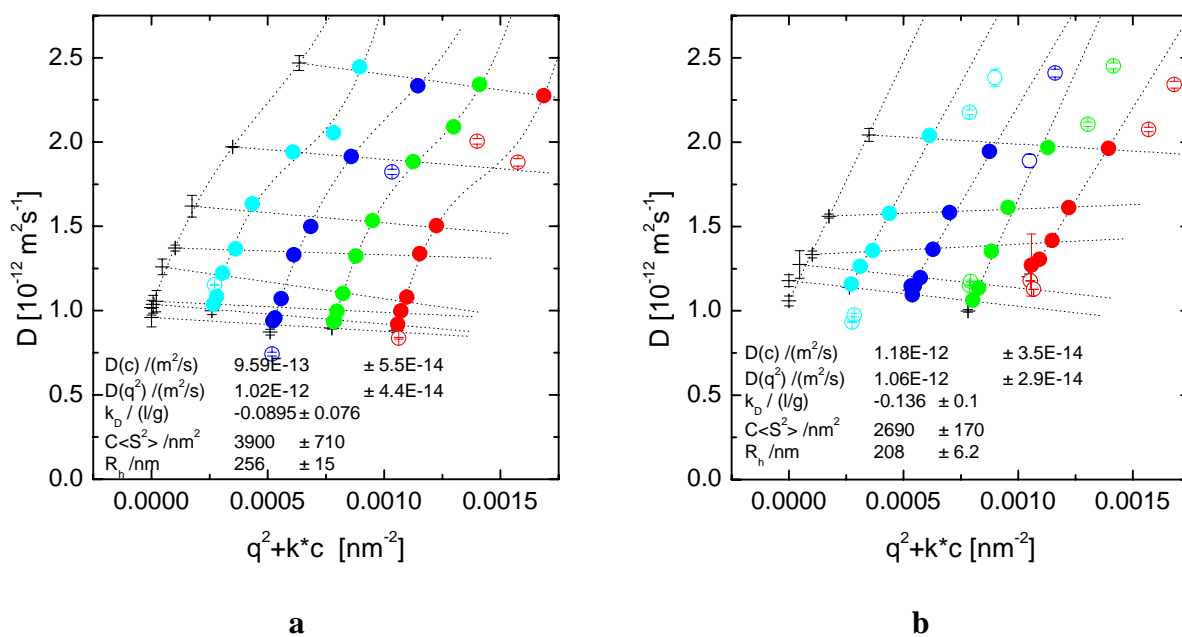


Figure 4.20. Dynamic Zimm-plots obtained from the DLS measurements carried out for the dilute phosphate buffer (pH = 7.2) solutions of the PEO-polyanion block copolymers: a) *PI-Ac*, b) *P2-Ac*.

Table 4.7. Experimental data obtained from DLS and SLS measurements for the dilute phosphate buffer solutions (pH = 7.2) of PEO-polyanion block copolymers, *P1-Ac* and *P2-Ac*.

Sample	$R_h$ [nm]	$R_g$ [nm]	$R_g/R_h$	$A_2$ [mol·L/g <sup>2</sup> ]	$M_w^{app}$ [g/mol]	$Z^{app}$
<i>P1-Ac</i>	256	188	0.73	$-1.6 \cdot 10^{-9}$	$1.0 \cdot 10^8$	13650
<i>P2-Ac</i>	208	181	0.87	$-4.5 \cdot 10^{-9}$	$6.2 \cdot 10^7$	5080

The sizes of the aggregates present in the solutions of *P1-Ac* and *P2-Ac* may suggest that these are vesicles; however, the corresponding masses are too low. As shown in appendix II the molecular weight of the aggregates is not sufficient for the formation of a membrane of a vesicle with  $R_h > 200$  nm. Calculated  $R_g/R_h$  values imply that the aggregates have a spherical shape. Furthermore, the negative values of  $A_2$  suggest the presence of strong attraction forces between the aggregates.

In order to obtain further information on the assemblies formed by PEO-polyanions in phosphate buffer, AUC measurements were performed. From the sedimentation velocity runs, sedimentation coefficient distributions,  $g(s)$ , could be obtained. In the solutions of *P1-Ac* and *P2-Ac*, sedimentation of one kind of species could be observed (Figure 4.21); mean values of sedimentation coefficient,  $s$  [S] (1S = 1 Svedberg =  $10^{-13}$  second), were 0.7 and 7.6, respectively.

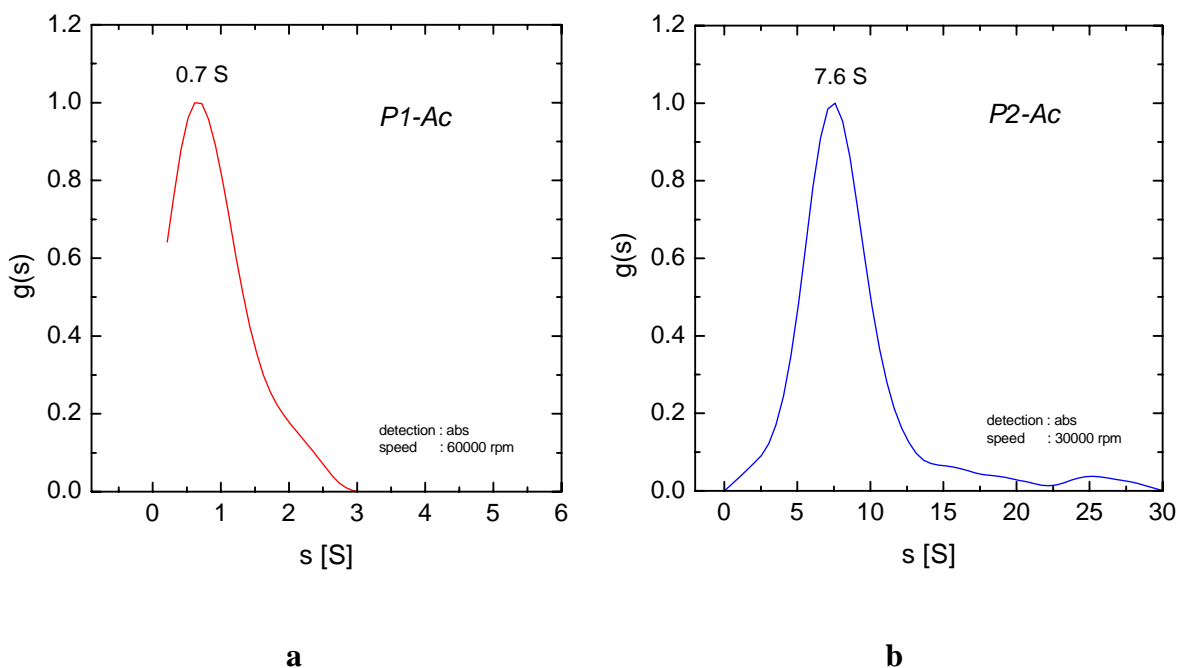


Figure 4.21. Sedimentation coefficient distributions,  $g(s)$ , obtained for the PEO-polyanion block copolymers in phosphate buffer: a) *P1-Ac*, b) *P2-Ac*.

It is known that particles, which are subjected to a centrifugal force sediment when their density is greater than that of the solvent. A low value for the sedimentation coefficient may imply that the mass of the particles is very low or that the density of the particles is very close to the density of the surrounding medium. However, the densities measured for *P1-Ac* and *P2-Ac* (summarised in Table 4.8) have a mean value of 1.2 g/cm<sup>3</sup>, whereas the density of the applied phosphate buffer is 0.995 g/cm<sup>3</sup>. Masses of the aggregates present in buffer solutions of *P1-Ac* and *P2-Ac* have values higher than 10<sup>7</sup> g/mol, as determined by means of SLS measurements. With such a difference in density and such a high mass, compact particles should sediment faster than observed. Slow sedimentation may also arise when the aggregates contain a relatively large amount of solvent, causing the low density difference between the particles and the surrounding medium. By combining the results obtained from the LS and AUC measurements and applying the equation (4.1) it is possible to calculate the partial specific volume of the aggregates,  $\bar{v}_a$ , which is the inverse of the density of the aggregates,  $\rho_a$ .

$$\bar{v}_a = \frac{1}{\rho_o} \cdot \left( 1 - \frac{sRT}{M_w D} \right) \quad (4.1)$$

where  $\rho_o$  is the density of the solvent,  $s$  is the sedimentation coefficient,  $R$  is the gas constant,  $T$  is the absolute temperature,  $M_w$  is the molecular weight of the particles and  $D$  is the diffusion coefficient. In Table 4.8 the calculated  $\rho_a$  values are summarised.

Table 4.8. Densities of the PEO-polyanion block copolymers,  $\rho_p$ , and densities of aggregates,  $\rho_a$ , in phosphate buffer solutions (pH = 7.2).

Sample	$\rho_p$ [g/cm <sup>3</sup> ]	$\rho_a$ [g/cm <sup>3</sup> ]
<i>P1-Ac</i>	1.241	0.997
<i>P2-Ac</i>	1.254	1.023

Obtained values of  $\rho_a$  are similar to the density of the phosphate buffer confirming that the sedimenting objects contain significant amounts of solvent. It was already discussed that these objects cannot be vesicles, in which the solvent could be incorporated inside. Therefore, the question arises as to what type of structure can satisfy all the parameters obtained from LS and AUC measurements. The most probable case seems to be the model where the

copolymers organise into micelles, which consequently form bigger clusters. Cluster formation is driven by attractive interactions between the micelles (negative  $A_2$  values). These interactions are based on the strong attraction between the micellar cores, which usually originates from van der Waals forces. However, in this case, the core-core attraction is highly increased due to the presence in the micellar cores of highly polarisable, charged sodium carboxylate groups. The clusters, although large, constitute a few loosely connected micelles and are highly swollen with the surrounding solvent, thus their low sedimentation rate.

The above model seems to be confirmed by AFM, which revealed the presence of small micellar objects. The solutions, originally at the concentration of 1 g/L, had to be diluted 500 times in order to disrupt the interactions between the micelles so as to be able to observe them separately. The exemplary micrographs taken for the PEO-polyanion block copolymer, *PI-Ac*, are presented in Figure 4.22. In this micrographs, aggregated micelles can be observed despite the high dilution of the sample, confirming the presence of relatively strong interactions between these micelles.

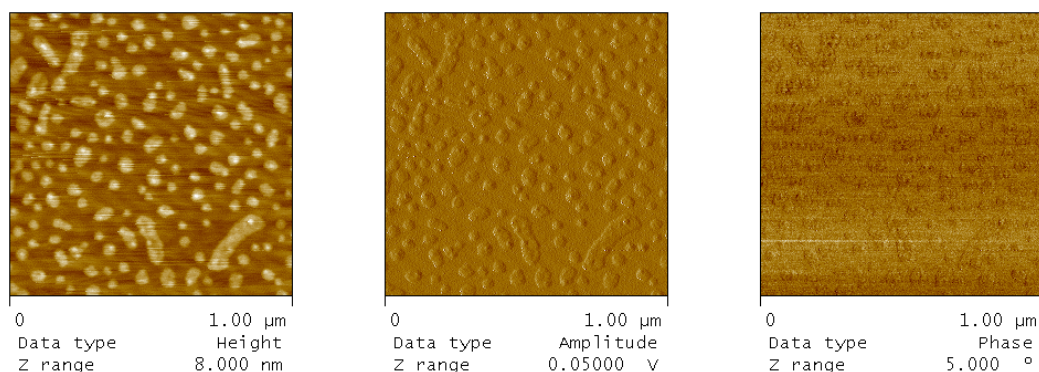


Figure 4.22. AFM micrographs of micelles formed by the PEO-polyanion block copolymer, *PI-Ac*; the solution (0.002 g/L) was spin-coated on graphite.

#### 4.2.1.2 PEO-polycation block copolymers

PEO-polycation block copolymers, *PI-Am* and *P2-Am*, were dissolved in phosphate buffer (pH = 7.2) and the obtained solutions were analysed by means of AUC, LS and AFM. In both samples AUC revealed the presence of two kinds of species. Figure 4.23 depicts the obtained sedimentation coefficient distributions,  $g(s)$ .



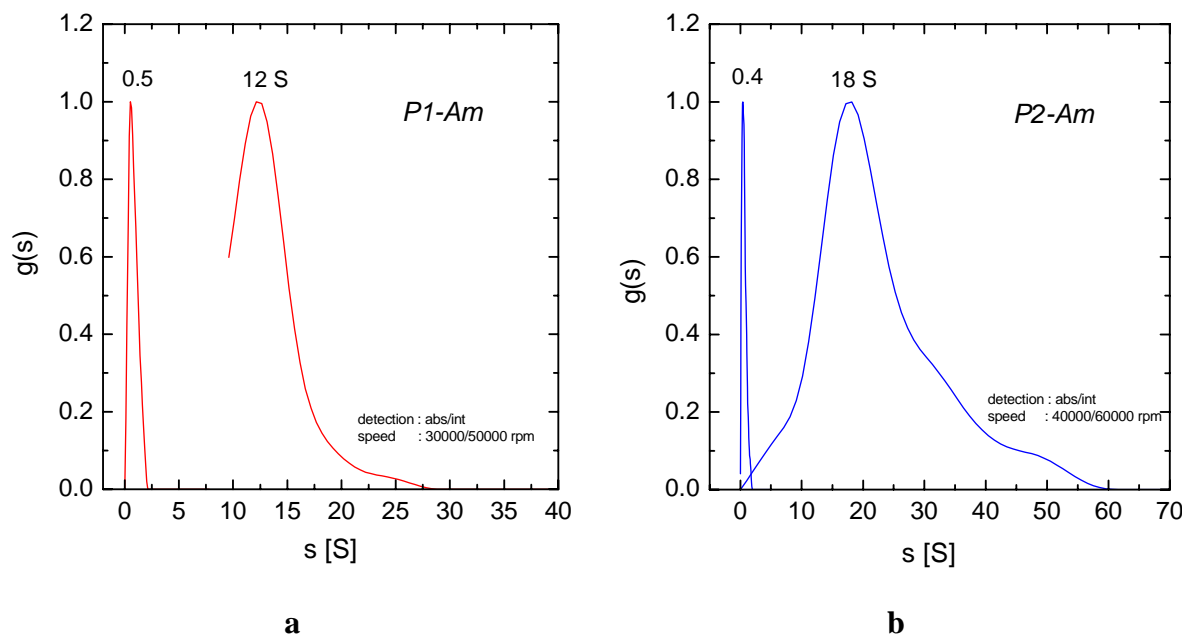


Figure 4.23. Sedimentation coefficient distributions,  $g(s)$ , obtained for the PEO-polycation block copolymers in phosphate buffer: a) sample *P1-Am*, b) sample *P2-Am*.

As can be seen, both samples exhibit similar bimodal sedimentation behaviour. From the fringe shift measured in the sedimentation velocity experiment, it was possible to calculate the contributions of both species in the total concentration of the copolymer in the samples (see section 3.3). For both, *P1-Am* and *P2-Am*, samples it was found, that the majority of the copolymer is incorporated into faster sedimenting species (higher  $s$  values), whereas the second peak around 0.5 S corresponds the minority of the total copolymer concentration. The mean values of the obtained sedimentation coefficients,  $s$ , as well as corresponding copolymer concentrations are summarized in Table 4.9.

Table 4.9. Sedimentation coefficients,  $s$ , obtained from AUC sedimentation velocity runs for the dilute phosphate buffer solutions (pH = 7.2) of PEO-polyion block copolymers.

Sample	$s_1$ [S]	$c_1$ [%]	$s_2$ [S]	$c_2$ [%]
<i>P1-Am</i>	0.5	29	12.6	71
<i>P2-Am</i>	0.4	16	19.2	84

For further characterisation of the aggregates formed by PEO-polycation block copolymers LS measurements were performed. DLS revealed a bimodal size distribution (Figure 4.24), pointing out that two kinds of species are present in the examined systems, which is in agreement with AUC results. In the *P1-Am* and *P2-Am* solutions, large aggregates

with  $R_h \sim 328$  nm and 233 nm, respectively, as well as smaller species with  $R_h \sim 20$  nm were detected. It was possible to divide the whole scattering intensity obtained from the angle dependent DLS into the contributions corresponding to the two populations present in the systems. Thus, obtained partial intensities could be separately visualised, similar to SLS data, in the angle/concentration dependent Zimm or Guinier plots, which provided the values of  $R_g$  and  $A_2$ .  $M_w$  values could also be determined, despite the bimodality of the whole system, since the contribution of the copolymer in every population was known from AUC measurements. Since the scattered intensity is proportional to the sixth power of the radius, the presence of large aggregates dominates the scattering. Thus, in case of the small aggregates, the quality of the obtained plots was not as high as for the larger aggregates, leading to difficulties in the data evaluation. Therefore, values obtained for smaller aggregates might possess a significant error. Results obtained from LS measurements are summarised in Table 4.10

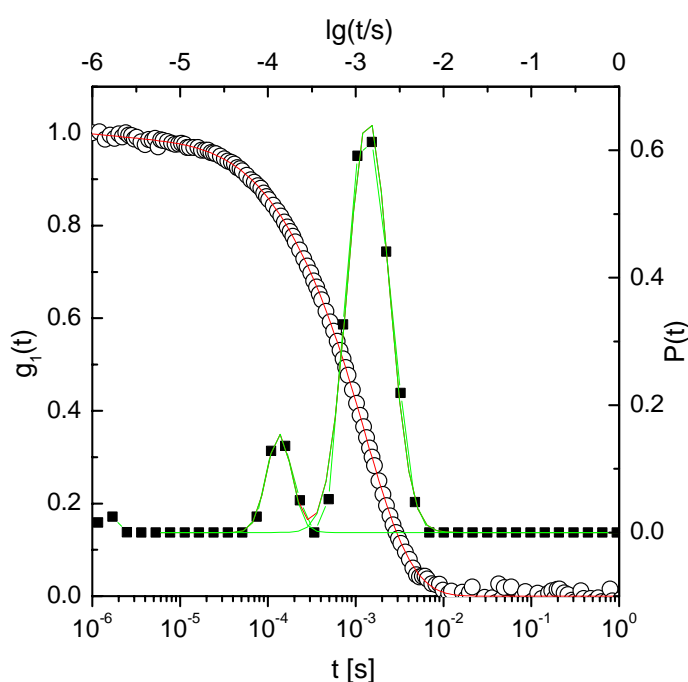


Figure 4.24. Field correlation function (circles) obtained from DLS of the PEO-polycation block copolymer, *PI-Am*, in phosphate buffer (0.985 g/L, 90°); evaluation of the data (squares) using program *Contin*.

Table 4.10. Experimental data obtained from DLS and SLS measurements for the dilute phosphate buffer solutions (pH = 7.2) of PEO-polycation block copolymers, *P1-Am* and *P2-Am*.

Sample	$R_h$ [nm]	$R_g$ [nm]	$R_g/R_h$	$A_2$ [mol·L/g <sup>2</sup> ]	$M_w^{app}$ [g/mol]	$Z$
<i>P1-Am</i>	328	215	0.65	$-1.2 \cdot 10^{-9}$	$5.7 \cdot 10^7$	7558
	19	41	2.16	$-8.2 \cdot 10^{-7}$	$5.1 \cdot 10^5$	68
<i>P2-Am</i>	233	202	0.87	$2.3 \cdot 10^{-9}$	$5.5 \cdot 10^7$	4375
	24	40	1.67	$-6.7 \cdot 10^{-8}$	$2.5 \cdot 10^6$	200

Like in the PEO-polyanion systems (section 4.2.1.1), the large aggregates detected in the solutions of PEO-polycation block copolymers might be clusters of loosely connected micelles. However, in the case of PEO-polycations, the micellar cores contain ammonium phosphate groups, which are less polarisable than sodium carboxylate groups present in PEO-polyanions. Hence, interactions between these micelles are weaker and apart from micellar clusters, also individual micelles can be observed. The small aggregates detected by LS should correspond individual micelles. By dividing  $Z$  numbers obtained for larger assemblies by  $Z$  number of individual micelles it was possible to calculate that one cluster contains about 20 (*P1-Am*) or 100 (*P2-Am*) micelles. Furthermore, the mean hydrodynamic volume of one cluster was compared with the volume of micelles. It was estimated that micelles constitute to only about 2 – 10% of the total volume of the cluster. Hence, clusters indeed contain large amounts of solvent, what explains their slow sedimentation rate in AUC experiments. Consequently, faster sedimenting species detected in sedimentation velocity runs should be separated micelles. As discussed before, in the *P1-Am* and *P2-Am* samples, the majority of the copolymer is incorporated into faster sedimenting species. Hence, it can be concluded that this solutions contain mostly individual micelles.  $R_g/R_h$  ratios calculated for this aggregates are significantly higher than 1, what may suggest a non-spherical morphology. However, AFM analysis did not reveal the presence of extended aggregates. Instead, spherical micelles could be observed as presented in Figure 4.25

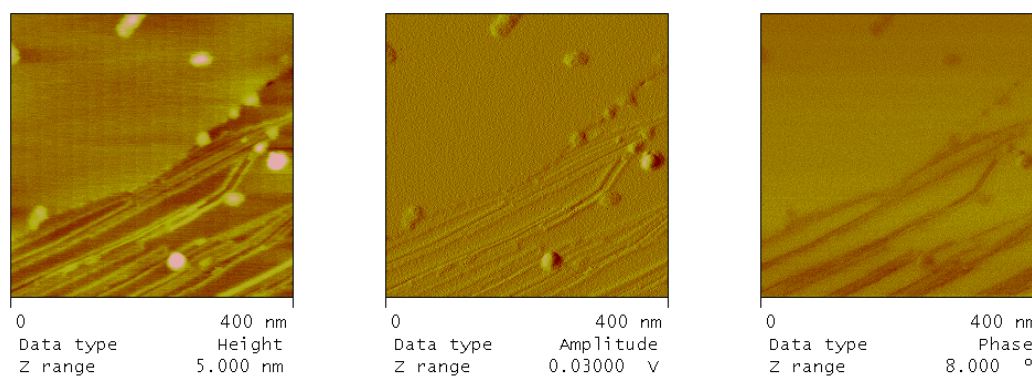


Figure 4.25. AFM micrographs of micelles formed by the PEO-polycation block copolymer, *PI-Am*; the solution was spin-coated on graphite.

#### 4.2.2 Diol-modified block copolymer

For investigations on the self-organisation of diol-modified copolymers, the block copolymer, *P2-Di*, having block lengths 40 and 132, respectively, was selected. This copolymer was synthesised as described in section 4.1.2.4 by radical addition of 3-mercaptopropanediol to the PB-PEO block copolymer precursor, *P2*.

The  $PB_{40}\text{-}PEO_{132}$  block copolymer precursor, *P2*, utilized in the synthesis of *P2-Di*, forms aggregates in aqueous solution with  $R_h = 26$  nm,  $R_g = 28$  nm, and  $M_w^{app} = 5.5 \cdot 10^6$  g/mol. Introduction of diol groups to the PB segment leads to a change of the  $\chi$  parameter as well as of the molecular volume and consequently has an influence on the self-organisation of this copolymer. In order to investigate the aggregation behaviour of *P2-Di*, aqueous solutions of this copolymer were prepared and characterised using dynamic and static LS. Angle-dependent measurements, performed on solutions within the concentration range between 0.25 and 1 g/L, revealed the presence of two types of species in the analysed system, with mean values of  $R_h$  of about 126 nm and 11 nm. However, as it was already mentioned in section 4.2.1.1, large aggregates give a much higher contribution to the scattering intensity than the small aggregates. In the DLS field correlation function, presented in Figure 4.26, the two populations can be very well seen, indicating that the amount of small particles is significantly higher than the amount of the large ones. Hence, it can be concluded that almost only small aggregates are present in the analysed sample. Assuming that the whole copolymer in the solution is incorporated into the small aggregates, it was possible to estimate their molecular weight as  $M_w^{app} = 6.5 \cdot 10^5$  g/mol. The corresponding  $Z$  number was calculated to be 53. The determined  $R_g$  was 36 nm, which when divided by the  $R_h$  value (11 nm) gives the

ratio of 3.3. Values of the  $R_g/R_h$  ratio, considerably higher than 1, are usually characteristic for rod-like aggregates.

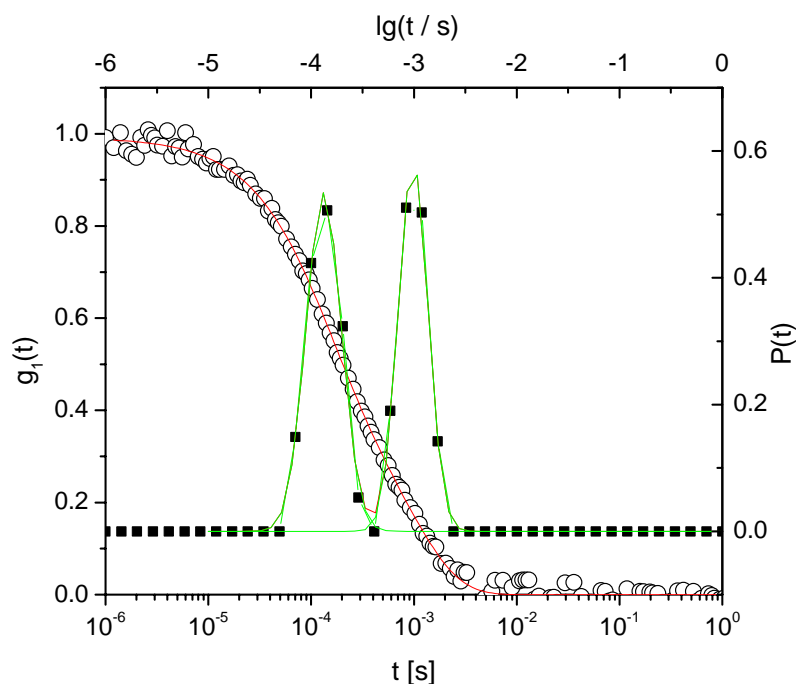


Figure 4.26. Field correlation function (circles) obtained from DLS of diol-modified copolymer, *P2-Di*, in water (1 g/L, 90°); evaluation of the data (squares) using program *Contin*.

The *P2-Di* solution was also characterised by means of AUC. Figure 4.27 depicts the sedimentation coefficient distributions,  $g(s)$ , of *P2-Di* and the corresponding precursor block copolymer, *P2*. As can be seen, the modified copolymer, *P2-Di*, sediments at a slower rate than the parent *P2*. This effect can be explained by the notably lower molecular weight of the aggregates formed in the solution of *P2-Di*. Also, their possible rod-like form can lead to more friction, slowing down the sedimentation process. The small fraction observed in *P2* sample, which sediments with  $s \sim 3$  S may correspond to aggregates containing only a few polymer chains, which were not detected by LS measurements. In the *P2-Di* sample only one sedimenting species was detected confirming the assumptions made by evaluation of the LS data.

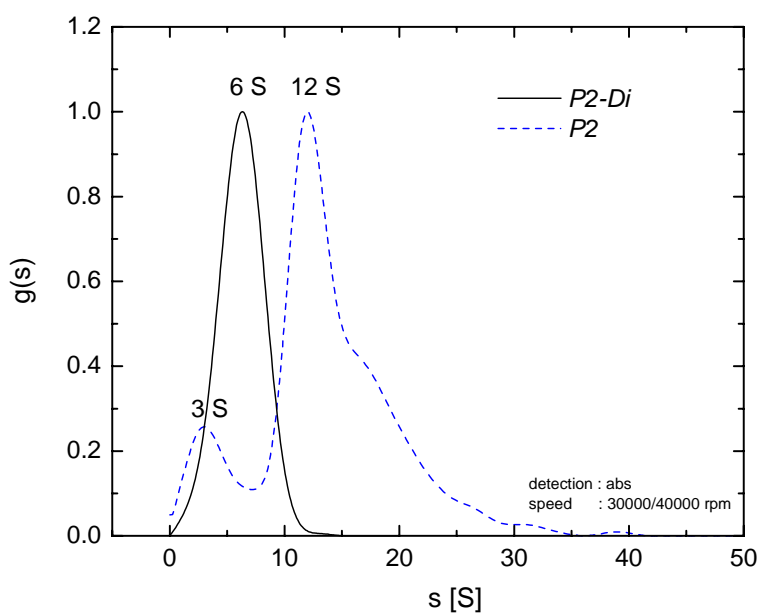


Figure 4.27. Sedimentation coefficient distributions,  $g(s)$ , of the diol-modified block copolymer,  $P2-Di$  (solid line), compared to the parent PB-PEO block copolymer,  $P2$  (dashed line), in aqueous solutions.

AFM analysis of  $P2-Di$  sample revealed the presence of rod-like aggregates presented in Figure 4.28. According to the data obtained from the cross-section analysis those aggregates are about 20 nm wide whereas their thickness is only about 2-3 nm. Hence, it seems reasonable, that the aggregates are flattened on the surface and their true thickness (diameter) in solution might be about 10-15 nm.

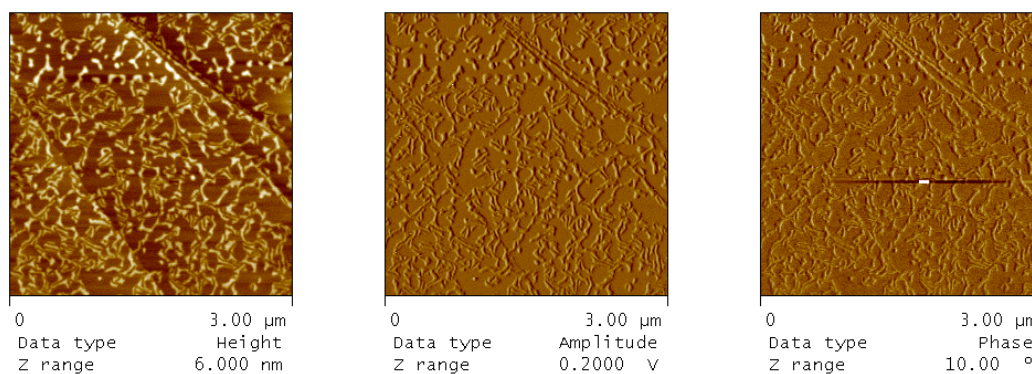


Figure 4.28. AFM micrographs of the aggregates formed by the diol-modified block copolymer,  $P2-Di$ , in aqueous solution; the solution was spin-coated on graphite.

### 4.2.3 Fluoro-modified block copolymer

In this study the self-organisation of a fluoro-modified  $PB_{40}$ - $PEO_{273}$  block copolymer,  $P3-Fl$ , in aqueous solutions is presented; details concerning the synthesis of this copolymer are described in section 4.1.2.5. Because of the high fraction of fluorinated chains, aqueous solutions of  $P3-Fl$  could not be prepared by direct dissolution of the copolymer in water. Therefore aggregates were prepared first by suspending the copolymer in water and then THF was added until the sample became optically clear. Subsequently the sample was let to stir until the complete evaporation of THF. Then the  $P3-Fl$  solution was analysed by means of AUC. Figure 4.29 depicts the sedimentation coefficient distribution obtained for the  $P3-Fl$  sample compared to that of the block copolymer precursor,  $P3$ . A change in the sedimentation behaviour of the copolymer after modification can be observed.

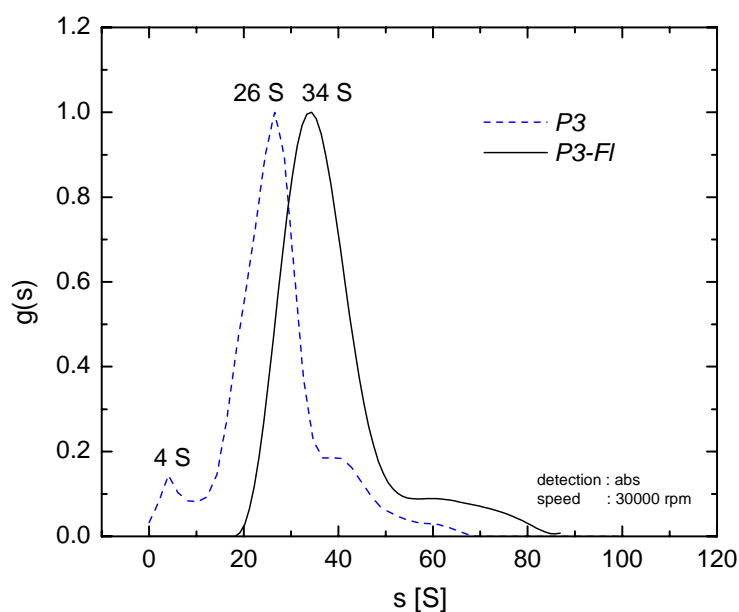


Figure 4.29. Sedimentation coefficient distributions,  $g(s)$ , of the fluoro-modified block copolymer,  $P3-Fl$  (solid line), compared to the parent PB-PEO block copolymer,  $P3$  (dashed line), in aqueous solutions.

LS measurements revealed the presence of two populations of aggregates as presented in Figure 4.30. Obtained  $R_h$  and  $R_g$  values are summarised in Table 4.11.

Table 4.11. Experimental data obtained from LS measurements of dilute solutions of fluoro-modified block copolymer, *P3-Fl*, in aqueous solutions.

Sample	$R_{h,1}$ [nm]	$R_{g,1}$ [nm]	$R_{g,1}/R_{h,1}$	$R_{h,2}$ [nm]	$R_{g,2}$ [nm]	$R_{g,2}/R_{h,2}$
<i>P3-Fl</i>	223	215	0.96	30	23	0.77

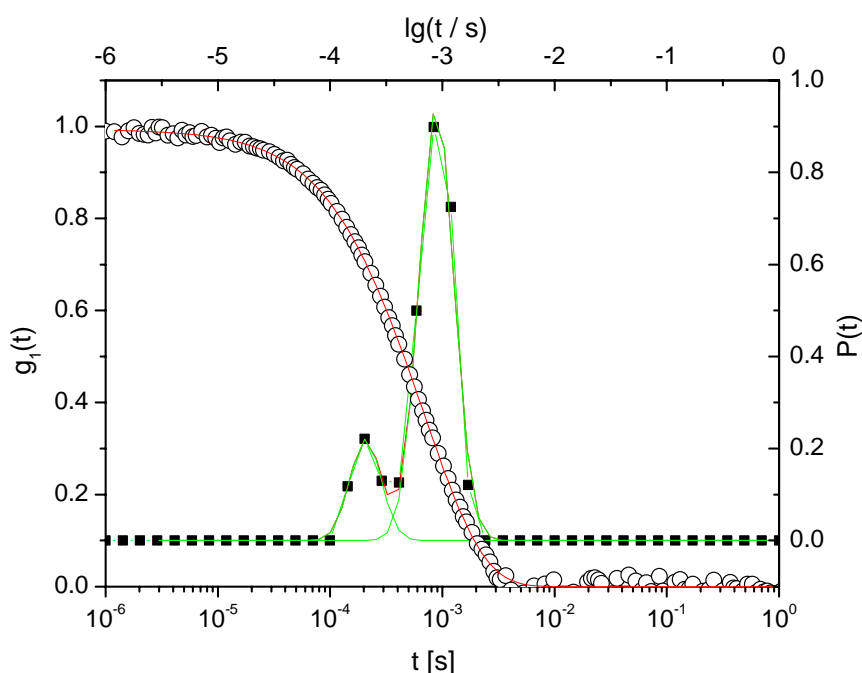


Figure 4.30. Field correlation function (circles) obtained from DLS of fluoro-modified copolymer, *P3-Fl*, in water (1,001 g/L, 90°); evaluation of the data (squares) using program *Contin*.

The  $R_g/R_h$  ratio calculated for the larger aggregates implies that this population contains vesicles, whereas in the case of the second population the  $R_g/R_h$  ratio indicates the presence of micelles. In the AFM micrographs (Figure 4.31) only one kind of aggregates can be observed, which, however, reveals a significant polydispersity. In the phase image, inside of each aggregate one can distinguish a small, bright spot. It may represent a domain, formed by fluorinated chains, which is embedded in the PEO matrix. As can be seen, some aggregates contain more than one spot, what may imply that within one aggregate more than one such a domain is present. Future investigations on this copolymer should include cryo-TEM analysis



in order to check, if the micellar cores exhibit a so-called multi-compartment character i.e. fluorinated chains and hydrocarbon parts form separated domains in the micellar core.

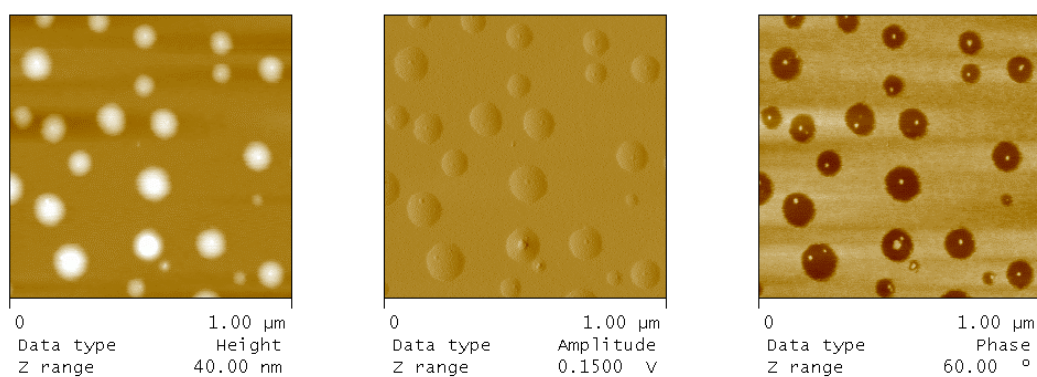


Figure 4.31. AFM micrographs of the aggregates formed by the fluoro-modified block copolymer, *P3-Fl*, in aqueous solution.

As already mentioned in section 4.1.2.5, the presence of partially fluorinated side chains should decrease the surface energy. In order to investigate this effect in the solution of *P3-Fl*, measurements of the surface tension using ring tensiometry were performed.<sup>139</sup> For this purpose, aqueous solutions within a broad range of concentrations were prepared ( $0.9 \cdot 10^{-6}$  – 2.4 mmol/L). The obtained surface tension isotherm is presented in Figure 4.32.

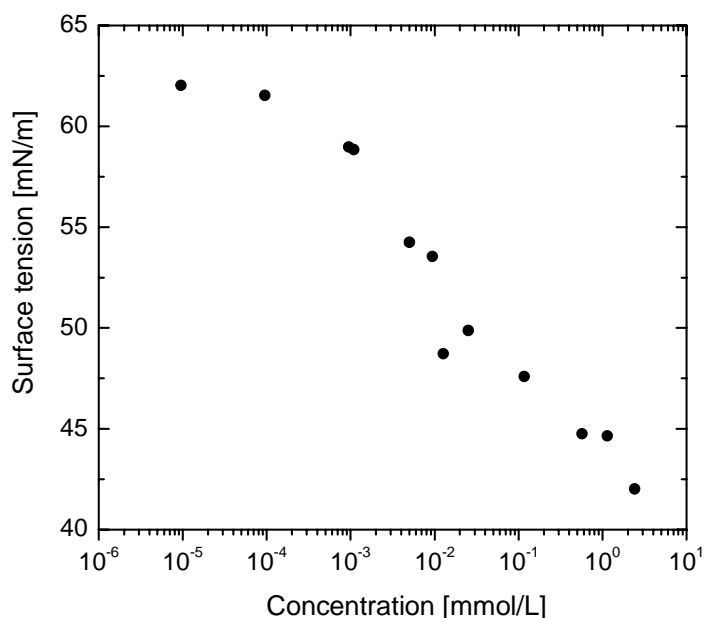


Figure 4.32. Surface tension isotherm obtained for the aqueous solutions of fluoro-modified copolymer, *P3-Fl*, concentration range:  $0.9 \cdot 10^{-6}$  – 2.4 mmol/L.

The surface tension starts to decrease at relatively low concentrations of *P3-Fl* and decreases continuously to the highest concentration investigated. For this concentration, the surface tension reaches the value of 42 mN/m. Further measurements at higher concentrations could not be performed due to a strongly increased viscosity of the *P3-Fl* copolymer solution. Nevertheless, it seems that the lower plateau cannot be reached because the exchange between the copolymer in micelles and at the water-air interface is rather slow and the equilibration of the system does not occur within the time frame of the measurement. In the case of low-molecular weight surfactants, this method allows also for determination of the critical micelle concentration (*cmc*). The *cmc* is in this case defined as the starting point of the lower plateau. However, this cannot be applied to block copolymers, since they start to build aggregates before the water-air interface is fully covered with polymer molecules and their *cmc* values are extremely low.<sup>140,141</sup> The obtained surface tension value is surprisingly high as compared to the values known for other fluorinated polymers; for example PTFE is characterised by surface tension energy of 18 mN/m. This effect seems to be connected with the experimental method applied. Low surface tension values can be obtained when the packing density of the molecules at the water-air interface is high. Small surfactant molecules can easily diffuse through the solution and organise at the interface. In the copolymer analysed here, fluorinated chains are grafted to the backbone of relatively large molecules. Therefore, diffusion is significantly slowed down and also the organisation of the fluorinated chains at the interface is hindered. Dense packing of the fluorinated chains is restricted because of sterical reasons arising from the presence of the large backbone as well as a loss of entropy due to the reduced degree of freedom of the chains at the interface.

An alternative method for the determination of the surface energy represents the measurement of the contact angle. In this method, the surface energy is determined for a polymer film instead of a polymer solution. Thus, the level of organisation of the chains at the interface should be increased. For the measurement, a silicon surface was covered with the *P3-Fl* block copolymer by drying a THF solution of the copolymer on the surface. Then, the contact angle for the drop of water on the surface was measured. The measurement was performed several times at different positions of the sample surface to obtain a representative average value. The determined mean contact angle,  $\theta$ , was of 100.4°. The surface energy can be calculated by applying the equation derived by Li and Neumann<sup>142</sup>

$$\cos \theta = -1 + 2(\gamma_s / \gamma_l)^{1/2} \exp(-\beta(\gamma_l - \gamma_s)^2) \quad (4.2)$$

where  $\beta$  is a constant ( $1.247 \cdot 10^{-4} \text{ m}^2/\text{mJ}^{-1}$ ). Thus, the surface energy of the solid,  $\gamma_s$ , can be determined from the experimentally obtained contact angle and the liquid surface tension,  $\gamma_l$  ( $\gamma_l$  for water = 72.3 mN/m). For the analysed film, the surface energy was calculated to be 22.5 mN/m. This value seems to be much more reasonable than the value obtained by ring tensiometry and confirms that the surface of *P3-Fl* block copolymer reveals the reduced surface energy.

#### 4.2.4 Influence of introduced groups on the self-organisation behaviour

In the previous sections, the self-organisation behaviour of four types of chemically modified block copolymers was described. Aqueous solutions of copolymers with introduced carboxylic acid, primary amine and hydroxyl groups as well as fluorinated chains were characterised in detail. Depending on the nature of the functional groups, the properties of the modified block changes and with it the aggregation behaviour of the block copolymer. Since it was possible to introduce various functional groups to the same copolymer precursor, a direct comparison of the change in aggregation behaviour can be done. For example, three different functional block copolymers obtained by modification of PB<sub>40</sub>-PEO<sub>132</sub> precursor (*P2*) can be compared. In Table 4.12 the characteristics of the aggregates formed by these copolymers in the aqueous solutions are summarised.

Table 4.12. Characteristics of the aggregates formed in aqueous solution of block copolymers obtained by modification of PB<sub>40</sub>-PEO<sub>132</sub> (*P2*) block copolymer precursor (*Ac*-carboxylic acid, *Am*-amine, *Di*-diol).

Sample	$R_h$ [nm]	$R_g$ [nm]	$R_g/R_h$	$A_2$ [mol·L/g <sup>2</sup> ]	$M_w^{app}$ [g/mol]	$Z$
<i>P2</i>	26	28	1.08	$6.7 \cdot 10^{-10}$	$5.5 \cdot 10^6$	682
<i>P2-Ac</i> *	208	181	0.87	$-4.5 \cdot 10^{-9}$	$6.2 \cdot 10^7$	5080
<i>P2-Am</i>	24	40	1.67	$-6.7 \cdot 10^{-8}$	$2.5 \cdot 10^6$	200
<i>P2-Di</i>	11	36	3.3	$-8.4 \cdot 10^{-8}$	$6.5 \cdot 10^5$	53

\* Data for micellar clusters

As was already discussed, in the solution of the *P2-Ac* copolymer, isolated aggregates could not be detected since they are incorporated in large clusters. Therefore, the data

obtained cannot be directly compared with other listed copolymers. Nevertheless, it can be concluded that the presence in the modified segment of highly polarisable carboxylate groups significantly changed the aggregation behaviour, when compared with the precursor block copolymer. By comparing the *P2* precursor with amine- (*P2-Am*) and diol- (*P2-Di*) modified block copolymers some trends can be observed. The size of the aggregates decreases with increasing polarity (hydrophilicity) of the introduced groups. Similar trend can be observed for  $M_w^{app}$  or  $Z$ . Aggregates formed by the precursor block copolymer, *P2*, have the highest values of the  $R_h$  and  $M_w^{app}$ . Slightly smaller in size aggregates are formed by *P2-Am*, which also reveal significantly lower  $M_w$  values. Furthermore, the  $R_g/R_h$  ratio suggests their elongated shape. However, by means of AFM, only spherical micelles were visualised. Between these micelles attracting interactions are present, therefore in the solution of *P2-Am* a small amount of large aggregates was also detected. The *P2-Di* block copolymer, containing two polar hydroxyl groups, is characterised by the smallest values of  $R_h$  and  $M_w^{app}$ . Moreover, formed aggregates have a non-spherical morphology, what differentiates them from the aggregates of *P2* and *P2-Am* block copolymers. The formation of rod-like aggregates could be possibly induced by the presence of additional energy contributions such as hydrogen bonding between the hydroxyl groups. Interestingly, in aqueous solutions of *P2-Di* prepared by dialysis from methanol or dioxane spherical aggregates were observed.<sup>143</sup>

Future investigations should include preparation of a series of modified block copolymers with introduced groups causing an increase in the hydrophobicity of the modified block. For example, introduction of alkyl or fluorinated chains represents one of possible modifications. It seems probable that for such a series of modified block copolymers opposite trends in aggregation behaviour will be observed.

### 4.3 Block copolymer complexes

As was already mentioned in section 2.4.3, combination of self-organisation with molecular recognition can lead to greater structural complexity and functionality. Additional energy contributions, originating from noncovalent interactions such as dipole-dipole, hydrogen bonding, van der Waals and electrostatic interactions are being applied to the self-organisation of polymers and preparation of complex macromolecular assemblies.<sup>4,76,77</sup> For example, mutual electrostatic interactions occurring in the mixtures of oppositely charged chains were found to act as a driving force for the formation of polyion complexes, *PIC*. This

strategy has been adopted by several groups for the production of various micellar<sup>84</sup> or vesicular<sup>85</sup> aggregates as well as solid state structures.<sup>86</sup> Another example is the self-organisation of polymers based on multiple hydrogen-bonding interaction, which has been extensively studied by the group of Rotello.<sup>94,95</sup>

In the following study, functionalised block copolymers are utilized for the preparation of complexes based on: (i) electrostatic or (ii) hydrogen-bonding interactions. Firstly, the formation of polyion complexes in the mixtures of oppositely charged ionic block copolymers is described. Two possibilities are taken into account, when oppositely charged blocks are of the same length and when block copolymers with unequal lengths of the charged blocks are mixed. Finally, investigations on the possible formation of hydrogen-bonded complexes between diol and acetoacetoxy units of suitable block copolymers in toluene are described.

#### **4.3.1 Polyion complexes of ionic block copolymers with equal lengths of the oppositely charged blocks**

The inspiration for these studies arose from the results of Harada and Kataoka on polyion complex (*PIC*) micelles prepared from a pair of oppositely charged block copolymers with a poly(ethylene oxide) block.<sup>87</sup> The charged blocks were poly(L-lysine) as the polycation and poly( $\alpha,\beta$ -aspartic acid) as the polyanion. They achieved the formation of *PIC* micelles in aqueous solution at a pH 7.29, where both block copolymers had a high degree of ionisation.

For the preparation of polyion complexes, PEO-polyion block copolymers were utilized (section 4.2.1). *PI-Ac* and *PI-Am* (shorter block lengths) as well as *P2-Ac* and *P2-Am* (longer block lengths) were dissolved in phosphate buffer at pH = 7.2. The solutions were mixed in an equal unit ratio of acid and amine residues in the block copolymers, aiming at electrostatically neutralized conditions. The obtained mixed solutions, *PI-AcAm* and *P2-AcAm*, were stirred overnight and then investigated by AUC to check whether complex formation took place. The sedimentation coefficient distribution of the copolymers in the mixture was compared to those obtained for the separated copolymers. The results of the AUC measurements for PEO-polyanions as well as PEO-polycations have been already discussed in section 4.2.1. If the copolymers do not interact with each other, the sedimentation coefficient distribution in the mixture should correspond to that of the separated copolymers. In the case a complex was formed, a change in the sedimentation coefficient distribution should be observed. Figure 4.33 depicts the sedimentation coefficient

distributions in the samples *P1-Ac*, *P1-Am* and in the mixture, *P1-AcAm*. In the solution of *P1-Ac* one species, sedimenting with a mean value of  $s \sim 0.7$  S, was detected and in the solution of *P1-Am* two kinds of species could be distinguished, with mean  $s$  values of  $\sim 0.5$  S and 12 S. The AUC measurement for the mixed sample *P1-AcAm* revealed a different sedimentation coefficient distribution than in the solutions of separated copolymers. The presence of new species, sedimenting with a mean  $s$  value of 3.6 S, strongly suggests the formation of a *PIC*.

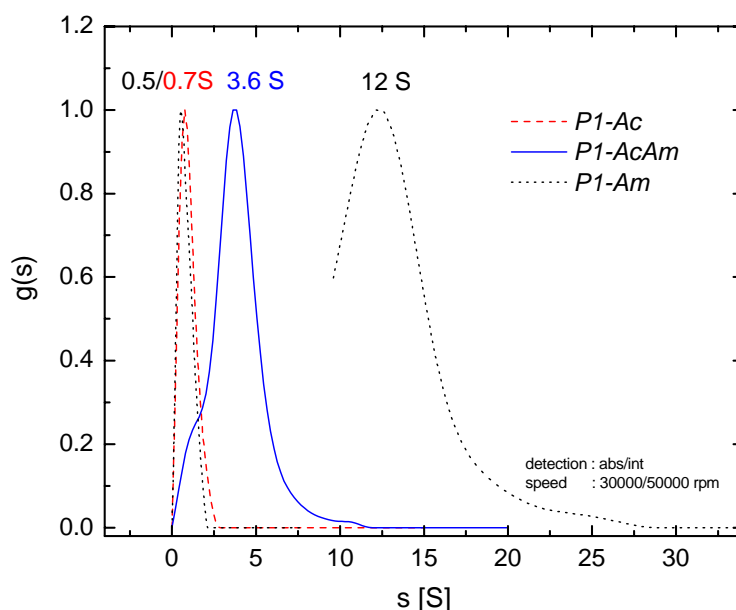


Figure 4.33. Sedimentation coefficient distributions of the samples PEO-polyanion (short), *P1-Ac* (dashed line), PEO-polycation (short), *P1-Am* (dotted line), and their mixture, *P1-AcAm* (solid line).

Figure 4.34 depicts the sedimentation coefficient distributions of the solutions containing copolymers with longer blocks: *P2-Ac*, *P2-Am* and *P2-AcAm*. *P2-Ac* reveals the presence of one kind of species sedimenting with the mean  $s$  value of 7.6 S. From the bimodal sedimentation coefficient distribution in the *P2-Am* sample two mean values of  $s$  can be distinguished  $\sim 0.4$  S and 18 S. From the fringe shift, measured in the sedimentation velocity experiment, it was possible to calculate the contributions of both species in the total concentration of the copolymer in the sample. It was found, that the majority, i.e. 84%, of the *P2-Am* copolymer sediments with the mean  $s$  value of  $\sim 18$  S, whereas the peak around 0.4 S corresponds to only 16% of the total copolymer concentration. In the mixed *P2-AcAm* sample also a bimodal sedimentation coefficient distribution can be observed. One species sediments

with the mean  $s$  value  $\sim 7$  S, which is similar to that of *P2-Am*. The second species sediments like the minority of *P2-Am* sample (0.4 S). However, the peak around 19 S, corresponding to the majority of the *P2-Am* copolymer, cannot be observed, what may indicate that this part of the *P2-Am* copolymer was incorporated into a complex.

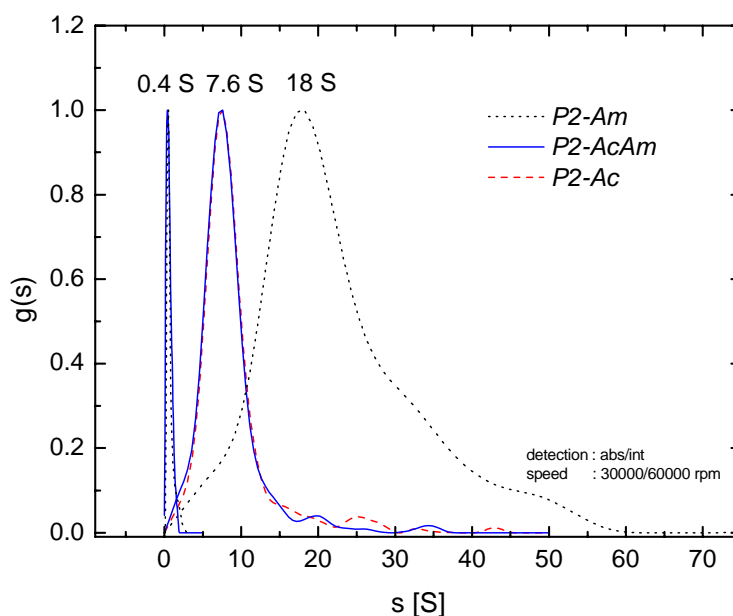


Figure 4.34. Sedimentation coefficient distributions of the solutions of PEO-polyanion (long), *P2-Ac* (dashed line), PEO-polycation (long), *P2-Am* (dotted line), and their mixture, *P2-AcAm* (solid line), in the phosphate buffer.

Dilute *P1-AcAm* and *P2-AcAm* solutions (1-0.25 g/L) were further characterised by means of LS, which revealed bimodal size distributions. Large species with  $R_h \sim 300$  nm as well as smaller particles with  $R_h \sim 20$  nm were detected. The obtained data were evaluated as was the case for PEO-polycation solutions (section 4.2.1.2) and provided further information on the analysed systems, summarised in Table 4.13 (for smaller species only  $R_h$  values are stated).

Table 4.13. Experimental data obtained from LS measurements for the mixtures of dilute solutions of block copolymers bearing carboxylic acid/primary amine functions in a pH = 7.2 phosphate buffer.

Sample	$R_h$ [nm]	$R_g$ [nm]	$R_g/R_h$	$A_2$ [mol·L/g <sup>2</sup> ]
<i>P1-AcAm</i>	345/23	278/-	0.80/-	$3.9 \cdot 10^{-10}$ /-
<i>P2-AcAm</i>	272/14	218/-	0.80/-	$8.9 \cdot 10^{-10}$ /-

The  $R_g/R_h$  ratios suggest that the analysed species have a spherical shape. Obtained  $A_2$  values are very low and possess a significant error ( $\sim 5 \cdot 10^{-10}$ ), therefore it is not clear whether any attraction between the aggregates is present. However, on the basis of AFM analysis, the presence of interactions between the aggregates can be supposed. Below, a series of micrographs obtained for the *P1-AcAm* sample is presented (Figure 4.35). The originally 1 g/L solution was diluted 10 times (a), 100 times (b) and than 500 times (c) so as to be able to observe separated micellar objects.

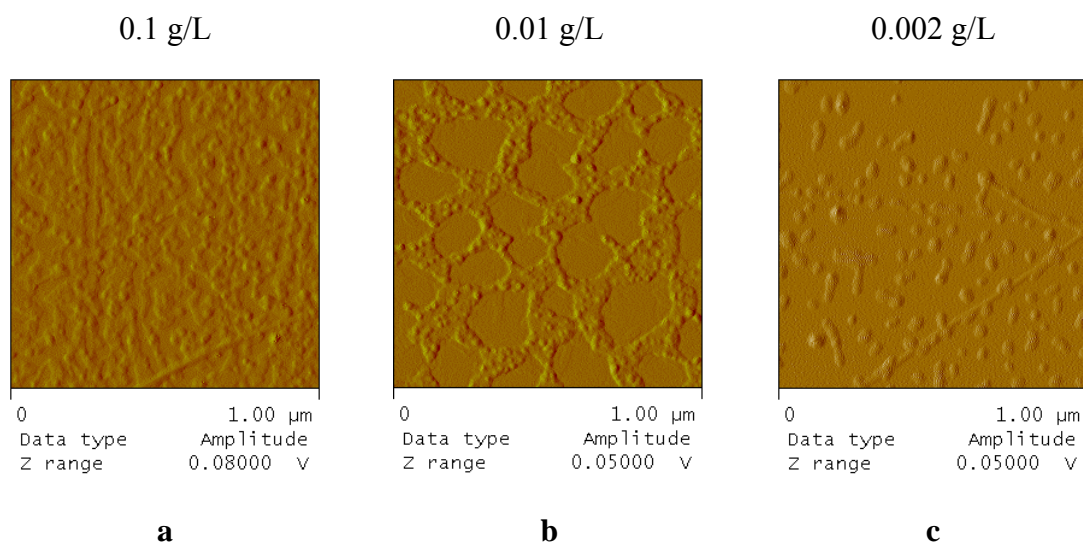


Figure 4.35. AFM micrographs of *PIC* micelles obtained by mixing of solutions of PEO-polyanion and PEO-polycation, sample *P1-AcAm*, concentrations: a) 0.1 g/L, b) 0.01 g/L, c) 0.002 g/L; solutions were spin-coated on graphite.

It was already discussed in section 4.2.1 that the separated PEO-polyion block copolymers form micelles, strongly attracting each other and thus forming micellar clusters. The same seems to hold true in the case of *PIC* resulting from mixing of these copolymers.



### 4.3.2 Polyion complexes of ionic block copolymers with unequal lengths of the oppositely charged blocks

In their investigations on the *PIC* micelles, Harada and Kataoka described that the formation of supramolecular assemblies from oppositely charged block copolymers is controlled by a so-called “chain length recognition”.<sup>88</sup> In the mixtures of copolymers with different block lengths, matched pairs with the same block lengths of polyanions and polycations formed exclusively. In order to prove whether chain length recognition takes place in the case of ionic block copolymers described here, mixtures of copolymers with different lengths of charged blocks were studied. For this purpose, phosphate buffer solutions of two PEO-polyanion and two PEO-polycation block copolymers (section 4.2.1) were utilized. Solutions of *PI-Ac* and *P2-Am* (short ionic and long cationic block) as well as *P2-Ac* and *PI-Am* (long ionic and short cationic block) were mixed together and the obtained mixed solutions *PIAc-P2Am* and *P2Ac-PIAm* were left to stir overnight to enable the formation of *PIC*. AUC sedimentation coefficient distributions of the mixed samples *PIAc-P2Am* and *P2Ac-PIAm* are presented in Figure 4.36 and Figure 4.37, respectively. Obtained results are compared to the sedimentation coefficient distributions of the corresponding separated PEO-polyion block copolymers. A significant change of sedimentation behaviour in the mixed samples can be observed: in both cases peaks originating from the separated copolymers are not present. Instead, a new peak appears confirming the formation of a *PIC*. Hence, it can be concluded that in the mixtures of oppositely charged copolymers described here, formation of *PIC* does not depend on the length of charged blocks.

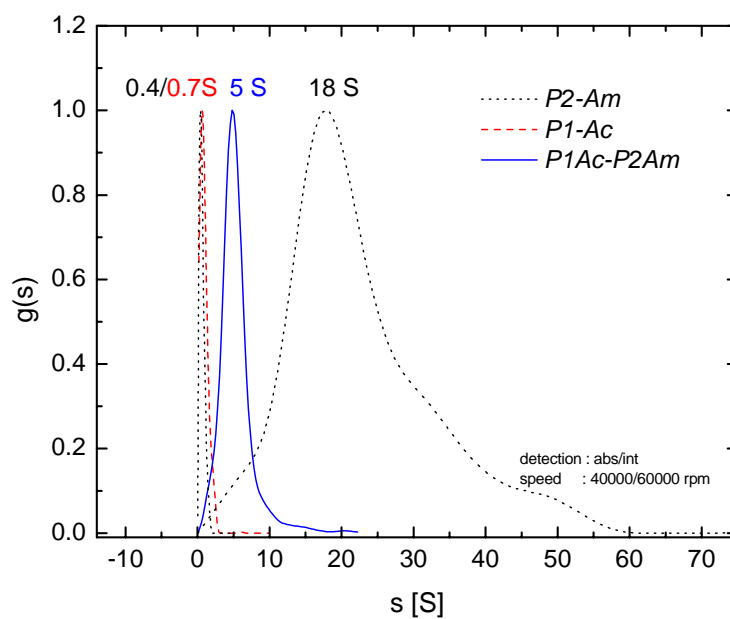


Figure 4.36. Sedimentation coefficient distributions of the PEO-polyanion (short),  $P1-Ac$  (dashed line), PEO-polycation (long),  $P2-Am$  (dotted line), and their mixture  $P1Ac-P2Am$  (solid line), in the phosphate buffer.

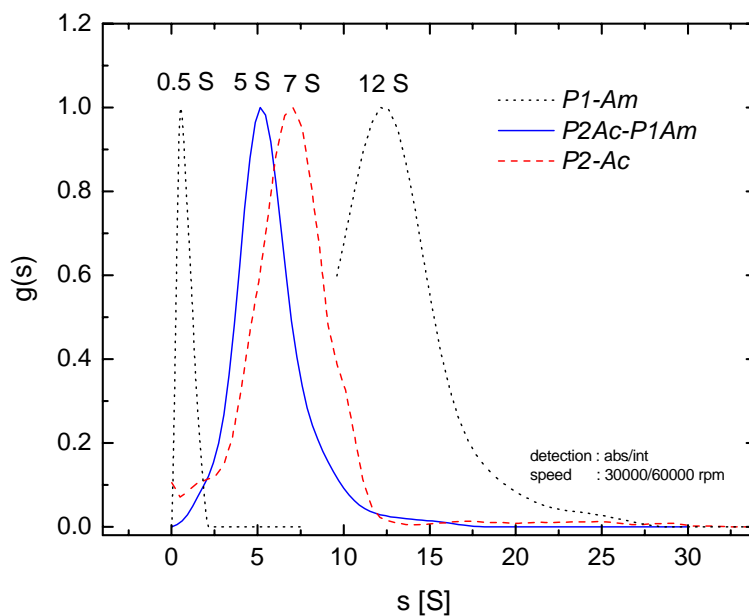


Figure 4.37. Sedimentation coefficient distributions of the PEO-polyanion (long),  $P2-Ac$  (dashed line), PEO-polycation (short),  $P1-Am$  (dotted line), and their mixture  $P2Ac-P1Am$  (solid line), in the phosphate buffer.

For dilute solutions of *PIAc-P2Am* and *P2Ac-PIAm* LS measurements were performed. The obtained results are summarised in Table 4.14. Two kinds of species, having  $R_h \sim 300$  nm and  $\sim 20$  nm, should correspond to micellar clusters and isolated micelles, respectively, as was already suggested for *PIC* of copolymers with equal chain lengths (section 4.3.1).

Table 4.14. Experimental data obtained from LS measurements for the mixtures of dilute solutions of block copolymers bearing carboxylic acid/primary amine functions in a pH = 7.2 phosphate buffer.

Sample	$R_h$ [nm]	$R_g$ [nm]	$R_g/R_h$	$A_2$ [mol·L/g <sup>2</sup> ]
<i>PIAc-P2Am</i>	296/13	218/-	0.74/-	$-6.3 \cdot 10^{-10}$ /-
<i>P2Ac-PIAm</i>	262/26	242/-	0.92/-	$2.4 \cdot 10^{-9}$ /-

### 4.3.3 Hydrogen-bonded complexes in toluene

The diol-modified block copolymer, *P2-Di*, contains two hydroxyl groups, which can play the role of hydrogen-bond donor centres for a molecule containing suitable hydrogen-bond acceptor sites. A suitable acceptor can be, for example an acetoacetoxy unit present in a poly((2-acetoacetoxy)ethyl methacrylate)-poly(*n*-butyl methacrylate) block copolymer, PAEMA-PBMA. Molecular recognition between these complementary hydrogen-bonding components might lead to the formation of a hydrogen-bonded complex as illustrated in Figure 4.38. The PAEMA-PBMA block copolymer (*R9*), having block lengths 30 and 206, respectively, was synthesised by Dr. Theodora Krasia.<sup>144</sup>

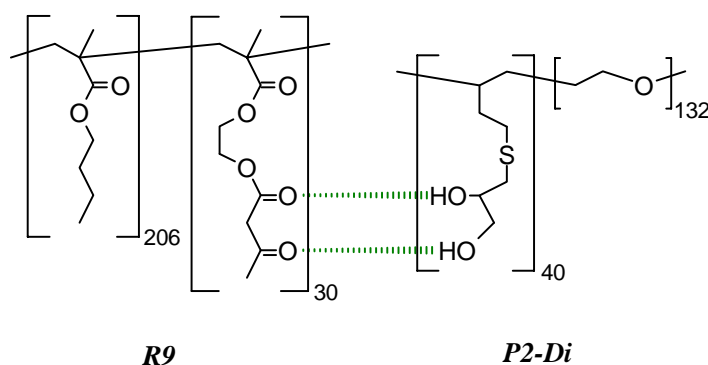


Figure 4.38. Schematic illustration of hydrogen bonding interactions between the acetoacetoxy units of poly((2-acetoacetoxy)ethyl methacrylate)-poly(*n*-butyl methacrylate), *R9*, and the diol groups of poly((2,3-dihydroxypropyl)thioethyl-ethylene)-poly(ethylene oxide), *P2-Di*.

For the complexation studies, solutions of the separated block copolymers in toluene were prepared. Toluene was chosen because this solvent acts as a weak hydrogen-bond donor and thus should promote the hydrogen-bonding interactions between the copolymers. The toluene solutions of *P2-Di* and *R9* were mixed together (1:1 molar ratio) and stirred overnight to enable formation of the complex. Then, AUC was applied to compare the sedimentation coefficient distributions of the copolymers in the separated solutions to that in the mixture (Figure 4.39). The results obtained from AUC measurements indicate that the complex indeed resulted: in the mixture, instead of separated sedimentation coefficient distributions corresponding to the separated copolymers, only one sedimenting species appeared.

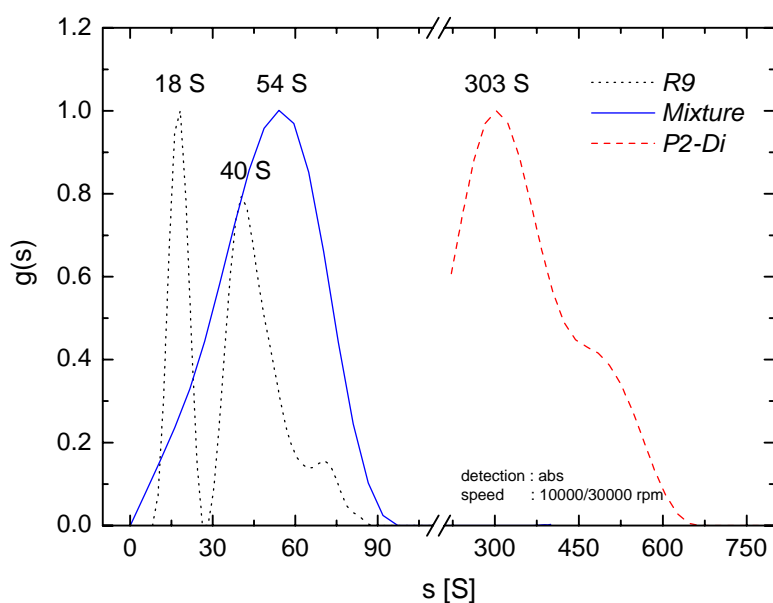


Figure 4.39. Sedimentation coefficient distributions,  $g(s)$ , of poly((2-acetoacetoxy)ethyl methacrylate)-poly(*n*-butyl methacrylate), *R9* (dashed line), the diol-modified copolymer, *P2-Di* (dotted line), and their mixture (solid line), in toluene.

Dilute solutions (0.25 – 1 g/L) of *P2-Di* were characterised by means of dynamic and static LS measurements. For unknown reason the quality of the obtained plots was not very high, as can be seen in Figure 4.40, and some of the experimental points were not considered.

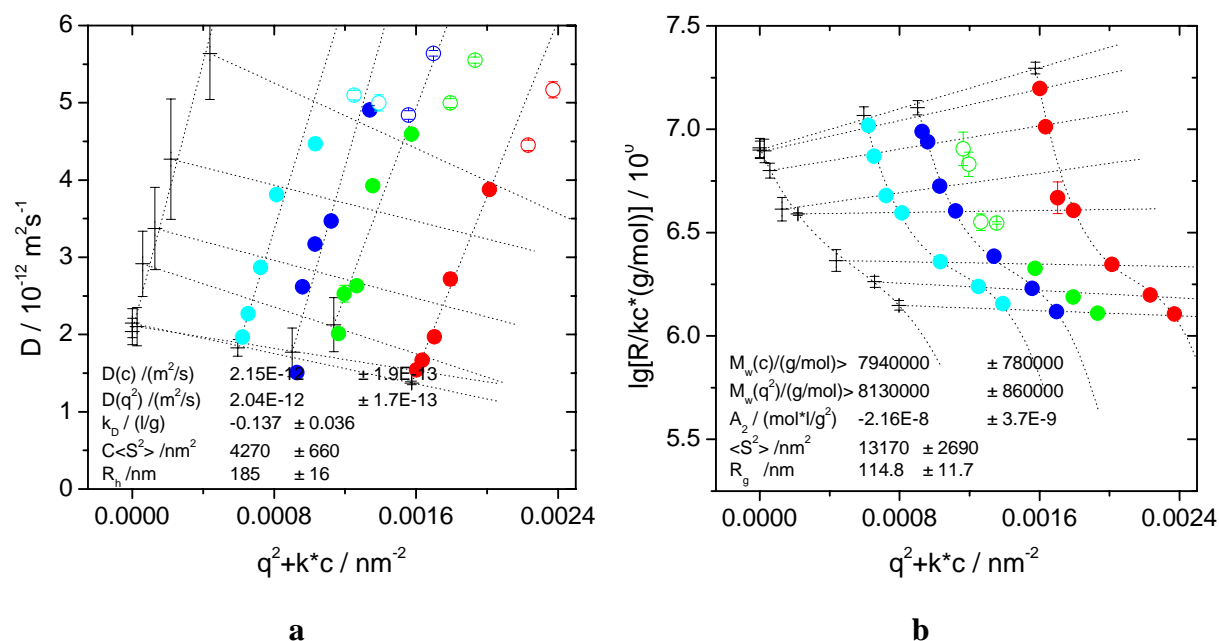


Figure 4.40. a) Dynamic Zimm-plot and b) Guinier-plot, obtained from LS measurements carried out for dilute aqueous solutions of the diol-modified copolymer, *P2-Di*.

Nevertheless, it was attempted to extract some information about the examined system. It could be estimated that the analysed species have  $R_h$  of about 185 nm and  $R_g$  of about 115 nm. The  $R_g/R_h$  ratio (0.62) indicates that the aggregates have spherical shape. Moreover, the negative value of  $A_2$  ( $-2.2 \cdot 10^{-8} \text{ mol} \cdot \text{L}/\text{g}^2$ ) implies the presence of attraction between the aggregates. The *R9* sample could not be characterised by means of LS due to similar refractive indices of PBMA block and toluene. For the same reason, a full characterisation of the mixed sample could not be achieved.

## 5 SUMMARY AND OUTLOOK

Well-defined block copolymers bearing desirable functional groups are of great interest. In this thesis, a modular synthetic approach allowing for the preparation of well-defined functional block copolymers has been presented. This approach is based on the chemical modification of PB-containing block copolymer precursors by radical addition of  $\omega$ -functional mercaptanes. Due to the commercial availability of various functional mercaptanes, this addition reaction represents a convenient route for the production of a library of functional block copolymers.

Functionalities were introduced by addition to the unsaturations of the PB block. It is known that PB can possess two types of microstructure, namely the 1,2- and 1,4-types. Since both types of PB reveal different reactivities, model reactions of methyl-3-mercaptopropionate with PB of the 1,2- and 1,4-type were performed. The obtained results proved that radical addition of mercaptanes to PB double bonds occurs in an anti-Markownikoff fashion and involves both the vinyl (1,2-type) as well as the in-chain (1,4-type) double bonds. The reaction proceeds smoothly without the formation of cross-linked products when the PB block contains a high amount of 1,2-type units.

Modifications of three different 1,2-polybutadiene-poly(ethylene oxide) (PB-PEO) block copolymers were performed with a series of  $\omega$ -functional mercaptanes. Firstly, model additions of methyl-3-mercaptopropionate were carried out. As a result, highly functionalised block copolymers were obtained. Importantly, the narrow molecular weight distributions of the block copolymer precursors are preserved during the modification process. In the following modifications, mercaptanes containing functional groups such as carboxylic acid, primary and tertiary amine were used. Consequently, copolymers containing a block, which can be charged under appropriate conditions, have been prepared. Thus, the addition of  $\omega$ -functional mercaptanes represents an alternative method for the production of ionic block copolymers. The addition reaction using protected amino acid (cysteine) may represent the first step in the direction of synthetic polymers with introduced oligopeptide sequences. Further development of this approach may lead to the production of so-called “molecular chimeras”, polymers containing synthetic and peptide blocks. Other interesting examples are hydroxyl (diol) functionalities as well as perfluoroalkyl chains, which were also successfully attached to the PB-PEO block copolymers. Finally, the extension of the concept to 1,2-

polybutadiene-polystyrene (PB-PS) block copolymers was demonstrated by the exemplary addition of methyl-3-mercaptopropionate. In all cases, modified copolymers were obtained in high yield and purity as demonstrated by  $^1\text{H}$  NMR, FT-IR and SEC analysis. In general, the applied modification method gives facile access to well-defined block copolymers bearing various functional groups. In the future, this library of functional block copolymers may be extended with samples containing, for example, phosphonates, oligopeptides, nucleobases and sugars.

Studies concerning the influence of the introduced groups on the self-organisation of the modified block copolymers in aqueous solution were also performed. Firstly, the aggregation behaviour of ionic block copolymers was described. In a pH 7.2 phosphate buffer, block copolymers possessing carboxylate or ammonium groups form aggregates of supposedly micellar character. Attractive interaction between these micelles leads to the formation of larger clusters, which are highly swollen with surrounding solvent. Further investigations on the self-organisation of the modified block copolymers involved the aggregation behaviour of the diol-modified block copolymer. It was observed, contrary to first expectations, that in aqueous solution this copolymer forms rod-like aggregates. The study of the aggregation behaviour of the copolymer with introduced fluorinated chains revealed that this copolymer forms spherical micelles in aqueous solution. AFM analysis allowed for visualisation of these aggregates, each containing a well observable area assigned to the fluorinated chains, embedded in the PEO matrix. Future investigations on this copolymer will include cryo-TEM analysis to investigate whether the micellar cores exhibit a so-called multicompartment character, i.e. separated domains of fluorinated and hydrocarbon regions. Studies of the aggregation behaviour allowed some general conclusions to be drawn concerning the influence of the introduced groups on the self-organisation of the modified copolymers. For a series of modified block copolymers with the same block lengths it was observed that the size of aggregates as well as the aggregation number decreases with increasing hydrophilicity of the introduced groups. Further investigations will include a similar series but with increasing hydrophobicity of the modified block to investigate whether opposite trends will be observed.

In the following studies, functionalised block copolymers were utilized for the preparation of complexes based on: (i) electrostatic and (ii) hydrogen-bonding interactions. Firstly, the formation of polyion complexes in mixtures of oppositely charged ionic block copolymers was described. Two possibilities are taken into account: (i) oppositely charged blocks are of

the same length; and (ii) oppositely charged blocks are of unequal lengths. In their study on polyion complex (*PIC*) micelles,<sup>87</sup> Harada and Kataoka observed that the formation of *PIC* micelles is controlled by the so-called “chain length recognition”.<sup>88</sup> Complex formation and aggregation occurred only in the case of block copolymers with equal lengths of the charged blocks. In the mixtures of block copolymers having different lengths *PIC* micelles were not observed. Interestingly, for the block copolymers analysed here, *PIC* formation occurred not only with copolymers having equal lengths of the charged blocks but also when short and long charged blocks were mixed. In toluene, studies on the possible formation of hydrogen-bonded complexes between diol and acetoacetoxy units of a poly((2-acetoacetoxy)ethyl methacrylate)-poly(*n*-butyl methacrylate) block copolymer were performed. Analytical ultracentrifugation measurements showed that complex formation, indeed, took place. However, complete analysis of the system by means of light scattering measurements could not be achieved.

There is no doubt that the synthetic approach presented here has great potential for the preparation of various functional block copolymers. The versatility of the applied method was confirmed by a number of examples of successfully performed modifications. Introduced moieties include carboxylic acid and ester groups, primary amine, amino acid, hydroxyl and perfluoroalkyl. Due to its modular character, this concept can be extensively extended. Future investigations may include introduction of different functional mercaptanes and utilization of other types of PB-containing block copolymers. Synthesis of various functional block copolymers based on the same backbone allows further systematic studies on aggregation behaviour. The method provides also an interesting opportunity to prepare copolymers bearing suitable complementary functionalities, which may be further utilized for the preparation of copolymer complexes.



## 6 EXPERIMENTAL PART

### 6.1 Solvents and Reagents

THF and toluene were distilled and dried over suitable drying agents: THF (Na/K alloy, LiAlH<sub>4</sub>, KOH), toluene (CaH<sub>2</sub>). Methanol, ethanol, benzene, DMSO, acetone, *n*-hexane, phosphate buffer (27 mM NaH<sub>2</sub>PO<sub>4</sub> in water, pH = 7.2) were used as received. All solvents used in NMR measurements were commercially obtained (Deutero GmbH) and used as received: CDCl<sub>3</sub>, D<sub>2</sub>O, DMF-d<sub>7</sub>, DMSO-d<sub>6</sub>, CD<sub>3</sub>OD-d<sub>4</sub>.

The following reagents were obtained commercially in the highest purity available from Sigma-Aldrich, Fluka or Acros and were used as received unless otherwise stated: *n*-butyl methacrylate, ethylene oxide, 1,3-butadiene, phosphazene base (*t*-BuP<sub>4</sub>), *sec*-butyl lithium (*sec*-BuLi), *n*-butyl lithium (*n*-BuLi), acetic acid, 1,4-polybutadiene (1,4-PB), *N,N*-azobis(isobutyronitrile) (AIBN), methyl-3-mercaptopropionate, 3-mercaptopropionic acid, 2-aminoethanethiol hydrochloride, 2-(diethylamino)ethanethiol hydrochloride, 3-mercapto-1,2-propanediol, *N*-acetyl-L-cysteine methyl ester. 1H,1H,2H,2H-perfluorooctanethiol was a commercial product of Fluorochem Ltd. (UK). All inorganic materials used (NaOH, KOH, Na, K, CaH<sub>2</sub>, LiAlH<sub>4</sub>, HCl) were of standard quality.

### 6.2 Synthetic procedures

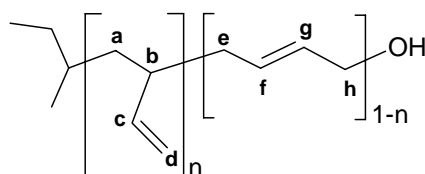
#### 6.2.1 Preparation of precursors by anionic polymerisation

All polymerisation reactions were performed on the Schlenk line (combined vacuum/argon line) equipped with Rotaflo<sup>®</sup> teflon valves. Argon was dried first by flowing through a column with an active drying and adsorption agent (silica gel blue, Fluka) and then “washed” through a system containing Na/K alloy in toluene. Utilized glass reactors were heated under vacuum to about 600 °C to exclude residues of moisture and, when necessary, ventilated with dry argon.

##### 6.2.1.1 Synthesis of 1,2-PB precursors

Distilled dry THF, left overnight above Na/K alloy to ensure absence of water, was condensed into the polymerisation reactor. 1,3-butadiene was dried over CaH<sub>2</sub> and then in *n*-

BuLi at  $-60\text{ }^{\circ}\text{C}$ . The reactor was kept at  $-78\text{ }^{\circ}\text{C}$  using ethanol/dry ice bath and then the initiator *sec*-BuLi was injected. Dry 1,3-butadiene was directly condensed into the reactor and left to polymerise overnight at  $-78\text{ }^{\circ}\text{C}$  (solution turned yellow). After 24 h the living polymer was quenched with ethylene oxide, which was previously purified over  $\text{CaH}_2$ , Na mirror and in *n*-BuLi. After the solution was stirred for 1 h at  $-78\text{ }^{\circ}\text{C}$ , it was left to warm to room temperature and was stirred at this temperature for next three days (solution turned colourless). The resulting polymer was precipitated into methanol yielding a yellow honey-like product, which was left to dry under vacuum. According to  $^1\text{H}$  NMR analysis, end capping of the chains was quantitative and the content of butadiene 1,2-adduct (*n*) was found to be  $\geq 93\%$ .



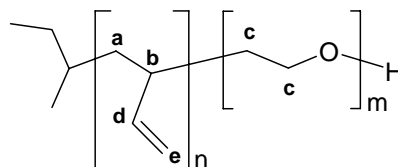
$^1\text{H}$  NMR (400 MHz,  $\text{CDCl}_3$ )  $\delta$  [ppm]: 5.60-5.20 (m, br, =CH, **c**, **f**, **g**), 5.00-4.75 (m, br, =CH<sub>2</sub>, **d**), 2.20-0.90 (br, polymer backbone: -CH<sub>2</sub>, **a**, **e**, **h**, -CH, **b**).

**FT-IR**,  $\tilde{\nu}$  ( $\text{cm}^{-1}$ ):  $\sim 3076$   $\nu$  (=C-H), 3000-2800  $\nu_{\text{as, s}}$  (-C-H),  $\sim 1640$   $\nu$  (C=C),  $\sim 1417$   $\delta$  (C-H),  $\sim 993$  and  $\sim 906$  “out of plane” C-H bending  $\gamma$  (-CH=CH<sub>2</sub>).

### 6.2.1.2 Synthesis of PB-PEO precursors

The PB-PEO precursor block copolymers used throughout these studies were prepared in two steps. Firstly, hydroxyl-terminated *1,2*-PBs were prepared by anionic polymerisation of 1,3-butadiene as described in section 6.2.1.1. In the second step, the *1,2*-PB macroinitiator was dissolved in the small amount of dry THF, placed in the reactor and dried overnight under dynamic vacuum. The polymerisation solvent, THF, was dried above Na/K alloy and condensed into the polymerisation reactor. After complete dissolution of the *1,2*-PB macroinitiator, phosphazene base (*t*-BuP<sub>4</sub>) was added using a syringe to affect deprotonation of the terminal -OH function allowing initiation of the polymerisation of ethylene oxide.<sup>145</sup> Ethylene oxide was purified over  $\text{CaH}_2$ , Na mirror and in *n*-BuLi before condensation into the reactor. The solution was stirred for 30 min. at  $-78\text{ }^{\circ}\text{C}$  then it was left to warm to room temperature and subsequently heated at  $40\text{ }^{\circ}\text{C}$  for three days. During the polymerisation, the

colour of the solution turned from yellow to deep violet. The polymerisation was quenched with acetic acid and the product was precipitated in cold acetone, re-dissolved in water and freeze-dried.

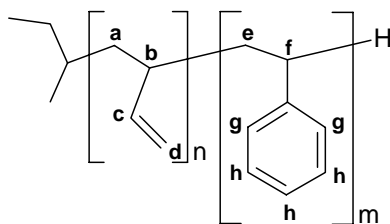


$^1\text{H NMR}$  (400 MHz,  $\text{CDCl}_3$ )  $\delta$  [ppm]: 5.60-5.20 (m, br, =CH, **d**), 5.00-4.75 (m, br, =CH<sub>2</sub>, **e**), 3.80-3.40 (br, -CH<sub>2</sub>, **c**), 2.20-0.90 (br, PB backbone: -CH<sub>2</sub>, **a**, -CH, **b**).

**FT-IR**,  $\bar{\nu}$  ( $\text{cm}^{-1}$ ):  $\sim 3076$   $\nu$  (=C-H), 3000-2800  $\nu_{\text{as, s}}$  (-C-H),  $\sim 1640$   $\nu$  (C=C),  $\sim 1460$   $\delta$  (C-H),  $\sim 1150$ - $1060$   $\nu_{\text{as}}$  (C-O-C),  $\sim 993$  and  $\sim 906$  “out of plane” C-H bending  $\gamma$  (-CH=CH<sub>2</sub>).

### 6.2.1.3 Synthesis of PB-PS precursor

PB-PS precursor was prepared by means of sequential living anionic polymerisation of 1,3-butadiene and styrene in THF. Dry THF was left overnight above Na/K alloy to ensure absence of water and then condensed into the polymerisation reactor. 1,3-butadiene was dried over  $\text{CaH}_2$  and after in *n*-BuLi at  $-60$  °C. The reactor was kept at  $-78$  °C using an ethanol/dry ice bath and then the initiator *sec*-BuLi was injected. Dry 1,3-butadiene was directly condensed into the reactor and left to polymerise overnight at  $-78$  °C (solution turned yellow). Styrene was dried over  $\text{AlLiH}_4$  for about 3 h and then transferred into the ampule containing *n*-BuLi *via* condensation and dried overnight. An aliquot was extracted from the polymerisation reactor and quenched with degassed methanol to be analysed by GPC. Styrene was condensed into the reactor and polymerised for 1 h at  $-78$  °C (orange) and then the polymerisation was quenched using degassed methanol (colourless). THF was partially evaporated under reduced pressure and the product was precipitated in methanol and dried under vacuum at  $40$  °C. The product was fractionated by the addition of methanol into the THF solution. According to  $^1\text{H NMR}$  analysis, the content of butadiene 1,2-adduct (**n**) in the copolymer was found to be 97%.



$^1\text{H NMR}$  (400 MHz,  $\text{CDCl}_3$ )  $\delta$  [ppm]: 7.35-6.85 (m, br, 3H, Ar-H, **h**), 6.85-6.25 (m, br, 2H, Ar-H, **g**), 5.60-5.20 (m, br, =CH, **c**), 5.00-4.80 (m, br, =CH<sub>2</sub>, **d**), 2.40-0.90 (br, polymer backbone: -CH<sub>2</sub>, **a**, **e**, -CH, **b**, **f**).

**FT-IR**,  $\tilde{\nu}$  ( $\text{cm}^{-1}$ ): 3084-3022  $\nu$  (=C-H) and  $\nu$  (Ar, C-H), 3000-2800  $\nu_{\text{as, s}}$  (-C-H),  $\sim 1639$   $\nu$  (C=C), 1600-1580 and 1492-1450 skeletal  $\sim \nu$  (Ar, C-H), 1182-1026  $\delta$  (Ar, C-H),  $\sim 993$  and  $\sim 906$  “out of plane” C-H bending  $\gamma$  (-CH=CH<sub>2</sub>),  $\sim 754$  and  $692$  “out of plane” C-H bending  $\gamma$  (Ar, C-H).

## 6.2.2 Radical addition of $\omega$ -functional mercaptanes

All radical addition reactions were performed in THF. The concentration in respect to a polymer was  $\sim 3\%$ . Utilized mercaptanes and radical initiator *N,N*-azobis(isobutyronitrile) (AIBN) were commercial products of the highest available purity and were used without further purification. The reactions were performed in a glass set with a cooler. After mixing of reagents, the mixtures were degassed and the reactions were carried out under an argon atmosphere at THF-reflux temperature.

### 6.2.2.1 Modification of PB homopolymers

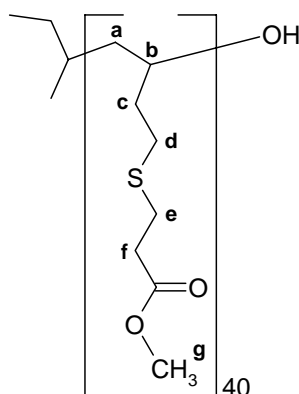
#### Radical addition of methyl-3-mercaptopropionate (*Es*) to 1,2-polybutadiene (1,2-PB)

1,2-PB and AIBN were dissolved in THF in the proportions given in Table 6.1. Then *Es* was added by means of a syringe and the solution was heated to reflux. After 24 h of reaction, the solution was left to cool to r.t. and the solvent was partially evaporated under reduced pressure. The polymer was precipitated twice from methanol, washed with water and dried under vacuum to constant weight. The yellow, honey-like product was isolated in 70 % yield.

Table 6.1. Amounts of reagents utilized in the exemplary modification of 1,2-polybutadiene, *1,2-PB*, with methyl-3-mercaptopropionate, *Es*.

Reagents	m [g]	M [g/mol]	n [mol]
<i>1,2-PB</i>	0.1	2160	$4.62 \cdot 10^{-5}$
<sup>a</sup> HS(CH <sub>2</sub> ) <sub>2</sub> COOCH <sub>3</sub>	2.221	120.17	$1.85 \cdot 10^{-2}$
<sup>b</sup> AIBN	0.101	164.21	$6.16 \cdot 10^{-4}$

<sup>a</sup>10 equivalents of double bonds of PB; <sup>b</sup>1/3 equivalents of double bonds of PB.



<sup>1</sup>H NMR (400 MHz, CDCl<sub>3</sub>) δ [ppm]: 3.65 (s, -CH<sub>3</sub>, **g**), 2.75 (m, -CH<sub>2</sub>, **e**), 2.59 (m, -CH<sub>2</sub>, **d**), 2.47 (m, -CH<sub>2</sub>, **f**), 2.20-0.90 (br, -CH<sub>2</sub>, **a**, -CH, **b**, -CH<sub>2</sub>, **c**).

FT-IR,  $\tilde{\nu}$  (cm<sup>-1</sup>): 3000-2800  $\nu_{\text{as, s}}$  (-C-H), ~1737  $\nu$  (C=O), ~1460  $\delta$  (C-H), ~1355  $\nu$  (-C-O-CH<sub>3</sub>), ~1240  $\nu$  (C-O).

#### Radical addition of methyl-3-mercaptopropionate (*Es*) to 1,4-polybutadiene (*1,4-PB*)

*1,4-PB* and AIBN were dissolved in THF in the proportions given in Table 6.2. Then *Es* was added by means of a syringe and the solution was heated to reflux. Within 1 h of reaction, a strong gelation of the solution occurred. Thus the mixture was left to cool to r.t. The gelatinous product was washed thoroughly with THF and dried under vacuum. The obtained product was insoluble in common organic solvents; hence sufficient purification as well as a detailed analysis of the resulting material was not possible.

Table 6.2. Amounts of reagents utilized in the exemplary modification of 1,4-polybutadiene, *1,4-PB*, with methyl-3-mercaptopropionate, *Es*.

Reagents	m [g]	M [g/mol]	n [mol]
<i>1,4-PB</i>	0.1	3000	$3.33 \cdot 10^{-5}$
<sup>a</sup> HS(CH <sub>2</sub> ) <sub>2</sub> COOCH <sub>3</sub>	2.203	120.17	$1.83 \cdot 10^{-2}$
<sup>b</sup> AIBN	0.10	164.21	$6.11 \cdot 10^{-4}$

<sup>a</sup>10 equivalents of double bonds of PB; <sup>b</sup>1/3 equivalents of double bonds of PB.

### 6.2.2.2 Modification of PB-PEO block copolymers

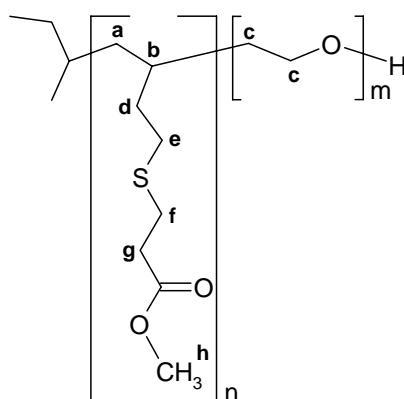
#### Radical addition of methyl-3-mercaptopropionate (*Es*)

PB<sub>25</sub>-PEO<sub>75</sub> (*PI*) and AIBN were dissolved in THF in the proportions given in Table 6.3. Then *Es* was added using a syringe and the solution was heated to reflux. After 24 h of reaction, the solution was left to cool to r.t. and the solvent was partially evaporated under reduced pressure. The polymer was precipitated twice from cold *n*-hexane, dissolved in water, dialysed (cut off: 1 kDa) and freeze-dried from the aqueous solution. The modified polymer was isolated in 55 % yield.

Table 6.3. Amounts of reagents utilized in the exemplary modification of PB-PEO block copolymer with methyl-3-mercaptopropionate, *Es*.

Reagents	m [g]	M [g/mol]	n [mol]
PB <sub>25</sub> -PEO <sub>75</sub> ( <i>PI</i> )	1.0	4700	$2.13 \cdot 10^{-4}$
<sup>a</sup> HS(CH <sub>2</sub> ) <sub>2</sub> COOCH <sub>3</sub>	6.408	120.17	$5.33 \cdot 10^{-2}$
<sup>b</sup> AIBN	0.292	164.21	$1.78 \cdot 10^{-3}$

<sup>a</sup>10 equivalents of double bonds of PB; <sup>b</sup>1/3 equivalents of double bonds of PB.



<sup>1</sup>H NMR (400 MHz, CDCl<sub>3</sub>)  $\delta$  [ppm]: 3.80-3.40 (br, -CH<sub>2</sub>, c, -CH<sub>3</sub>, h), 2.75 (m, -CH<sub>2</sub>, f), 2.59 (m, -CH<sub>2</sub>, e), 2.48 (m, -CH<sub>2</sub>, g), 2.20-0.90 (br, -CH<sub>2</sub>, a, -CH, b, -CH<sub>2</sub>, d).

**FT-IR**,  $\tilde{\nu}$  ( $\text{cm}^{-1}$ ): 3000-2800  $\nu_{\text{as, s}}$  ( $-\text{C}-\text{H}$ ),  $\sim 1741$   $\nu$  ( $\text{C}=\text{O}$ ),  $\sim 1460$   $\delta$  ( $\text{C}-\text{H}$ ),  $\sim 1150$ - $1060$   $\nu_{\text{as}}$  ( $\text{C}-\text{O}-\text{C}$ ).

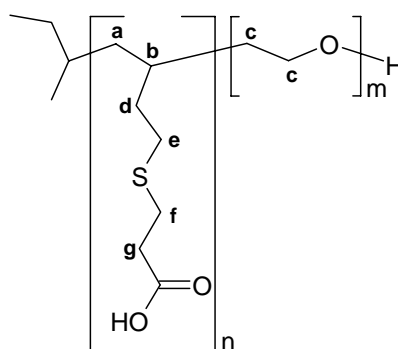
#### Radical addition of 3-mercaptopropionic acid (*Ac*)

PB<sub>40</sub>-PEO<sub>132</sub> (*P2*) and AIBN were dissolved in THF in the proportions given in Table 6.4. *Ac* was added by means of a syringe and the solution was heated to reflux. After 24 h of reaction the solution was left to cool to r.t. and the solvent was partially evaporated under reduced pressure. The polymer was precipitated twice from cold *n*-hexane, dissolved in water, dialysed (cut off: 1 kDa) and freeze-dried from the water solution. The modified polymer was isolated in 90 % yield. For conversion of the modified polymer into the sodium salt, NaOH was added to the aqueous solution (10 fold excess with respect to the carboxylic acid groups) and the polymer was dialyzed against water and freeze-dried.

Table 6.4. Amounts of reagents utilized in the exemplary modification of PB-PEO block copolymer with 3-mercaptopropionic acid, *Ac*.

Reagents	m [g]	M [g/mol]	n [mol]
PB <sub>40</sub> -PEO <sub>132</sub> ( <i>P2</i> )	0.2	8000	$2.5 \cdot 10^{-5}$
<sup>a</sup> HS(CH <sub>2</sub> ) <sub>2</sub> COOH	1.061	106.14	$1.0 \cdot 10^{-2}$
<sup>b</sup> AIBN	0.055	164.21	$3.33 \cdot 10^{-4}$

<sup>a</sup>10 equivalents of double bonds of PB; <sup>b</sup>1/3 equivalents of double bonds of PB.



**<sup>1</sup>H NMR** (400 MHz, DMSO)  $\delta$  [ppm]: 3.85-3.15 (br,  $-\text{CH}_2$ , **c**),  $\sim 2.62$  (m,  $-\text{CH}_2$ , **f**), 2.50-2.35 (m,  $-\text{CH}_2$ , **e, g**), 2.20-0.90 (br,  $-\text{CH}_2$ , **a**,  $-\text{CH}$ , **b**,  $-\text{CH}_2$ , **d**).

**FT-IR**,  $\tilde{\nu}$  ( $\text{cm}^{-1}$ ): 3000-2800  $\nu_{\text{as, s}}$  ( $-\text{C}-\text{H}$ ),  $\sim 1717$   $\nu$  ( $\text{C}=\text{O}$ ),  $\sim 1460$   $\delta$  ( $\text{C}-\text{H}$ ),  $\sim 1150$ - $1060$   $\nu_{\text{as}}$  ( $\text{C}-\text{O}-\text{C}$ ).

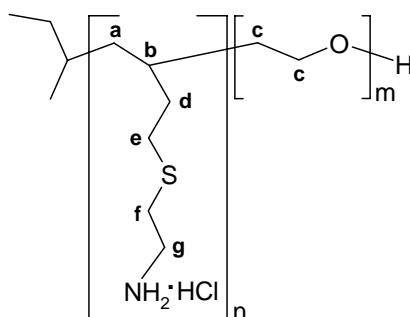
### Radical addition of 2-aminoethanethiol hydrochloride (*Am-HCl*)

PB<sub>40</sub>-PEO<sub>132</sub> (*P2*), AIBN and *Am-HCl* (proportions given in Table 6.5) were stirred in THF at r.t. until both polymer and AIBN were dissolved; *Am-HCl* is insoluble in THF. The mixture was heated to reflux and the reaction was carried out for 24 h. The mixture was then left to cool to r.t. and the solvent was evaporated under reduced pressure. The residue was dissolved in water, dialysed against water (cut off: 1 kDa) and then freeze-dried. The modified polymer was isolated in 78 % yield. For conversion of the modified polymer into the free amine form, NaOH was added to the aqueous solution (10 fold excess to the amine hydrochloride groups) and the polymer was freeze-dried.

Table 6.5. Amounts of reagents utilized in the exemplary modification of PB-PEO block copolymer with 2-aminoethanethiol hydrochloride, *Am-HCl*.

Reagents	m [g]	M [g/mol]	n [mol]
PB <sub>40</sub> -PEO <sub>132</sub> ( <i>P2</i> )	0.5	8000	$6.25 \cdot 10^{-5}$
<sup>a</sup> HS(CH <sub>2</sub> ) <sub>2</sub> NH <sub>2</sub> ·HCl	2.840	113.61	$2.50 \cdot 10^{-2}$
<sup>b</sup> AIBN	0.137	164.21	$8.33 \cdot 10^{-4}$

<sup>a</sup>10 equivalents of double bonds of PB; <sup>b</sup>1/3 equivalents of double bonds of PB.



<sup>1</sup>H NMR (400 MHz, CDCl<sub>3</sub>)  $\delta$  [ppm]: 3.80-3.40 (br, -CH<sub>2</sub>, **c**), 3.0 (m, -CH<sub>2</sub>, **f**), 2.70 (m, -CH<sub>2</sub>, **e**), 2.54 (m, -CH<sub>2</sub>, **g**), 2.20-0.90 (br, -CH<sub>2</sub>, **a**, -CH, **b**, -CH<sub>2</sub>, **d**).

FT-IR,  $\tilde{\nu}$  (cm<sup>-1</sup>): 3000-2800  $\nu_{as, s}$  (-C-H),  $\sim$ 2800  $\nu_{as, s}$  (-NH<sub>3</sub><sup>+</sup>),  $\sim$ 1575  $\delta$  (-NH<sub>3</sub><sup>+</sup>),  $\sim$ 1460  $\delta$  (C-H),  $\sim$ 1150-1060  $\nu_{as}$  (C-O-C).



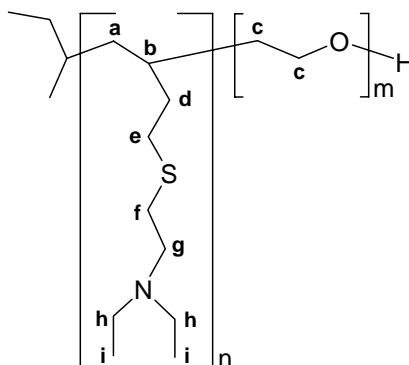
Radical addition of 2-(diethylamino)ethanethiol hydrochloride (*TAm-HCl*)

PB<sub>25</sub>-PEO<sub>75</sub> (*PI*), AIBN and *TAm-HCl* (proportions used as in Table 6.6) were stirred in THF at r.t. until the polymer and AIBN were dissolved; *TAm-HCl* is insoluble in THF. The mixture was heated to reflux and the reaction was carried out for 24 h. The mixture was then left to cool to r.t. and the solvent was evaporated under reduced pressure. The residue was dissolved in water, dialysed against water (cut off: 1 kDa) and then freeze-dried. The modified polymer was isolated in 66 % yield.

Table 6.6. Amounts of reagents utilized in the exemplary modification of PB-PEO block copolymer with 2-(diethylamino)ethanethiol hydrochloride, *TAm-HCl*.

Reagents	m [g]	M [g/mol]	n [mol]
PB <sub>25</sub> -PEO <sub>75</sub> ( <i>PI</i> )	0.2	4700	4.26·10 <sup>-5</sup>
<sup>a</sup> HS(CH <sub>2</sub> ) <sub>2</sub> N(C <sub>2</sub> H <sub>5</sub> ) <sub>2</sub> ·HCl	1.807	169.72	1.06·10 <sup>-2</sup>
<sup>b</sup> AIBN	0.058	164.21	3.55·10 <sup>-4</sup>

<sup>a</sup>10 equivalents of double bonds of PB; <sup>b</sup>1/3 equivalents of double bonds of PB.



<sup>1</sup>H NMR (400 MHz, CDCl<sub>3</sub>) δ [ppm]: 3.80-3.40 (br, -CH<sub>2</sub>, **c**), ~2.62 (m, -CH<sub>2</sub>, **g**), 2.55-2.35 (m, -CH<sub>2</sub>, **e, f, h**), ~1.01 (m, -CH<sub>3</sub>, **i**), 2.20-0.90 (br, -CH<sub>2</sub>, **a**, -CH, **b**, -CH<sub>2</sub>, **d**).

FT-IR,  $\tilde{\nu}$  (cm<sup>-1</sup>): 3000-2800  $\nu_{as, s}$  (-C-H), ~2800  $\nu$  (NH<sup>+</sup>), ~1460  $\delta$  (C-H), ~1150-1060  $\nu_{as}$  (C-O-C).

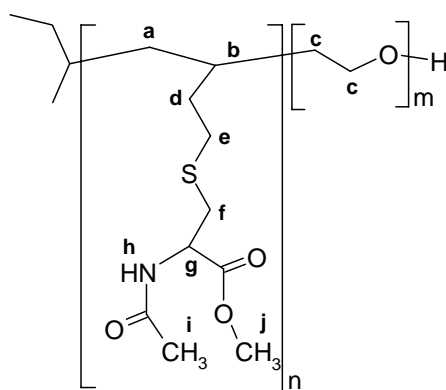
Radical addition of N-acetyl-L-cysteine methyl ester (PCys)

PB<sub>40</sub>-PEO<sub>132</sub> (*P2*), AIBN and PCys were dissolved in THF in the proportions given in Table 6.7. The mixture was heated to reflux and the reaction was carried out for 24 h. The solution was then left to cool to r.t. and the solvent partially was evaporated under reduced pressure. The polymer was precipitated from cold *n*-hexane, dissolved in water, dialysed (cut off: 1 kDa) and freeze-dried from the aqueous solution. The modified polymer was isolated in 68 % yield.

Table 6.7. Amounts of reagents utilized in the exemplary modification of PB-PEO block copolymer with N-acetyl-L-cysteine methyl ester, PCys.

Reagents	m [g]	M [g/mol]	n [mol]
PB <sub>40</sub> -PEO <sub>132</sub> ( <i>P2</i> )	0.2	8000	$2.5 \cdot 10^{-5}$
<sup>a</sup> HS(CH <sub>2</sub> ) <sub>2</sub> COOH	1.772	177.22	$1.0 \cdot 10^{-2}$
<sup>b</sup> AIBN	0.055	164.21	$3.33 \cdot 10^{-4}$

<sup>a</sup>10 equivalents of double bonds of PB; <sup>b</sup>1/3 equivalents of double bonds of PB.



<sup>1</sup>H NMR (400 MHz, CDCl<sub>3</sub>)  $\delta$  [ppm]:  $\sim$ 6.50 (very br, -NH, **h**), 4.79 (br, -CH, **g**), 3.75 (s, -CH<sub>3</sub>, **j**), 3.70-3.40 (br, -CH<sub>2</sub>, **c**), 2.94 (m, -CH<sub>2</sub>, **f**), 2.65-2.35 (br, -CH<sub>2</sub>, **e**), 2.03 (s, -CH<sub>3</sub>, **i**), 2.20-0.90 (br, -CH<sub>2</sub>, **a**, -CH, **b**, -CH<sub>2</sub>, **d**).

FT-IR,  $\tilde{\nu}$  (cm<sup>-1</sup>):  $\sim$ 3280  $\nu$  (N-H), 3000-2800  $\nu_{as, s}$  (-C-H),  $\sim$ 1742  $\nu$  (C=O),  $\sim$ 1657 Amid I  $\nu$  (C=O),  $\sim$ 1532 Amid II  $\delta$  (N-H),  $\sim$ 1460  $\delta$  (C-H),  $\sim$ 1150-1060  $\nu_{as}$  (C-O-C).

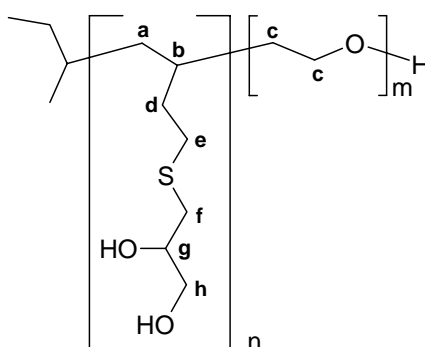
Radical addition of 3-mercapto-1,2-propanediol (*Di*)

PB<sub>40</sub>-PEO<sub>132</sub> (*P2*) and AIBN were dissolved in THF in the proportions given in Table 6.8. *Di* was added by means of a syringe and the solution was heated to reflux. After 24 h of reaction the solution was left to cool to r.t. and the solvent was evaporated under reduced pressure. Then MeOH was added and the solution was ultrafiltrated through a 1 kDa membrane. MeOH was evaporated under reduced pressure and the modified polymer was dissolved in about 10 mL of THF and precipitated twice from cold *n*-hexane. The modified polymer was isolated in 88 % yield.

Table 6.8. Amounts of reagents utilized in the exemplary modification of PB-PEO block copolymer with 3-mercapto-1,2-propanediol, *Di*.

Reagents	m [g]	M [g/mol]	n [mol]
PB <sub>40</sub> -PEO <sub>132</sub> ( <i>P2</i> )	0.5	8000	6.25·10 <sup>-5</sup>
<sup>a</sup> HSCH <sub>2</sub> CH(OH)CH <sub>2</sub> OH	2.704	108.16	2.50·10 <sup>-2</sup>
<sup>b</sup> AIBN	0.137	164.21	8.33·10 <sup>-4</sup>

<sup>a</sup>10 equivalents of double bonds of PB; <sup>b</sup>1/3 equivalents of double bonds of PB.



<sup>1</sup>H NMR (400 MHz, CD<sub>3</sub>OD)  $\delta$  [ppm]: 3.70 (m, CH, **g**), 3.65-3.40 (br, -CH<sub>2</sub>, **c**, **h**), 2.75-2.45 (m, -CH<sub>2</sub>, **e**, **f**), 2.20-0.90 (br, -CH<sub>2</sub>, **a**, -CH, **b**, -CH<sub>2</sub>, **d**).

FT-IR,  $\tilde{\nu}$  (cm<sup>-1</sup>): ~3350  $\nu$  (O-H), 3000-2800  $\nu_{as, s}$  (-C-H), ~1460  $\delta$  (C-H), ~1150-1060  $\nu_{as}$  (C-O-C).

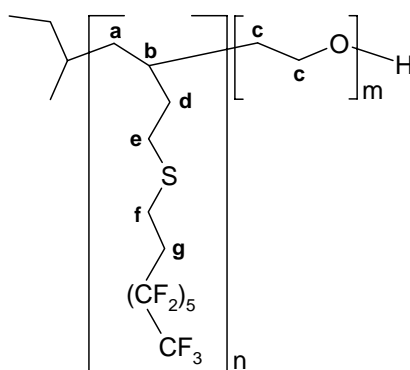
Radical addition of 1H,1H,2H,2H-perfluorooctanethiol (*Fl*)

PB<sub>40</sub>-PEO<sub>273</sub> (*P3*) and AIBN were dissolved in THF in the proportions given in Table 6.9. Then *Fl* was added by means of a syringe and the solution was heated to reflux. After 24 h of reaction, the second portion of AIBN in 0.5 mL of THF was added and the solution was left to react for the next 24 h. After cooling to r.t., the solvent was partially evaporated under reduced pressure. The polymer was precipitated twice from cold *n*-hexane, dissolved in water, dialysed (cut off: 1 kDa) and freeze-dried from the aqueous solution. The modified polymer was isolated in 88 % yield.

Table 6.9. Amounts of reagents utilized in the exemplary modification of PB-PEO block copolymer with 1H,1H,2H,2H-perfluorooctanethiol, *Fl*.

Reagents	m [g]	M [g/mol]	n [mol]
PB <sub>40</sub> -PEO <sub>273</sub> ( <i>P3</i> )	0.3	14200	$2.11 \cdot 10^{-5}$
<sup>a</sup> HS(CH <sub>2</sub> ) <sub>2</sub> (CF <sub>2</sub> ) <sub>5</sub> CF <sub>3</sub>	3.210	380.17	$8.44 \cdot 10^{-3}$
<sup>b</sup> AIBN	2·0.05	164.21	$2.81 \cdot 10^{-4}$

<sup>a</sup>10 equivalents of double bonds of PB; <sup>b</sup>2·1/3 equivalents of double bonds of PB.



<sup>1</sup>H NMR (400 MHz, CDCl<sub>3</sub>) δ [ppm]: 5.60-4.75 (m, br, =CH<sub>2</sub>, remaining PB double bonds), 3.80-3.40 (br, -CH<sub>2</sub>, **c**), 2.85 (m, -CH<sub>2</sub>, **f**), 2.50 (m, -CH<sub>2</sub>, **e**), 1.55 (m, -CH<sub>2</sub>, **g**), 2.20-0.90 (br, -CH<sub>2</sub>, **a**, -CH, **b**, -CH<sub>2</sub>, **d**).

FT-IR,  $\tilde{\nu}$  (cm<sup>-1</sup>): 3000-2800  $\nu_{as,s}$  (-C-H), ~1460  $\delta$  (C-H), ~1200  $\nu$  (C-F), ~1150-1060  $\nu_{as}$  (C-O-C).

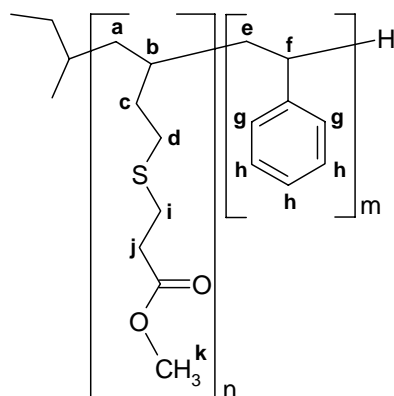
### 6.2.2.3 Modification of PB-PS block copolymers

PB<sub>85</sub>-PS<sub>351</sub> and AIBN were dissolved in THF in the proportions given in Table 6.10. *Es* was then added by means of a syringe and the solution was heated to reflux. After 24 h of reaction, the solution was left to cool to r.t. and the solvent was partially evaporated under reduced pressure. The polymer was precipitated twice from methanol, washed with water and dried under vacuum to constant weight. The product was isolated in 78 % yield.

Table 6.10. Amounts of reagents utilized in the exemplary modification of PB-PS block copolymer with methyl-3-mercaptopropionate, *Es*.

Reagents	m [g]	M [g/mol]	n [mol]
PB <sub>85</sub> -PS <sub>351</sub>	0.2	41200	4.85·10 <sup>-6</sup>
<sup>a</sup> HS(CH <sub>2</sub> ) <sub>2</sub> COOCH <sub>3</sub>	0.496	120.17	4.12·10 <sup>-3</sup>
<sup>b</sup> AIBN	0.023	164.21	1.37·10 <sup>-4</sup>

<sup>a</sup>10 equivalents of double bonds of PB; <sup>b</sup>1/3 equivalents of double bonds of PB.



<sup>1</sup>H NMR (400 MHz, CDCl<sub>3</sub>) δ [ppm]: 7.35-6.85 (m, br, 3H, Ar-H, **h**), 6.85-6.25 (m, br, 2H, Ar-H, **g**), 3.68 (s, -CH<sub>3</sub>, **k**), 2.76 (m, -CH<sub>2</sub>, **i**), 2.60 (m, -CH<sub>2</sub>, **d**), 2.49 (m, -CH<sub>2</sub>, **j**), 2.40-0.90 (br, polymer backbone: -CH<sub>2</sub>, **a**, **e**, -CH, **b**, **f**).

FT-IR,  $\tilde{\nu}$  (cm<sup>-1</sup>): 3084-3022  $\nu$  (Ar, C-H), 3000-2800  $\nu_{as, s}$  (-C-H), ~1734  $\nu$  (C=O), 1600-1580 and 1492-1450 skeletal  $\sim \nu$  (Ar, C-H), 1182-1026  $\delta$  (Ar, C-H), ~754 and 692 “out of plane” C-H bending  $\gamma$  (Ar, C-H).

### 6.3 Experimental techniques

**Nuclear Magnetic Resonance (NMR)** spectra were recorded at room temperature on a Bruker DPX-400 Spectrometer operating at 400.1 MHz. Solvents used were:  $\text{CDCl}_3$  ( $\delta = 7.24$  ppm),  $\text{DMSO-d}_6$  ( $\delta = 2.49$  ppm),  $\text{DMF-d}_7$  ( $\delta = 8.01, 2.91, 2.74$  ppm),  $\text{CD}_3\text{OD-d}_4$  ( $\delta = 4.78$  and  $3.30$  ppm),  $\text{D}_2\text{O}$  ( $4.67$  ppm) and  $\text{CCl}_4$ . For assignment of the NMR signals, abbreviations such as s (singlet), d (doublet), t (triplet), m (multiplet) and br (broad) were used. WinNMR (Bruker) program was used for analysis of spectra. Signals were assigned with the aid of the ACD/ChemSketch V3.00 software and literature references.<sup>131,132</sup>

**Fourier-Transform Infra Red (FT-IR)** spectra were recorded on a BioRad 6000 FT-IR. All samples were measured in the solid state using a Single Reflection Diamond ATR. For classifying the molecular vibrations appearing in IR spectra, abbreviations such as  $\nu$  (stretching),  $\delta$  (bending) and  $\gamma$  ("out of plane" bending), s (symmetrical), as (asymmetrical) were used. Signals were assigned with the aid of literature references.<sup>131,132</sup>

**Size Exclusion Chromatography (SEC)** was performed on Thermo Separation Products setups being equipped with UV (TSP UV1000) and RI (Shodex RI-71) detectors.

THF was used as the eluent at a flow rate of 1.0 mL/min at 25 °C. The employed column set consisted of three  $300 \times 8$  mm MZ-SD*plus* (spherical polystyrene gel with an average particle size of 5  $\mu\text{m}$ ) having a pore size of  $10^3$ ,  $10^5$ , and  $10^6$  Å, respectively.

N-methylpyrrolidone + 0.5 wt % LiBr was used at 70 °C at a flow rate of 0.8 mL/min, column set: two  $300 \times 8$  mm PSS-GRAM (spherical polyester gel with an average particle size of 7  $\mu\text{m}$ ) with a pore size of  $10^2$  and  $10^3$  Å, respectively.

All samples were filtered prior use and 100  $\mu\text{l}$  of approximately 0.2% w/v of polymer solution was injected in the GPC column. For calibration 1,2-PB, PEO, PS standards (PSS GmbH, Mainz, Germany) were used. Molecular weights and molecular weight distributions were calculated using the Program-Packet NTeqGPC V5.1.5 (hs GmbH, Oberhilbersheim, Germany).

**Dynamic (DLS)** and **Static Light Scattering (SLS)** measurements were carried out on a commercial spectrometer from ALV-GmbH (Langen, Germany) consisting of an goniometer with temperature controller ( $\pm 0.05\text{K}$ ) and an ALV 5000 multi-tau correlator. The refractive index increment  $\text{dn/dc}$  was measured using an NFT-Scanref differential refractometer. SLS

experiments were performed at scattering angles from  $15^\circ$  to  $150^\circ$  at  $5^\circ$  intervals. However, due to the large fluctuations in the scattered intensities at the lower angle-range, the data from  $15^\circ - 30^\circ$  were often excluded from the calculations. Obtained data were evaluated by a standard Zimm or Guinier analysis.

All solutions were filtered through  $5\ \mu\text{m}$  millipore filters prior measurement. The cylindrical quartz cuvettes (1 cm diameter) were extensively cleaned first with THF and ethanol followed by cleaning with ultrasound using a Tensid solution (Hellmanex, Hellma). They were subsequently washed several times with distilled water to completely remove any Tensid remained. Finally, they were washed with acetone in a dust-free fountain for 20 minutes and placed in a desiccator.

**Analytical ultracentrifugation** measurements (sedimentation velocity) were performed on a Beckman Optima XL-I (Beckman Coulter, Palo Alto, CA) at  $25\ ^\circ\text{C}$ , using self-made 12 mm titanium centrepieces. Detection of the sedimenting boundary was carried out using UV-Vis absorption and interference optics.

**Atomic Force Microscopy (AFM)** was performed on a Nano-Scope IIIa Microscope (Digital Instruments, USA) using a  $10\times 10\ \mu\text{m}$  cantilever (Model TESP; resonant frequency: 300 KHz; force constant: 42 N/m). All measurements were carried out with Tapping Mode. Dilute sample solutions were spin-coated on graphite surface to be visualised by AFM.

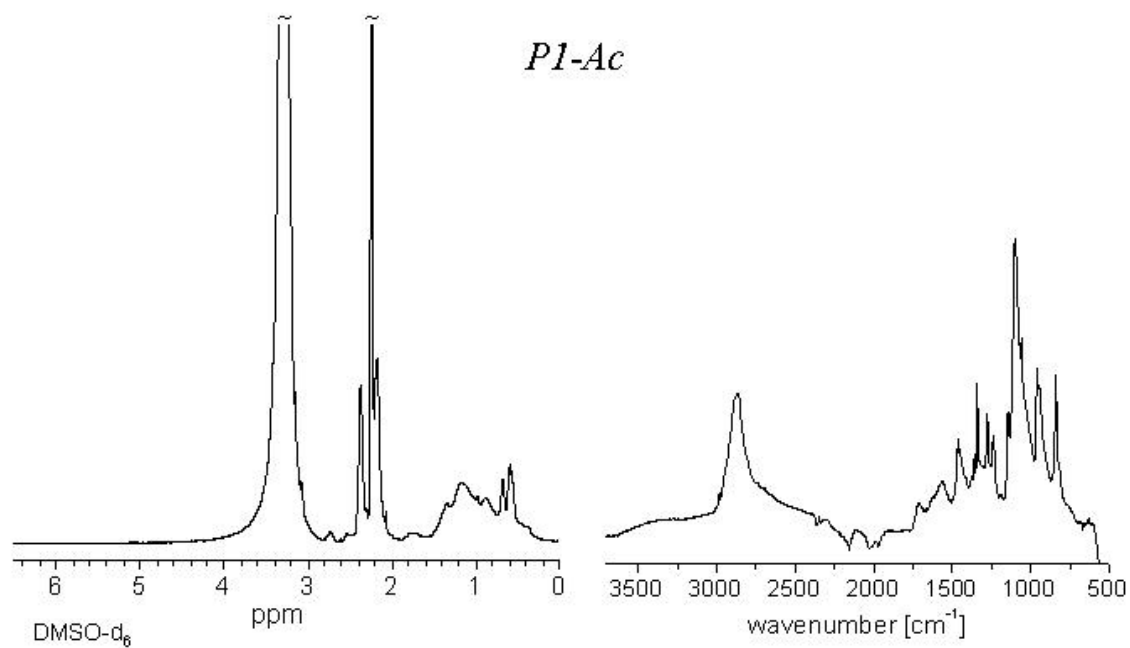
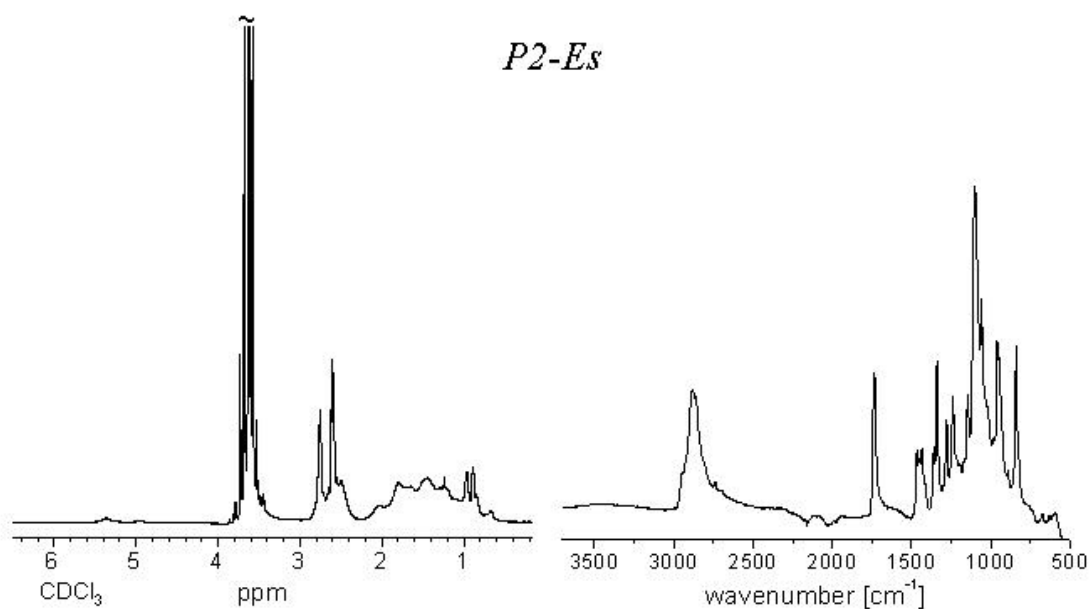
**Density measurements** were carried out on a density meter DMA 5000 (Anton Paar, Germany) at  $25\ ^\circ\text{C}$ . The specific density of the bulk polymer was extrapolated from the density data measured for a particular solvent and a 0.75 wt % solution of the polymer in the same solvent.

**Surface tension** measurements were performed on a Prozessor Tensiometer K12 (Krüss GmbH, Germany) using the DuNoüy ring method.

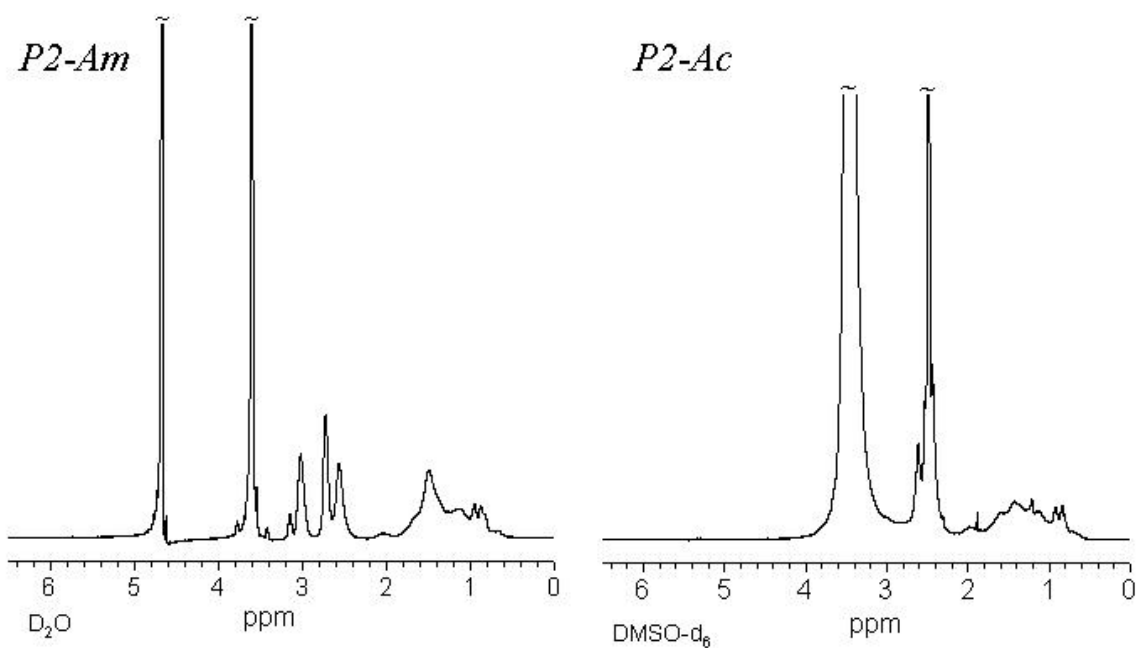
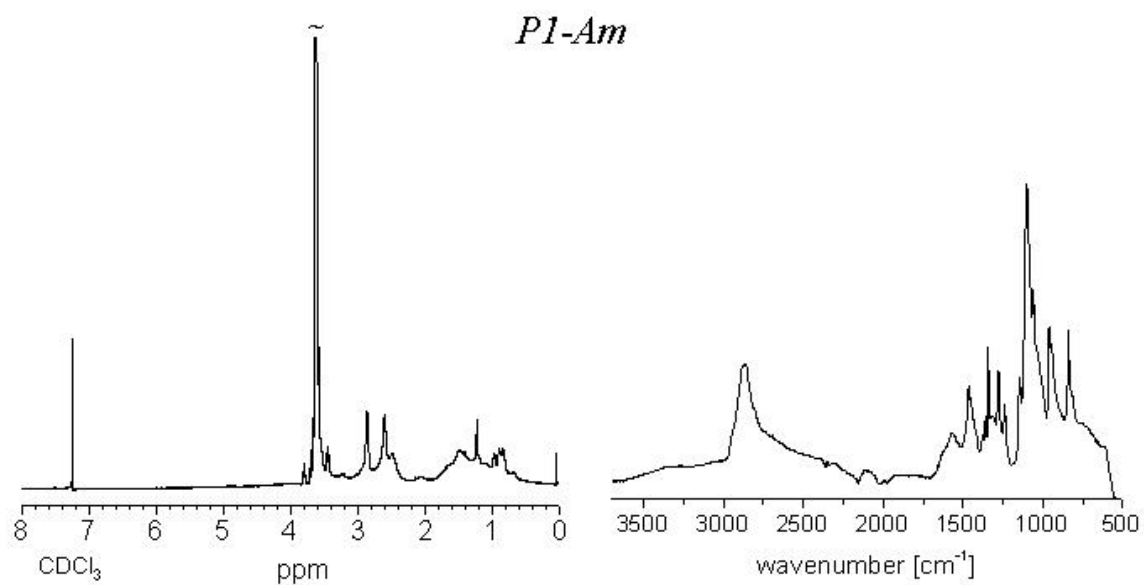
**Contact Angle** measurements were performed on a G10 contact angle goniometer (Krüss GmbH, Germany) using water as test liquid. The angle reported here is the average of five measurements.

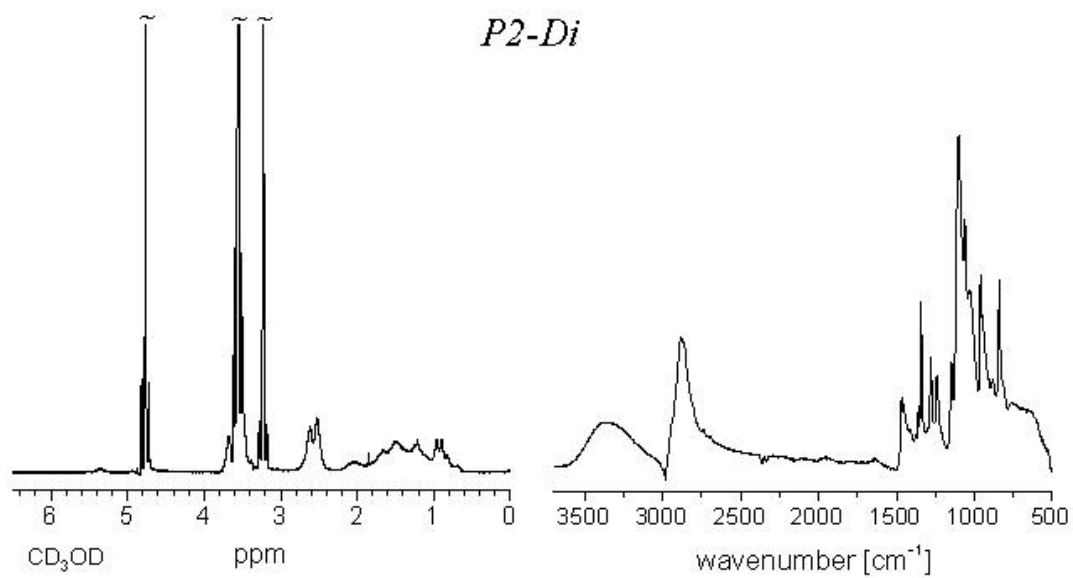
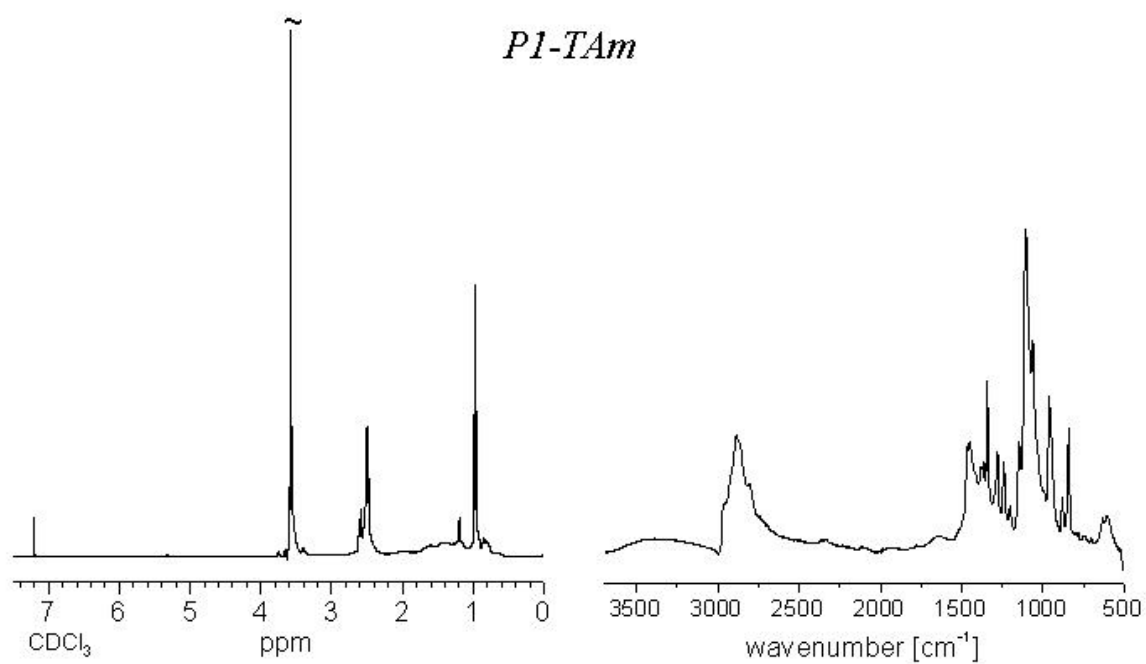
## 7 APPENDIX

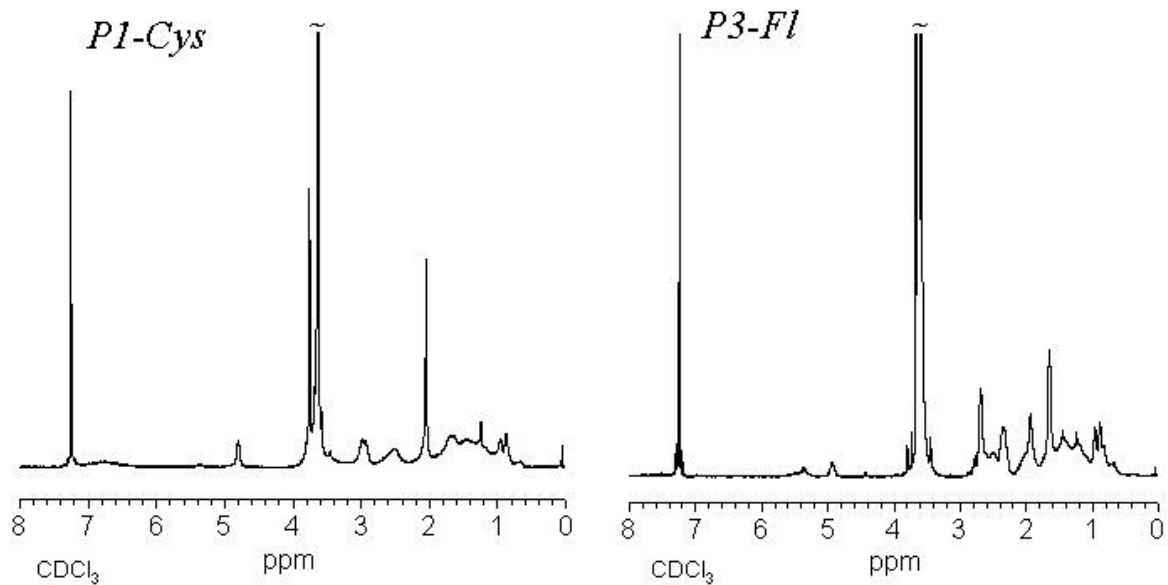
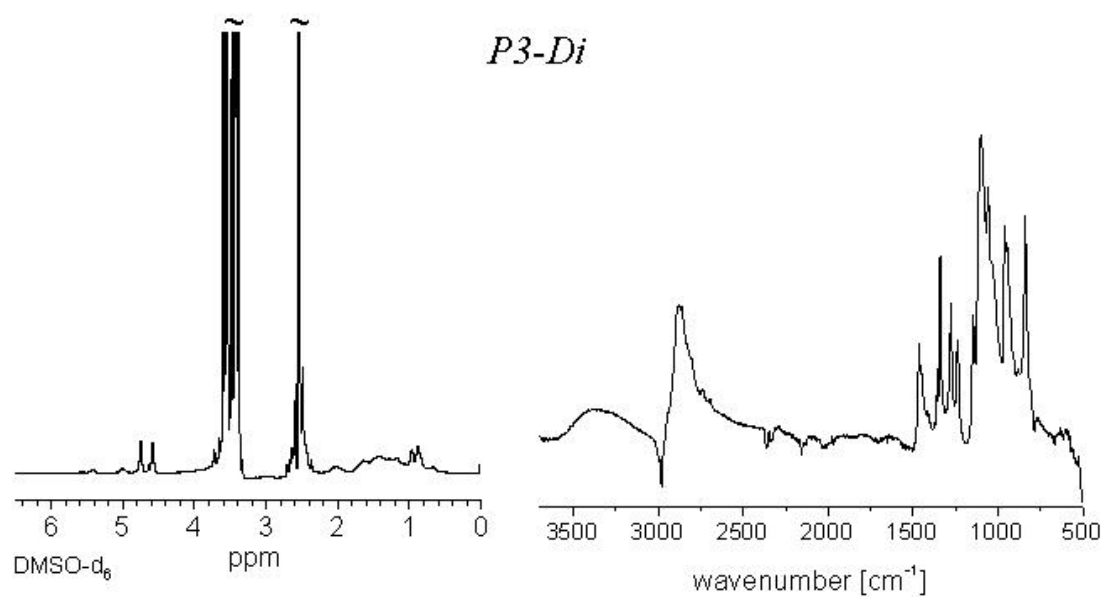
### I. $^1\text{H}$ NMR AND FT-IR SPECTRA (REFER SECTION 4.1.2)











II. CALCULATION OF THE THICKNESS OF THE VESICLE MEMBRANE,  $d$ , (REFER SECTION 4.2.1.1)

The volume of the vesicle,  $V_{ves}$ , can be calculated by

$$V_{ves} = \frac{4}{3}\pi R^3 \quad (7.1)$$

where  $R$  is the radius of the vesicle

The volume of the inner sphere of the vesicle,  $V_{in}$ , which is filled with a solvent can be calculated by

$$V_{in} = \frac{4}{3}\pi(R-d)^3 \quad (7.2)$$

By subtracting the volume of the inner sphere from the volume of the vesicle one can obtain the volume of the polymer building the vesicle membrane,  $V_{pol}$

$$V_{pol} = V_{ves} - V_{in} = \frac{4}{3}\pi(R^3 - (R-d)^3) = \frac{M}{\rho N_A} \quad (7.3)$$

where  $M$  is the molecular weight of the vesicle,  $\rho$  is the density of the polymer and  $N_A$  is Avogadro's number.

Thus, the thickness of the vesicles membrane can be calculated as follows

$$d = R - \sqrt[3]{R^3 - \frac{3M}{4\pi\rho N_A}} \quad (7.4)$$

In Table 7.1 the values utilized for the calculations as well as  $d$  values obtained for samples *P1-Ac* and *P2-Ac* are summarised

Table 7.1. Values utilized for calculations and obtained thickness of the vesicle membrane,  $d$ .

Sample	$R_h$ [nm]	$M_w$ [g/mol]	$\rho$ [g/cm <sup>3</sup> ]	$d$ [nm]
<i>P1-Ac</i>	256	$1.01 \cdot 10^8$	1.241	<b>0.165</b>
<i>P2-Ac</i>	208	$6.25 \cdot 10^7$	1.254	<b>0.154</b>

## 8 ABBREVIATIONS

$A_2$	Second virial coefficient
AFM	Atomic force microscopy
AIBN	<i>N,N</i> -azobis(izobutyronitrile)
ATRP	Atom transfer radical polymerisation
AUC	Analytical ultracentrifugation
BuLi	Butyl lithium
<i>cmc</i>	Critical micelle concentration
$D$	Diffusion coefficient
DLS	Dynamic light scattering
DMF	Dimethylformamide
DMSO	Dimethylsulfoxide
$DP$	Degree of polymerisation
FT-IR	Fourier-transform infrared spectroscopy
GC	Gas chromatography
GPC	Gel permeation chromatography
HTPB	Hydroxyl-terminated polybutadiene
<i>IPEC</i>	Interpolyelectrolyte complex
LS	Light scattering
MeOH	Methanol
$M_n$	Number averaged molecular weight
$M_w$	Weight averaged molecular weight
$M_w^{app}$	Apparent weight averaged molecular weight
NMR	Nuclear magnetic resonance
PAA	Poly(acrylic acid)
PAEMA	Poly((2-acetoacetoxy)ethyl methacrylate)
PB	Polybutadiene
PBMA	Poly( <i>n</i> -butyl methacrylate)

---

<i>PDI</i>	Polydispersity index
PEO	Poly(ethylene oxide)
<i>PIC</i>	Polyion complex
ppm	Parts per million
PTFE	Poly(tetrafluoroethylene)
PS	Polystyrene
RAFT	Reversible addition-fragmentation chain-transfer polymerisation
$R_g$	Radius of gyration
$R_h$	Hydrodynamic radius
RI	Refractive index
$R(\theta)$	Rayleigh ratio
<i>s</i>	Sedimentation coefficient
SBR	Styrene/butadiene random copolymer
SEC	Size exclusion chromatography
SLS	Static light scattering
<i>t</i> -BuP <sub>4</sub>	Phosphazene base P <sub>4</sub>
T	Absolute temperature
TEM	Transmission electron microscopy
THF	Tetrahydrofuran
UV-Vis	Ultraviolet-visible
$\chi$	Flory-Huggins interaction parameter
<i>Z</i>	Aggregation number
$Z^{app}$	Apparent aggregation number

## 9 ACKNOWLEDGEMENTS

I would like to thank all the people who contributed to this thesis:

Prof. Dr. Markus Antonietti for the opportunity to work on this interesting project and for the fruitful discussions, which helped to find answers to many questions.

Dr. habil. Helmut Schlaad for his continuous help, many useful suggestions, numerous discussions and for being a great supervisor.

Dr. Reinhard Sigel for all the discussions and his help on the interpretation of the light scattering results. Birgit Schonert for numerous light scattering measurements and Dr. Andreas Erbe for his general help.

Antje Völkel for AUC measurements and for fulfilling all the wishes according to data evaluation ☺. Thanks also to Dr. habil. Helmut Cölfen for his help on the interpretation of AUC results.

Marlies Gräwert for innumerable SEC measurements and not only... Olaf Niemeyer for the similarly large amount of NMR experiments.

Anne Heilig for AFM analysis as well as lots of encouragement, Irina Shekova for titration and surface tension measurements, Margit Barth for density measurements, Rona Pitschke and Dr. Jürgen Hartmann for SEM and TEM analysis.

Dr. Hans Börner for the discussions on the “synthetic part” of my thesis.

Ines Below for all her help both in and out of the lab. Dr. Theodora Krasia (Theodorek) for her help and the unforgettable atmosphere during my first months in the institute. Thanks also to Zofia Hordyjewicz, Matthias Meyer, Dr. Mattijs ten Cate, Yufei Luo, Liangchen You, Dr. Yan Geng for the friendly atmosphere in the lab.

“Thank you” also to all the people who supported my work by various contributions: Doreen Eckhardt, Georg Garnweitner, Hartmut Rettig, Steffen Kozempel, Dr. Charl Faul, Laura Hartmann, Dr. Matthijs Groenewolt, Dr. Cornelia Sinn, Jessica Brandt, Katharina Otte, Annette Pape, Katarina Zesch and also to all present and former members of our department.

A special “Thank you” goes to Danielle Franke for all the corrections and discussions on my thesis as well as for being a great office-mate.

Dr. Christoph Kozlowski is gratefully acknowledged for the reason he knows.

A big “Thank you” goes to Dr. Magdalena Łosik for everything she taught me and especially for her friendship and continuous support in everyday life.

A very special “more than Thank you” goes to Stephan for all his love, patience and support as well as for our “physicochemical discussions”.

And last but not least, I would like to thank my parents and all my family for the moral support throughout these years.



**10 LITERATURE**

- (1) Förster, S.; Antonietti, M. *Adv. Mater.* **1998**, *10*, 195-217.
- (2) Wegner, G. *Acta mater.* **2000**, *48*, 253-262.
- (3) Bates, F. S.; Fredrickson, G. H. *Physics Today* **1999**, *52*, 32-38.
- (4) Ikkala, O.; ten Brinke, G. *Science* **2002**, *295*, 2407-2409.
- (5) Hamley, I. W., Ed. *Developments in Block Copolymer Science and Technology*; John Wiley & Sons, Ltd: Chichester, 2004.
- (6) Hsieh, H. L.; Quirk, R. P. *Anionic Polymerization: Principles and Practical Applications*; Marcel Dekker: New York, 1996.
- (7) Matyjaszewski, K., Ed. *Controlled radical polymerization*; American Chemical Society: Washington, DC, 1998.
- (8) Bohme, K.; Schmidt-Naake, G. *Macromolecular Materials and Engineering* **2004**, *289*, 254-263.
- (9) Petersen, H.; Fechner, P. M.; Fischer, D.; Kissel, T. *Macromolecules* **2002**, *35*, 6867-6874.
- (10) Lefebvre, H.; Fradet, A. *Macromol. Symp.* **1997**, *122*, 25-31.
- (11) Faust, R.; Kennedy, J. P. *J. Polym. Sci., Part A: Polym. Chem.* **1987**, *25*, 1847-1869.
- (12) Faust, R.; Zsuga, M.; Kennedy, J. P. *Polymer Bulletin* **1989**, *21*, 125-131.
- (13) Miyamoto, M.; Sawamoto, M.; Higashimura, T. **1984**, *17*, 265-268.
- (14) Nuyken, O.; Riess, G.; Loontjens, J.; Vanderlinde, R. *J. Macromol. Sci., Pure Appl. Chem.* **1995**, *A32*, 459-466.
- (15) Szwarc, M.; Van Beylen, M. *Ionic Polymerization and Living Polymers*; Chapman & Hall: New York, 1993.
- (16) Elias, H.-G. *An Introduction to Polymer Science*; VCH: Weinheim, 1997.
- (17) Varshney, S. K.; Hautekeer, J. P.; Fayt, R.; Jérôme, R.; Teyssié, P. *Macromolecules* **1990**, *23*, 2618.
- (18) Szwarc, M.; Levy, M.; Milkovich, R. *J. Am. Chem. Soc.* **1956**, *78*, 2656-2657.
- (19) Szwarc, M. *Nature* **1956**, *178*, 1168.
- (20) Faust, R.; Schlaad, H. In *Applied Polymer Science: 21st Century*; Elsevier Science: Amsterdam, 2000; pp 999-1020.
- (21) Ramireddy, C.; Tuzar, Z.; Prochazka, K.; Webber, S. E.; Munk, P. *Macromolecules* **1992**, *25*, 2541-2545.
- (22) Cram, D. J. *Fundamentals of Carbanion Chemistry*; Academic Press: New York, 1965.
- (23) Jagur-Grodzinski, J. *J. Polym. Sci., Part A: Polym. Chem.* **2002**, *40*, 2116-2133.
- (24) Hirao, A.; Nagahama, H.; Ishizone, T.; Nakahama, S. *Macromolecules* **1993**, *26*, 2145-2150.
- (25) Ueda, K.; Hirao, A.; Nakahama, S. *Macromolecules* **1990**, *23*, 939-945.
- (26) Tohyama, M.; Hirao, A.; Nakahama, S.; Takenaka, K. *Macromol. Chem. Phys.* **1996**, *197*, 3135-3148.
- (27) Reed Jr, S. F. *J. Polym. Sci., Part A: Polym. Chem.* **1972**, *10*, 1187-1194.
- (28) Nakahama, S.; Hirao, A. *Prog. Polym. Sci.* **1990**, *15*, 299-335.
- (29) Aoshima, S.; Iwasa, S.; Kobayashi, E. *Polym. J.* **1994**, *26*, 912-919.
- (30) Forder, C.; Armes, S. P.; Billingham, N. C. *Polym. Bull.* **1995**, *35*, 291 - 297.
- (31) Morishima, Y.; Hashimoto, T.; Itoh, Y.; Kamachi, M.; Nozakura, S.-I. *J. Polym. Sci., Polym. Chem. Ed.* **1982**, *20*, 299-310.

- (32) Wang, J.; Varshney, S. K.; Jerome, R.; Teyssie, P. *J. Polym. Sci., Part A: Polym. Chem.* **1992**, *30*, 2251-2261.
- (33) Feldthusen, J.; Ivan, B.; Müller, A. H. E. *Macromolecules* **1998**, *31*, 578-585.
- (34) Eisenberg, A.; Kim, J.-S. *Introduction to Ionomers*; John Wiley & Sons: New York, 1998.
- (35) Nugay, N.; Hosotte, C.; Nugay, T.; Riess, G. *European Polymer Journal* **1994**, *30*, 1187-1190.
- (36) Vink, H. *Makromol. Chem.* **1970**, *131*, 133-145.
- (37) Thaler, W. A. *Macromolecules* **1983**, *16*, 623-628.
- (38) Mango, L. A.; Lenz, R. W. *Makromol. Chem.* **1973**, *163*, 13-36.
- (39) Hahn, S. F. *J. Polym. Sci., Part A: Polym. Chem.* **1992**, *30*, 397-408.
- (40) Rosedale, J. H.; Bates, F. S. *J. Am. Chem. Soc.* **1988**, *110*, 3542-3545.
- (41) Mohammadi, N. A.; Rempel, G. L. *Macromolecules* **1987**, *20*, 2362-2368.
- (42) Antonietti, M.; Förster, S.; Hartmann, J.; Oestreich, S. *Macromolecules* **1996**, *29*, 3800-3806.
- (43) Ramakrishnan, S. *Macromolecules* **1991**, *24*, 3753-3759.
- (44) Nishikubo, T.; Kameyama, A. *Prog. Polym. Sci.* **1993**, *18*, 963-995.
- (45) Gimenez, V.; Mantecon, A.; Cadiz, V. *J. Polym. Sci., Part A: Polym. Chem.* **1996**, *34*, 925-934.
- (46) Frey, W.; Dederichs, B.; Klesper, E. *Eur. Polym. J.* **1986**, *22*, 745-753.
- (47) Iyengar, D. R.; Perutz, S. M.; Dai, C.-A.; Ober, C. K.; Kramer, E. J. *Macromolecules* **1996**, *29*, 1229-1234.
- (48) Antonietti, M.; Förster, S.; Micha, M.; Oestreich, O. *Acta Polym.* **1997**, *48*, 262-268.
- (49) Oestreich, S. *Amphiphile Blockcopolymer - Synthese, Strukturbildung und Anwendung*; Thesis, University of Potsdam: Potsdam, 1997.
- (50) Schlaad, H.; Krasia, T.; Patrickios, C. S. *Macromolecules* **2001**, *34*, 7585-7588.
- (51) Bates, F. S.; Fredrickson, G. H. *Annu. Rev. Phys. Chem.* **1990**, *41*, 525-557.
- (52) Förster, S.; Plantenberg, T. *Angew. Chem. Int. Ed.* **2002**, *41*, 688-714.
- (53) Hamley, I. W. *The Physics of Block Copolymers*; Oxford University Press: New York, 1998.
- (54) Leibler, L. *Macromolecules* **1980**, *13*, 1602-1617.
- (55) Matsen, M. W.; Bates, F. S. *Macromolecules* **1996**, *29*, 1091-1098.
- (56) Förster, S.; Khandpur, A. K.; Zhao, J.; Bates, F. S.; Hamley, I. W.; Ryan, A. J.; Bras, W. *Macromolecules* **1994**, *27*, 6922-6935.
- (57) Khandpur, A. K.; Förster, S.; Bates, F. S.; Hamley, I. W.; Ryan, A. J.; Bras, W.; Almdal, K.; Mortensen, K. *Macromolecules* **1995**, *28*, 8796-8806.
- (58) Nyrkova, I. A.; Khokhlov, A. R.; Doi, M. *Macromolecules* **1993**, *26*, 3601-3610.
- (59) Riess, G. *Prog. Polym. Sci.* **2003**, *28*, 1107-1170.
- (60) Schillen, K.; Brown, W.; Johnsen, R. M. *Macromolecules* **1994**, *27*, 4825-4832.
- (61) Antonietti, M.; Heinz, S.; Schmidt, M.; Rosenauer, C. *Macromolecules* **1994**, *27*.
- (62) Discher, D. E.; Eisenberg, A. *Science* **2002**, *297*, 967-973.
- (63) Soo, P. L.; Eisenberg, A. *J. Polym. Sci., Part B: Polym. Physics* **2004**, *42*, 923-938.
- (64) Israelachvili, J. N. *Intermolecular and Surface Forces*; Academic Press: London, 1985.
- (65) Förster, S.; Zisenis, M.; Wenz, E.; Antonietti, M. *J. Chem. Phys.* **1996**, *104*, 9956-9970.
- (66) Antonietti, M.; Förster, S. *Adv. Mater.* **2003**, *15*, 1323-1333.
- (67) Luo, L.; Eisenberg, A. *Langmuir* **2001**, *17*, 6804-6811.
- (68) Shen, H.; Eisenberg, A. *Angew. Chem. Int. Ed.* **2000**, *39*, 3310-3312.

- (69) Choucair, A.; Eisenberg, A. *Eur. Phys. J. E* **2003**, *10*, 37-44.
- (70) Zhang, L.; Yu, K.; Eisenberg, A. *Science* **1996**, *272*, 1777-1779.
- (71) Auschra, C.; Stadler, R. *Macromolecules* **1993**, *26*, 2171-2174.
- (72) Breiner, U.; Krappe, U.; Stadler, R. *Macromol. Rapid Commun.* **1996**, *17*, 567-575.
- (73) Li, Z.; Kesselman, E.; Talmon, Y.; Hillmyer, M. A.; Lodge, T. P. *Science* **2004**, *306*, 98-101.
- (74) Lehn, J.-M. *Supramolecular Chemistry - Concepts and Perspectives*; VCH: Weinheim, 1995.
- (75) Whitesides, G. M.; Grzybowski, B. *Science* **2002**, *295*, 2418-2421.
- (76) Ruokolainen, J.; Mäkinen, R.; Torkkeli, M.; Mäkelä, T.; Serimaa, R.; ten Brinke, G.; Ikkala, O. *Science* **1998**, *280*, 557-560.
- (77) Stupp, S. I.; LeBonheur, V.; Walker, K.; Li, L. S.; Huggins, K. E.; Keser, M.; Amstutz, A. *Science* **1997**, *276*, 384-389.
- (78) Lee, M.; Cho, B.-K.; Zin, W.-C. *Chem. Rev.* **2001**, *101*, 3869-3892.
- (79) Chen, J. T.; Thomas, E. L.; Ober, C. K.; Mao, G.-P. *Science* **1996**, *273*, 343-346.
- (80) Chen, J. T.; Thomas, E. L.; Ober, C. K.; Hwang, S. S. *Macromolecules* **1995**, *28*, 1688-1697.
- (81) Schlaad, H.; Kukula, H.; Smarsly, B.; Antonietti, M.; Pakula, T. *Polymer* **2002**, *43*, 5321-5328.
- (82) Cornelissen, J. J. L. M.; Fischer, M.; Sommerdijk, N. A. J. M.; Nolte, R. J. M. *Science* **1998**, *280*, 1427-1430.
- (83) Cornelissen, J. J. L. M.; Donners, J. J. J. M.; de Gelder, R.; Graswinckel, W. S.; Metselaar, G. A.; Rowan, A. E.; Sommerdijk, N. A. J. M.; Nolte, R. J. M. *Science* **2001**, *293*, 676-680.
- (84) Kabanov, A. V.; Bronich, T. K.; Kabanov, V. A.; Yu, K.; Eisenberg, A. *Macromolecules* **1996**, *29*, 6797-6802.
- (85) Schrage, S.; Sigel, R.; Schlaad, H. *Macromolecules* **2003**, *36*, 1417-1420.
- (86) Antonietti, M.; Wenzel, A.; Thünemann, A. *Langmuir* **1996**, *12*, 2111-2114.
- (87) Harada, A.; Kataoka, K. *Macromolecules* **1995**, *28*, 5294-5299.
- (88) Harada, A.; Kataoka, K. *Science* **1999**, *283*, 65-67.
- (89) Harada, A.; Kataoka, K. *Macromolecules* **2003**, *36*, 4995-5001.
- (90) Harada, A.; Togawa, H.; Kataoka, K. *European Journal of Pharmaceutical Sciences* **2001**, *13*, 35-42.
- (91) Harada, A.; Kataoka, K. *J. Control. Release* **2001**, *72*, 85-91.
- (92) Gohy, J.-F.; Varshney, S. K.; Jérôme, R. *Macromolecules* **2001**, *34*, 2745-2747.
- (93) Gohy, J.-F.; Khoussakoun, E.; Willet, N.; Varshney, S. K.; Jerome, R. *Macromol. Rapid Commun.* **2004**, *25*, 1536-1539.
- (94) Ilhan, F.; Gray, M.; Rotello, V. M. *Macromolecules* **2001**, *34*, 2597-2601.
- (95) Shenhar, R.; Sanyal, A.; Uzun, O.; Nakade, H.; Rotello, V. M. *Macromolecules* **2004**, *37*, 4931-4939.
- (96) Bazzi, H. S.; Bouffard, J.; Sleiman, H. F. *Macromolecules* **2003**, *36*, 7899-7902.
- (97) Grubisic, Z.; Rempp, P.; Benoit, H. *J. Polym. Sci., Part B - Polymer Letters* **1967**, *B5*, 753-759.
- (98) Tyndall, J. *Phil. Mag.* **1869**, *37*, 384.
- (99) Lord Rayleigh, J. W. *Phil. Mag.* **1871**, *41*, 107.
- (100) Debye, P. *J. Appl. Phys.* **1944**, *15*, 338.
- (101) Debye, P. *Phys. Colloid. Chem.* **1947**, *51*, 32.
- (102) Mie, G. *Ann. Physik* **1908**, *25*, 377.
- (103) Zimm, B. H. *J. Chem. Phys.* **1948**, *16*, 1093.

- (104) Kratky, O.; Porod, G. *Rec. Trav. Chim. Pays-Bas* **1949**, *68*, 1106-1122.
- (105) Brown, W., Ed. *Dynamic Light Scattering*; Oxford Science Publications: Oxford, 1993.
- (106) Siebert, A. J. F. *MIT Rad. Lab.* **1943**, 465.
- (107) Provencher, S. W. *Computer Phys. Commun.* **1982**, *27*, 214-228.
- (108) Svedberg, T.; Nichols, J. B. *J. Am. Chem. Soc.* **1923**, *45*, 2910.
- (109) Schachman, H. K. *Ultracentrifugation in Biochemistry*; Academic Press: New York, 1959.
- (110) Nernst, W. *Z. Physik. Chem.* **1888**, *2*, 613.
- (111) Signer, R.; Gross, H. *Helv. Chim. Acta* **1934**, *17*, 726.
- (112) Binning, G.; Quate, C.; Gerber, C. *Phys. Rev. Lett.* **1986**, *56*, 930.
- (113) McLean, R. S.; Sauer, B. B. *Macromolecules* **1997**, *30*, 8314-8317.
- (114) Zhang, H. L.; Bremmell, K.; Kumar, S.; Smart, R. S. C. *Journal of Biomedical Materials Research Part A* **2004**, *68A*, 479-488.
- (115) Griesbaum, K. *Angew. Chem.-Int. Edit.* **1970**, *9*, 273-287.
- (116) Ceausescu, E.; Bittman, S.; Fieroiu, V.; Badea, E. G.; Gruber, E.; Ciupitoiu, A.; Apostol, V. *Journal of Macromolecular Science-Chemistry* **1985**, *A22*, 525-539.
- (117) Ajiboye, O.; Scott, G. *Polymer Degradation and Stability* **1982**, *4*, 415-425.
- (118) Ajiboye, O.; Scott, G. *Polymer Degradation and Stability* **1982**, *4*, 397-413.
- (119) Kularatne, K. W. S.; Scott, G. *Eur. Polym. J.* **1979**, *15*, 827-832.
- (120) Cunneen, J. I.; Shipley, F. W. *J. Polym. Sci.* **1959**, *36*, 77-90.
- (121) Boutevin, G.; Ameduri, B.; Boutevin, B.; Joubert, J.-P. *J. Appl. Polym. Sci.* **2000**, *75*, 1655-1666.
- (122) Boutevin, B.; Hervaud, Y.; Mouledous, G. *Polym. Bull.* **1998**, *41*, 145-151.
- (123) Schapman, F.; Couvercelle, J. P.; Bunel, C. *Polymer* **1998**, *39*, 4955-4962.
- (124) Ciardelli, F.; Aglietto, M.; Passaglia, E.; Picchioni, F. *Polymers for Advanced Technologies* **2000**, *11*, 371-376.
- (125) Romani, F.; Passaglia, E.; Aglietto, M.; Ruggeri, G. *Macromol. Chem. Phys.* **1999**, *200*, 524-530.
- (126) Odian, G. *Principles of Polymerization*; John Wiley & Sons, Inc.: New York, 1991.
- (127) Bywater, S. In *Comprehensive Polymer Science. The Synthesis, Characterization, Reactions & Applications of Polymers*; Sir Allen, G., Ed.; Pergamon Press: Oxford, 1989; Vol. 3.
- (128) Serniuk, G. E.; Banes, F. W.; Swaney, M. W. *J. Am. Chem. Soc.* **1948**, *70*, 1804-1808.
- (129) Salle, R.; Pham, Q. T. *J. Polym. Sci. Pol. Chem.* **1977**, *15*, 1799-1810.
- (130) Herczynska, L.; Lestel, L.; Boileau, S.; Chojnowski, J.; Polowinski, S. *Eur. Polym. J.* **1999**, *35*, 1115-1122.
- (131) Silverstein, R. M.; Bassler, G. C.; Morrill, T. C. *Spectrometric identification of organic compounds*; John Wiley & Sons, Inc.: New York, 1991.
- (132) Hesse, M.; Meier, H.; Zeeh, B. *Spektroskopische Methoden in der organischen Chemie*; Thieme: Stuttgart, 1987.
- (133) Antonietti, M.; Henke, S.; Thunemann, A. *Adv. Mater.* **1996**, *8*, 41-&.
- (134) Guan, Z.; DeSimone, J. M. *Macromolecules* **1994**, *27*, 5527-5532.
- (135) Webber, S. E.; Munk, P.; Tuzar, Z., Eds. *Solvents and Self-Organization of Polymers*; Kluwer Academic Publishers: Dordrecht, 1996; Vol. 327.
- (136) Luo, L. B.; Ranger, M.; Lessard, D. G.; Le Garrec, D.; Gori, S.; Leroux, J. C.; Rimmer, S.; Smith, D. *Macromolecules* **2004**, *37*, 4008-4013.

- (137) Yusa, S. I.; Fukuda, K.; Yamamoto, T.; Ishihara, K.; Morishima, Y. *Biomacromolecules* **2005**, *6*, 663-670.
- (138) Justynska, J.; Schlaad, H. *Macromol. Rapid Commun.* **2004**, *25*, 1478-1481.
- (139) DuNoüy, P. L. *Gen. Physiol.* **1919**, *1*, 521.
- (140) Astafieva, I.; Zhong, X. F.; Eisenberg, A. *Macromolecules* **1993**, *26*, 7339.
- (141) Astafieva, I.; Khougaz, K.; Zhong, X. F.; Eisenberg, A. *Macromolecules* **1995**, *28*, 7127.
- (142) Li, D.; Neumann, A. W. *J. Colloid. Interface Sci.* **1992**, *148*, 190.
- (143) Tjiu, W. C. *Aggregation Behaviour of Diblock Copolymers in Solution*; Master thesis, TU Berlin: Berlin, 2005.
- (144) Krasia, T. *Synthesis and Colloidal Properties of a Novel Type of Block Copolymers Bearing  $\beta$ -dicarbonyl Residues*; Thesis, University of Potsdam: Potsdam, 2003.
- (145) Schlaad, H.; Kukula, H.; Rudloff, J.; Below, I. *Macromolecules* **2001**, *34*, 4302-4304.